LXRα INTERACTS WITH CAP350

THE LIVER X RECEPTOR α INTERACTS WITH THE CENTROSOME-ASSOCIATED

PROTEIN 350 (CAP350)

By

OMAR HASSANI

B.Sc. (Hons.)

A Thesis

Submitted to the School Of Graduate Studies in Partial Fulfillment of the

Requirements for the Degree Master of Science

McMaster University

Master of Science (2006)   McMaster University

(Biochemistry)   Hamilton Ontario

TITLE: LXRα interacts with the Centrosome-Associated Protein 350 (CAP350)

AUTHOR: Omar Hassani, B.Sc. (Hons.) (Queen's University)

SUPERVISOR: Dr. John Capone

NUMBER OF PAGES: xiii, 126

ABSTRACT

The Liver X receptor (LXR) is a type II nuclear receptor that is known to be a master regulator of cholesterol levels in the body through its transcriptional control of target genes involved in the handling of cholesterol. The regulation of LXR occurs at multiple levels including ligand and protein availability, post-translational modifications, protein-protein interactions with various cofactors and/or chaperones and a new concept of regulation that involves compartmentalization. This involves the establishment of regions where proteins can be active or inactive. Type II nuclear receptors have recently been found to shuttle between the cytoplasm and the nucleus, thus a compartmentalization component is likely to be involved. It was recently implicated that the centrosome-associated protein 350 (CAP350) can sequester PPARα into nuclear bodies, and to regions in the cytoplasm. The significance of this appears to be the control of PPAR action. CAP350 is a large protein that has the ability to interact with nuclear receptors via an LXXLL motif, and with the cytoskeleton via a CAP-Gly motif. CAP350 is suggested to play a role in the organization of nuclear receptors in the nucleus, and their retention in compartments. In this report, LXRα was confirmed to interact with CAP350 *in vitro*, using a GST-binding assay. Utilizing fluorescent protein chimeras with both nuclear receptors and CAP350 allowed the monitoring of this interaction *in vivo*. CAP350 was observed to form nuclear bodies that were capable of recruiting LXRα. This recruitment was dependant on the integrity of the LXXLL motif. The mutated LXXLL motif of CAP350 was not able to colocalize with LXRα. The significance of this interaction remains unknown. It is likely to be similar to that observed with PPARα, since the nuclear bodies formed by CAP350 seem to correspond to transcriptionally silent regions in the nucleus.

ACKNOWLEDGMENTS

TABLE OF CONTENTS

LIST OF ABBREVIATIONS

ABCA1	ATP-binding cassette transporter A1
ABCG1	ATP-binding cassette transporter G1
ABCG5	ATP-binding cassette transporter G5
ABCG8	ATP-binding cassette transporter G8
Ada2p	alteration/deficiency of activation 2 protein
AR	androgen receptor
AF-1	activation function-1 domain of NRs
AF-2	activation function-2 domain of NRs
ApoE	apolipoprotein E
BFP	blue fluorescent protein
BRG1	brahma related gene-1
BSA	bovine serum albumin
CAP350	centrosome associated protein 350
CAP-Gly domain	centrosome-associated protein-glycine conserved domain
CBP/p300	CREB (cAMP response element binding protein) binding protein/p300
CFP	cyan fluorescent protein
9-cis-RA	9-cis-retinoic acid
CoRNR box	corepressor/nuclear receptor box
CT	C-terminal domain of RNA polymerase II
CYP7A1	cholexterol 7α-hydroxylase
DBD	DNA-binding domain
DR-1	direct repeat-with 1bp-spacer

DR-4	direct repeat-with 4bp-spacer
DRIP150	vitamin D receptor-interacting protein 150
ER	estrogen receptor
FRET	fluorescence resonance energy transfer
GFP	green fluorescent protein
GNAT	GCN5-like *N*-acetyltransferases
GR	glucocorticoid receptor
GRIP1	glucocorticoid receptor interacting protein-1
HAT	histone acetyltransferase
HDAC	histone deacetylase
HDL	high density lipoprotein
HRE	hormone response element
Hsp90	heat shock protein 90
LBD	ligand binding domain
LXR	liver-X receptor
LXRE	LXR response element
MCS	multiple cloning site
mRFP	monomeric red fluorescent protein
MYST	MOZ/YBF2/SAS2/Tip60 family
N-CoR	nuclear receptor co-repressor
NcoA-1	nuclear receptor co-activator-1
NES	nuclear export sequence
NLS	nuclear localization sequence
NR(s)	nuclear receptor(s)
p/CAF	p300/CBP associated factor

PIC	pre-initiation complex
PPAR	peroxisome proliferator activated receptor
PR	progesterone receptor
PTF	PSE-binding factor
RAR	retinoic acid receptor
RIP-140	receptor interacting protein 140
RLU	relative light units
RNA Pol II	RNA polymerase II
RXR	retinoid-X receptor
SAGA	Spt/Ada/Gcn5 acetyltransferase
SMRT	silencing mediator of retinoid and thyroid hormone receptor
Src-1	steroid receptor co-activator 1
SREBP-1c	sterol regulatory element binding protein 1c
TBP	TATA box binding protein
Tip60	tat interacting protin 60
TR	thyroid hormone receptor
VDR	vitamin D receptor
YFP	yellow fluorescent protein

LIST OF FIGURES

INTRODUCTION

1.1   *General Transcription:*

In order to elicit a physiological response in a spatiotemporal manner, a collection of gene networks need to interact and influence each other. Genes exist on the DNA of chromosomes whose structure is very dynamic. At any specific time, access to genes is regulated with expression occurring when access is favorable, while when access is unfavorable expression is inhibited. Gene expression involves transcription, which transcribes information possessed by a gene into an mRNA molecule that carries the blueprint of the protein to the ribosomes. The mRNA sequences are read by the ribosomes allowing translation to a polypeptide, based on that sequence. Following post-translational modification and transport to its functional location, the protein can exert its effects, and a cellular response is observed. An important step of gene expression is transcription, which is a highly regulated event that ensures proper expression to achieve a desired response.

Transcription takes place in the nucleus at DNA sites on chromosomes. Class II transcription (one of three types of transcription) transcribes RNA from class II genes that code for proteins. These genes involve a control region with a promoter and TATA box. The machinery uses the RNA polymerase II (RNA pol II) enzyme and a collection of general transcription factors that influence the basal rate of transcription.

Transcription is often separated into 3 phases: initiation, elongation and termination. Prior to the initiation phase, a pre-initiation complex (PIC) must form on the promoter upstream of a target gene. This involves the recognition of the core promoter by the general transcription factor TFIID (reviewed in Hernandez, N.

1993), and the stepwise recruitment of TFIIB and TFIIA, along with the subsequent recruitment of RNA Pol II and TFIIF. Recruitment of TFIIH by TFIIE, to the forming PIC, stimulates the phosphorylation of the C-terminal domain (CTD) of RNA Pol II forming the closed-PIC (reviewed in Orphanides *et al.* 1996). These general transcription factors are responsible for bringing in the RNA pol II to form the stable complex that will allow for the physical unwinding of the DNA. This exposes the start site allowing for RNA synthesis to occur according to the template. The assembly of this basal transcriptional machinery occurs at a rate unique to the target gene. Fluctuations of this rate will allow for regulation of expression.

Transcriptional control involves the basal transcriptional machinery, sequence-specific DNA-binding factors, chromatin-remodeling factors, enzymes responsible for covalent modifications of histones, and proteins and cofactors that bridge these interactions. Compartmentalization of the various proteins also is a mechanism of control. Chemical signals that occur in response to environmental or metabolic stimuli indicate whether a desired response is needed and are responsible for cues to inhibit or enhance transcription. Chemical signals rely on finding target effectors, or modify effectors by altering pH or temperature.

Inhibition of transcription is based on the negative repression brought about by the physical constraints of chromosome structure. The chromosome is a dynamic structure with machinery that maintains it in a tightly coiled repressed state that blocks access to the information contained within. Enhancement of transcription is based on the release of the negative repression by utilizing the chromatin modification activity of various coactivators that cause the chromosome to unwind and enter a permissive state.

1.2   Nuclear Receptors:

Small hydrophobic molecules derived from cholesterol, fatty acids, fat-soluble vitamins, and other lipids act as signaling molecules that can directly effect transcription. Once activated these hormones mediate their effects using nuclear receptors (NRs), a superfamily of ligand-activated transcription factors.

1.2.1 Nuclear Receptor structure:

Nuclear receptors are a superfamily of DNA-binding proteins that share a conserved amino acid sequence. Despite varying ligand specificities and functions they have a similar structural organization that is composed of 5 domains (Figure 1). An amino-terminal A/B domain has a ligand-independent transcriptional activation function (AF-1) (Kumar and Thompson *et al.* 2003). The core DNA-binding domain (DBD; C domain) contains two highly conserved zinc-finger motifs that target the receptor to specific DNA sequences known as hormone response elements (HRE; Claessens and Gewirth 2004). The D domain (hinge region) separates the DBD from the ligand-binding domain and permits protein flexibility to tolerate simultaneous dimerization and DNA binding. The ligand-binding domain (LBD; E domain) confers specificity to a particular hormone. Despite the variability of hormones, the ligand-binding domains across NRs share a common fold referred to as an antiparallel α-helical 'sandwich' in a 3-layer structure composed of 12 α-helices and 2 to 4 β-strands (Wurtz *et al.* 1996). Dimerization interfaces are found in both the LBD and DBD (reviewed in Mangelsdorf and Evans 1995). F-domain extensions at the C-terminal end are often found, and have a ligand-dependant activation function (AF-2; Danielian *et al.* 1992; Barettino *et al.* 1994; and Durand *et al.* 1994). Ligand binding occurs via a mouse-trap model (Renaud, *et al.* 1995), where the LBD acts as a molecular switch. The

highly conserved C-terminal amphipathic helix 12 (in the α-helical sandwich of the LBD) projects outwards away from the core structure. The hydrophobic residues that line the ligand-binding pocket allows the ligand to be directed inward, after which a conformational change follows, that results in the ligand being embedded in the pocket within the protein closed off from the exterior. The conformational change allows for helix 12 to fold up against the core creating a 'lid' over the ligand-binding pocket. This results in the AF-2 domain becoming available for the binding of coactivators.

The full transcriptional activity of a NR is achieved through synergism between its activation function domains. Moreover, the transcriptional potential of each activation function domain is dependant on external determinants such as promoter context, cell type, and posttranslational modifications (Aronica and Katzenellenbogen 1993; Tzukerman et al. 1994). All AF-1 regions of NRs studied thus far belong to the large category of intrinsically disordered activation domains. The AF-1 consists of modules that have a poor propensity to form α-helical secondary structure and/or formation of hydrophobic surfaces. Protein-protein interaction surfaces can still form, the importance of these modules in AF-1 activated transcription is suggested by the role of inter- or intra-protein dynamics in forming these surfaces (Almlof et al. 1997). In contrast, the AF-2 domain is highly structured and consists of a surface created by specific structural elements in the LBD. Thus the conformation of the LBD is of crucial importance for AF-2 function. As described above the proper positioning of helix 12 of the LBD determines the confirmation of the AF-2 domain that allows it to generate the surface to which co-activators bind. Almost all recognized AF-2 interacting coactivators contain conserved leucine-rich motifs with the consensus sequence LXXLL (Heery et al. 1997). NRs recruit general

transcription factors or co-activators using these domains, the basis for these recruitments is the formation of protein-protein interactions to stabilize the PIC or remodel chromatin.
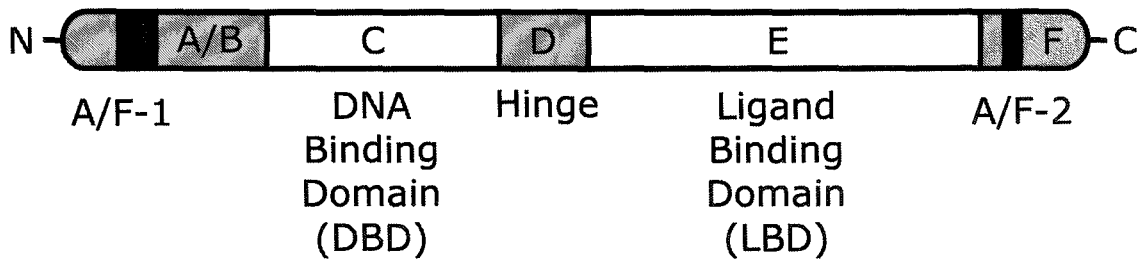
Figure 1. Schematic representation of a typical nuclear receptor.

The schematic emphasizes the domain architecture, with the black bars representing the activation-function regions that lie within the A/B-domain and the F-domain. The C-domain is also referred to as the DNA binding domain (DBD). The D-domain is the hinge region. And the E-domain is the ligand binding domain (LBD).

1.2.2   Nuclear Receptor types and model:

NRs classically, are divided in two types (Figure 2) based on cellular localization, dimerization status, and DNA binding (Chawla *et al.* 2001a). Type I NRs are the steroid receptors including the androgen receptor (AR), progesterone receptor (PR), estrogen receptor (ER) and the glucocorticoid receptor (GR). These are constitutively found in the cytoplasm bound with the chaperone protein Hsp90 (Brinkmann *et al.* 1999) and undergo a ligand dependant import into the nucleus. Ligand binding causes a conformational change in the receptor that results in dissociation of the chaperone complex allowing the receptor to be imported into the nucleus (Gobinet *et al.* 2002). Once in the nucleus type I NRs bind DNA as homodimers, at an HRE that is composed of a palindromic (symmetric) hexanucleotide repeat with sequence 5′-AGAACA-3′ (Zilliacus *et al.* 1995; Shoenmakers *et al.* 2000).

Type II NRs include the vitamin D receptor (VDR), thyroid hormone receptor (TR), retinoic acid receptor (RAR), peroxisome proliferator-activated receptor (PPAR), the liver-X receptor (LXR) and the Retinoid-X Receptor (RXR). They are currently thought to have a predominantly nuclear localization (Baumann *et al.* 1999). In the nucleus type II NRs heterodimerize with RXR and are bound unliganded to an HRE that is a direct repeat with the canonical sequence 5′-AGGTCA-3′ (Mangelsdorf and Evans 1995). This unliganded heterodimer recruits NCoR/SMRT that in turn recruits Sin3A and several histone deacetylases (HDACs) forming a corepressor complex that acts to repress transcription of the target gene (Figure 3). Ligand binding causes a conformational change in the NR that results in displacement of the corepressor complex and active recruitment of coactivators Src-1/NcoA-1, CBP/p300, and p/CAF that have intrinsic histone acetyl transferase (HAT) activity to remodel chromatin and

bring in the transcription machinery to enhance gene expression (Xu *et al.* 1999; Qi *et al.* 2002).
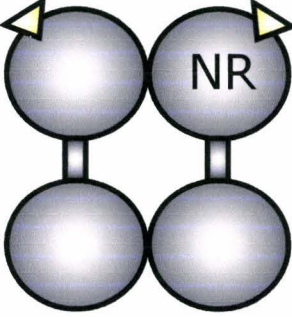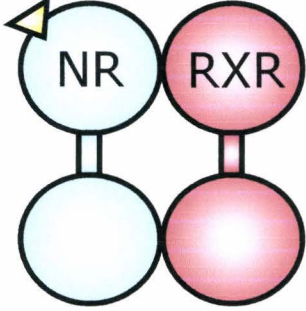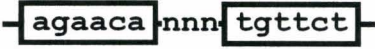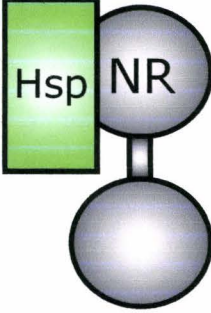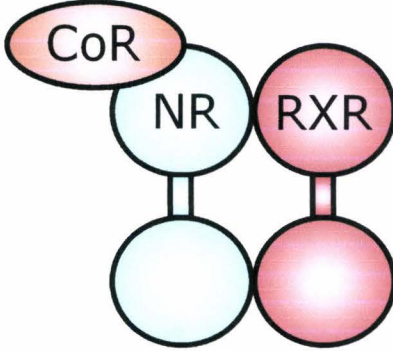
	Type I (Steroid Receptors)	Type II
Functional form	Liganded homodimer	Heterodimer with RXR
Hormone Response Element	Palindromic hexanucleotide with 3-bp spacer	Direct Repeat with 1-bp to 5-bp spacer
Cellular localization	Cytoplasmic	Predominantly Nuclear
Nuclear import	Ligand dependant	Ligand indendant

Figure 2. Comparison of Type I and Type II nuclear receptors.

Type I and Type II nuclear receptors are compared in terms of dimerization partners, DNA binding, and Localization. ◁ Refers to ligand.
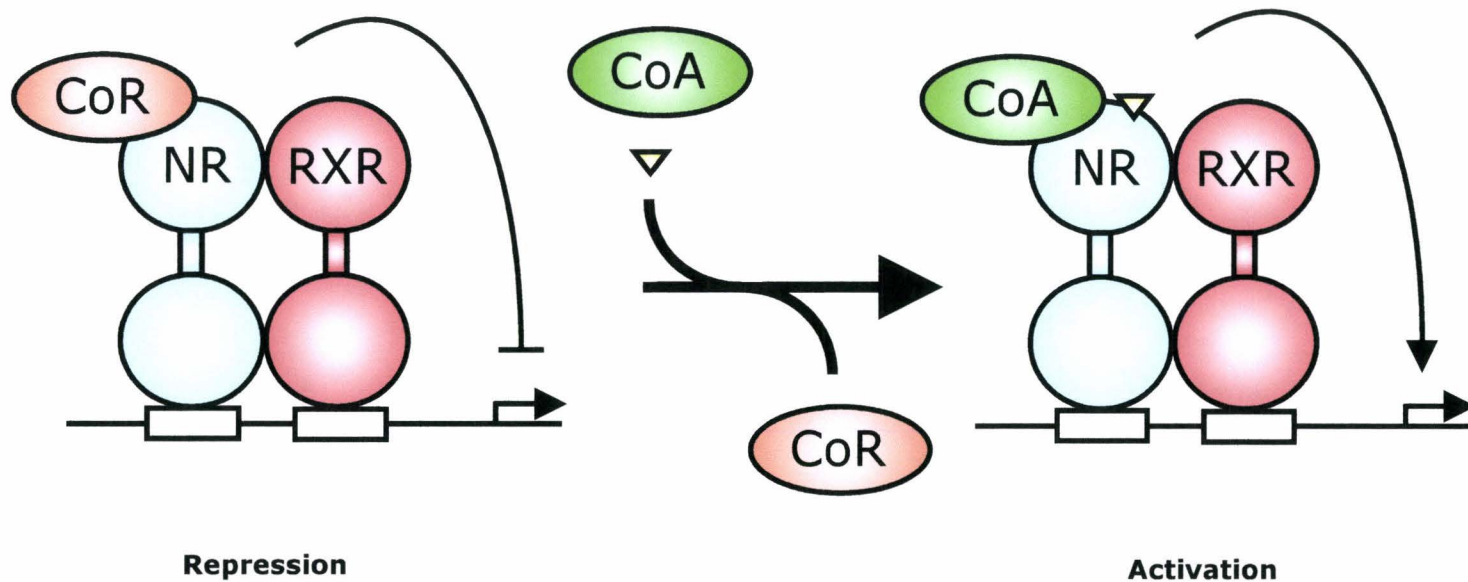
Figure 3. Model of Type II nuclear receptor action.

The diagram represents the current model of type II NR action. This all occurs in the nucleus. The repression of transcription occurs in the absence of ligand with the type II heterodimer in complex with co-repressors on the response element upstream of a target gene. Activation of transcription occurs in the presence of ligand, and results in dissociation of the co-repressor complex and active recruitment of the co-activator complex.

1.2.3   Nuclear Receptor function:

In general NRs work to modulate transcription of a gene network. Each NR has a specific set of genes which it controls An NR is activated once a ligand interacts with the LBD. The HRE is composed of two half sites separated by a spacer. Each half of an NR dimer binds to one half-site. The HRE of type I NRs is composed of palindromic repeats of a hexanucleotide half-site with consensus sequence 5'-AGAACA-3', separated by a 3-bp spacer. The type II NRs recognize direct repeats of a half-site with the consensus sequence of 5'-AGGTCA-3'. Their inter-half-site spacing are known to be from 1-bp to 5-bp, and differentiates which heterodimer binds (Mangelsdorf and Evans 1995). These types of repeats are referred to by their inter-half site spacing ie. DR-1 (direct repeat-with 1bp spacer). For example PPARs are known to interact with a DR-1 and LXR with a DR-4.

NRs enhance the expression of target genes in a number of ways. Chromatin structure generally represents a barrier to transcription by inhibiting the binding of transcription factors to their cognate site (Orphanides and Reinberg 2000). However, NRs have the ability to access their binding sites in this repressive chromatin structure (Colingwood *et al.* 1999; Deroo and Archer 2001; Hsiao *et al* 2002). NRs bind DNA and alter the structural configuration of the DNA, resulting in DNA bending (Leidig *et al.* 1992), this bending leads to the disruption of the nucleosome influencing the availability of DNA sequences for interactions with transcription factors. To these sites, NRs recruit components of intermediary multiprotein complexes that mediate their effects on activation of transcription. This involves multiple coactivators that act in both a sequential and combinatorial manner to reorganize chromatin templates (Pollard and Peterson 1998), and to modify and recruit basal factors of the PIC along with RNA pol II, allowing the stabilization of the

PIC at the promoters of hormone responsive genes (Dilworth and Chambon 2001; Beato and Sanchez-Pacheco 1996).

The coactivator proteins facilitate the communication between NRs, the basal transcriptional machinery and the chromatin environment (reviewed in Torchia *et al.* 1998). Coactivators are shared across many NR pathways resulting in transcriptional interference, where NRs compete for binding of a particular co-activator, squelching the response of the other NRs (Meyer *et al.* 1989). Two main groups of coactivators have been characterized, termed ligand-dependant coactivators that bind to the AF-2 domain, and coactivators that are associated with the N-terminal AF-1 domain (Mckenna *et al.* 1999; Glass and Rosenfeld 2000). Several coactivators are known to bind directly to the AF-1 of NRs, but the structural basis of these interactions is not well established. Some of these coactivators include TBP, Ada2p, CBP, DRIP150, (Ford *et al.* 1997; Henriksson *et al.* 1997; Almlof *et al.* 1998; Hittelman *et al.* 1999) contain no known sequence homologies.

Coactivators that bind the AF-2 domain include the p160 family, that comprises SRC-1/NcoA-1 (Onate *et al.* 1995; Kamei *et al.* 1996), pCIP/AIBI/ACTR/RAC3/TRAM-1 (Torchia *et al.* 1997; Anzick *et al.* 1997; Chen *et al.* 1997; Li *et al.* 1997; Takeshita *et al.* 1997), and TIF2/GRIP1/NcoA-2 (Voegel *et al.* 1996; Hong *et al.* 1996, 1997; Torchia *et al.* 1997). These coactivators include an amino-terminal bHLH and PAS domains, along with domains for interaction with NRs and CBP, and C-terminal activation domains (reviewed in Xu and Li 2003). They recruit HATs and methyltransferases to facilitate chromatin unwinding and assembly of general transcription factors. This interaction occurs through a highly conserved NR box that is made up of a short α-helical LXXLL motif that forms an amphipathic α-helix (Heery *et al.* 1997; Voegel *et al.* 1998). Almost all AF-2 interacting coactivators

that have been described, interact with NRs using this recognition surface. The LXXLL is a leucine-rich motif, where X is any amino acid. Although this motif is necessary to mediate the binding of these proteins, amino acid residues flanking the core motif are important in the recognition of NRs. Several coactivators have been shown to contain NR box with single or multiple copies of the LXXLL motif forming the NR interacting domain. The variety in number and sequence among the coactivators may account for the observed differences in binding to selected NRs (Heery *et al.* 1997; Torchia *et al.* 1997; Voegel *et al.* 1998; McInerney *et al.* 1998).

NRs are known to recruit two classes of proteins that alter the chromatin structure of the promoter region, ATP-dependant chromatin-remodeling proteins and histone-modifying proteins. The ATP-dependant chromatin remodeling proteins are multi-subunit complexes that use the energy of ATP hydrolysis to locally disrupt or alter the association of histones with DNA. All ATP-dependant chromatin-remodeling factors identified thus far belong to the Swi2/Snf2 ATPase superfamily (Eisen *et al.* 1995). The SWI/SNF complex is evolutionary conserved and consists of at least 9 proteins including the invariant core complex and variable subunits that contribute to transcriptional activation. This large enzymatic complex structurally disrupts the histone-DNA contacts within nucleosomes increasing the accessibility of DNA for transcription factor binding (reviewed in Vignali *et al.* 2000).

NRs also recruit histone-modifying proteins, as another strategy to disrupt chromatin architecture. Histones undergo a variety of post-translational modifications that include phosphorylation, methylation, ubiquitination, ADP ribosylation and acetylation (Cheung *et al.* 2000; Strahl and Allis 2000). The outcome of histone modification results in the alteration of chromatin structure and/or presentation of the nucleosome surface for interaction with proteins

important for transcriptional activation at the promoter (Grunstein 1997). The best studied histone-modification is acetylation. Acetylation of the N-terminal tails of the core histones disrupts the histone octamer, and results in loss of the highly ordered structure in the nucleosome. The addition of the acetyl group to the lysine residues of the N-terminal tails neutralizes their positive charge thereby weakening the electrostatic interaction with DNA (Hong *et al.* 1993), and interactions between neighboring nucleosomes (Luger *et al.* 1997). Acetylation is performed by enyzymes known as histone acetyltransferases (HATs) that include 3 families, the GNAT (SAGA/pCAF/GCN5), the MYST (NuA4/Tip60) and the p300/CBP family (Brown *et al.* 2000; Narlikar *et al.* 2002). HATs are recruited to the ligand-activated NR by the AF-2 binding coactivators described above. Many of those NR coactivators also exhibit HAT activity, including ACTR and SRC-1 (Perlmann and Evans 1997, Torchia *et al.* 1998). To balance HAT activity and maintain a dynamic chromatin structure, there are proteins with histone deacetylase activity (HDAC) that repress transcription which is discussed below.

Type II NRs are able to lower basal promoter activity in the absence of ligand, repressing transcription. A number of different repression mechanisms have been proposed that lie within either active or passive repression models. Passive repression refers to competition either for DNA binding or for dimerization partners that both result in steric hindrance by the unliganded receptor on the promoter blocking access of coactivators or basal factors (Hudson *et al.* 1990). Inactive heterodimer formation as documented for TR is also a passive mechanism (Glass *et al.* 1989; Forman and Samuels 1990). Active repression models describe that unliganded NRs either directly affect transcription initiation, or recruit an array of factors that create an environment incompatible with proper assembly of a PIC.

NRs interact with corepressors that include the nuclear receptor corepressor (NCoR) and the silencing mediator of retinoic acid and thyroid hormone receptors (SMRT) (Chen and Evans, 1995; Horlein *et al.* 1995; Ordentlich *et al.* 1999). NCoR and SMRT both contain a conserved bipartite NR-interacting domain (NRID) (Li *et al.* 1997; Seol *et al.* 1996; Zamir *et al.* 1996) and 3 independent repressor domains that can actively repress a heterologous DNA-binding domain (Chen and Evans, 1995; Horlein *et al.* 1995; Ordentlich *et al.* 1999). Further analysis of the NRIDs revealed that each contains a critical LXXXIXXX-I/L motif, which includes the L/I-XX-I/V-I motif termed the CoRNR box (Hu and Lazar 1999; Nagy *et al.* 1999; Perissi *et al.* 1999). This LXXXIXXX-I/L motif is similar to the LXXLL recognition motif present in nuclear receptor coactivators (Heery *et al.* 1997; McInerney *et al.* 1998) but is predicted to form an extended α-helix one turn longer than the coactivator motif. NCoR-1 and NCOR-2/SMRT recruit Sin3A and associated HDAC-1 and HDAC-2 to form a repressive complex that will maintain histones deacetylated, resulting in a repressed state (Chen *et al.* 1996; Horlein *et al.* 1995).

1.3   PPAR, LXR, and RXR:

The focus of this project is on the study of the regulation of nuclear receptors and in particular the type II NRs Peroxisome Proliferator-Activated Receptor (PPAR), the Liver-X Receptor (LXR) and the Retinoid-X Receptor (RXR). PPAR and LXR are NRs that are regulators for various genes that are involved with fatty acid metabolism and cholesterol metabolism. While RXR is the heterodimeric partner for all type II NRs.

1.3.1   Peroxisome Proliferator-Activated Receptor (PPAR):

PPARs were named for there ability to be activated by a class of compounds known as peroxisome proliferators (Issemann and Green, 1990). These compounds have the ability to induce peroxisome proliferation in the liver and kidney of rodents (reviewed in Reddy *et al.* 1982) and include polyunsaturated fatty acids and eicosanoids (Wilson *et al.* 2000). The first PPAR was cloned in 1990 (Issemann and Green, 1990), and within a short-period of time the α, β/δ, and γ subtype were cloned from various organisms. The sequence of the three subtypes of PPARs display homology, with greater homology with PPARs from the same organism than with subtypes from different organisms (reviewed in Lemberger *et al.* 1996). Using gene knockout studies each PPAR subtype was determined to perform a specific function in fatty acid homeostasis.

PPARα is a transcriptional regulator of many processes involved in fatty acid metabolism. It is viewed as a global regulator of fatty acid catabolism, where PPARα target genes function together to coordinate the complex metabolic changes necessary to conserve energy during fasting and feeding. Target genes are involved with serum triglyceride transport, liberation of fatty acids, import of fatty acids into the mitochondria, peroxisomal β-oxidation, ketogenesis and gluconeogenesis (reviewed in Schoonjans *et al.* 1996). PPARα regulates these effects in the liver, kidney, heart and brown adipose tissue.

PPARγ is a key regulator of adipogenesis, and plays an important role in cellular differentiation, insulin sensitization, artherosclerosis and cancer (Rosen and Spiegelman 2001). Ligands for PPARγ include fatty acids and other arachidonic acid metabolites. PPARγ promotes fat storage by increasing adipocyte differentiation and transcription of a number of important lipogenic proteins. In macrophages, PPARγ induces the lipid transporter ABCA1 through an indirect mechanism involving the LXR

pathway, which in turn promotes cellular efflux of phospholipids and cholesterol into HDL (Chawla et al. 2001b; Chinetti et al. 2001).

1.3.2   Liver-X Receptor (LXR):

LXRα, first cloned in 1995, exhibits a pattern of expression that is prominent in enterohepatic tissues such as the intestine, kidney and spleen, with the highest expression occurring in the liver (Willy et al. 1995). The LXR subfamily consists of two members, LXRα and LXRβ, where LXRβ is ubiquitously expressed at low levels in all tissues (Repa et al. 2000) while LXRα is restricted to those tissues rich in lipid metabolism. LXRβ exhibits a 77% identity at the amino acid level with LXRα in the ligand- and DNA-binding domain, but LXRβ lacks the AF-2 region (Teboul et al. 1995). Both types form obligate heterodimers with RXR, and preferentially bind a hormone response element separated by 4 nucleotides (DR4; Willy and Mangelsdorf 1997; Wiebel and Gustafsson 1997).

LXR activators are a select group of oxysterols derived from tissue-specific cholesterol metabolism in the liver, brain, and gonads. The most potent LXR activators identified are 22(R)-hydroxycholesterol, 24(S)-hydroxycholesterol, and 24(S),25-epoxycholesterol (Janowski et al. 1996; Lehmann et al. 1997). LXR activation can be antagonized by other small lipophillic agents, including 22(S)-hydroxycholesterol, geranylgeranyl pyrophosphate and certain unsaturated fatty acids (Spencer et al. 2001; Ou et al. 2001; Gan et al. 2001).

The role of LXR as the body's cholesterol sensor, maintains cholesterol homeostasis through regulating cholesterol catabolism, storage, absorption, and transport. This is conducted through the transcriptional control of key target genes involved in these processes. The liver is the primary site of cholesterol elimination.

The generation of oxysterols in hepatocytes due to excess cholesterol (Zhang *et al.* 2001) allows LXR to sense the need to remove this excess. This stimulates the transcription of cholesterol 7α-hydroxylase (CYP7A1), the rate-limiting enzyme in bile acid biosynthesis. The increased CYP7A1 catalyzes the conversion of cholesterol into bile acids, which is secreted in bile and eliminated in feces (Russell and Setchell *et al.* 1992; Princen *et al.* 1997). LXRα controls this by activating CYP7A1 transcription through an LXRE in the CYP7A1 promoter (Lehmann *et al.* 1997; Peet *et al.* 1998). LXRα knockout mice, fail to up-regulate CYP7A1 in response to cholesterol and develop toxic levels of hepatic cholesterol (Peet *et al.* 1998).

Since the liver is a major site of cholesterol catabolism, there are mechanisms that deal with elevated cholesterol by esterification and storage within the cell, or efflux of free cholesterol to circulation for transport to the liver for handling. LXRs regulate esterification and storage by an indirect means that involves the coordinate regulation of fatty acid biosynthesis. Under high levels of cholesterol, LXRs upregulate transcription of sterol regulatory element binding protein 1c (SREBP-1c; Schultz *et al.* 2000; Repa *et al.* 2000a) which results in increased cleavage of this ER membrane bound bHLH transcription factor. The increase in active SREBP-1c increases the transcription of a number of fatty acid-synthesizing enzymes. One of the products of the fatty acid synthesis pathway, oleolyl-CoA, becomes abundant due to this upregulation, and is the preferred substrate for acyl-CoA:cholesterol acyltransferase, promoting the esterification of cholesterol for storage. This increased fatty acid synthesis also allows for more phospholipid synthesis allowing incorporation into lipoproteins.

When cholesterol levels exceed storage capacity in the cell, efflux of the excess cholesterol back into the serum where it is transported to the liver by a

process known as reverse cholesterol transport. Cellular efflux of free cholesterol is achieved through a number of membrane ATP-binding cassette (ABC) transporters that deliver cholesterol to HDL that serve as the primary transport in the serum to the liver. LXRs prevent the accumulation of sterols in the intestine and macrophage by the induction of multiple ABC transporters and acceptor proteins involved in this pathway (Repa et al. 2000b; Costet et al. 2000; Venkateswaran et al. 2000a; Laffitte et al. 2001). In the macrophage, activation of the RXR-LXR heterodimer by oxysterols stimulates transcription of the ABCA1 and ABCG1 (Repa et al. 2000b; Venkateswaran et al. 2000a) and is dependant on LXR activity at Abca1 and Abcg1 promoters (Costet et al. 2000; Venkateswaren et al. 2000b). ABCA1 is responsible for the cellular efflux of free cholesterol and phospholipids to apolipoprotein acceptors. ABCG1 is another transporter expressed in macrophages that plays a role in cellular efflux of cholesterol and phospholipids. In addition, LXRs also increase the availability of HDL acceptor particles through upregulation of ApoE contributing to the formation of HDL particles (Laffitte et al. 2001; Linton et al. 1995). HDL delivers cholesterol esters to the liver for catabolism and excretion (Glass and Witztum 2001). In the small intestine an increase in dietary and/or secreted biliary cholesterol activates LXR and increases transcription of at least 3 ABC transporters, ABCA1, ABCG5, and ABCG8. These transporters increase cholesterol efflux into the intestinal lumen and thereby prevent net sterol absorption (Repa et al. 2000b; McNeish et al. 2000).

The role of LXR as a cholesterol sensor that governs transport, absorption, and catabolism of sterols provides new possibilities for intervention in the treatment of hypercholesterolemia that would help prevent the progression of artherosclerosis. Ideally, an LXR drug would have 3 potent anti-artherogenic effects: 1. increased

catabolism of cholesterol through upregulation of CYP7A1; 2. inhibition of dietary cholesterol absorption by upregulating intestinal transporters (ABCA1, ABCG5, and ABCG8); 3. increased cholesterol transport from peripheral tissures through upregulation of efflux transporters (ABCA1 and ABCG1) and apolipoproteins (ApoE). One potential problem with an LXR drug is its ability to also upregulate fatty acid synthesis, resulting in hypertriglyceridemia. The future design of LXR drugs would have to dissociate this process from the beneficial effects on cholesterol metabolism.

1.3.3   Retinoid-X Receptor (RXR):

RXRs were identified as orphan receptors that have a high sequence homology with RARs (Mangelsdorf *et al.* 1990). There are 3 separate RXR genes in mammals encoding 3 subtypes α, β, and γ. RXR is expressed throughout development in the embryo. In the adult, RXRβ mRNA is widespread, while RXRα and RXRγ expression is more restricted. RXRα is found in liver, kidney, and skin among other tissues. RXRγ in the muscle and heart. In embryos RXRα and RXRβ are expressed in a range of tissues, while RXRγ expression is more restricted. RXR is the obligate heterodimer partner for all the type II NRs. Thus, RXRs typically do not function alone, but rather serve as master regulators of several crucial regulatory pathways. RXR can be influenced by its ligand 9-cis-RA. This activation can influence some of the activation of the RXR heterodimers. This has led to the finding of potent synthetic RXR agonists (rexinoids) that have dramatic effects on lipid homeostasis since all the lipid-sensing receptors are RXR heterodimers (Mukherjee *et al.* 1998; Repa *et al.* 2000b).

1.4   NR Regulation:

Control of NR activity occurs at multiple levels (Figure 4). NRs need to be activated. An important level of control is ligand availability. All NR ligands are fat soluble and readily pass through many of the body's barriers, thus the concentration of ligand at the target needs to be limited. Ligands are synthesized *de novo*, or from lipid precursors in the diet, or are metabolites of a pathway; for example thyroxine (McNabb 1995), retinoic acid (Petkovich 2001) and oxysterols (Olkkonen and Lehto 2004) respectively. The concentration of ligand is maintained at an appropriate level defined by the cell in a balance between synthesis and degradation. Also some of the ligands are known to have cellular binding proteins such as cellular retinoic acid binding protein that sequester the ligands limiting their action (Noy 2000).

The concentration of NR protein is tightly regulated and involves a balance between synthesis and degradation. The amount of NR protein at any one time is tightly controlled, however a reserve is needed to be able to produce an effect. This reserve is regulated by various protein-protein interactions with its binding proteins that affect NR activity. Chaperones sequester NRs and hold them in a non-active confirmation such as in the case of type I NRs with heat shock proteins. NRs could also experience squelching when in complex with corepressors or coactivators, or RXR. Post-translational modification such as phosphorylation may also have an effect on NR activity.

Another aspect of NR regulation and the focus of this work is compartmentalization. Compartmentalization is a regulatory mechanism that allows specific process to occur more efficiently in a particular region than in another. An example is that for transcription factors to perform their function they must be in the nucleus. And their import and/or export imposes the regulatory aspect of this compartmentalization.

Thus NR regulation includes ligand availability, receptor abundance and stability, protein-protein interactions, posttranslational modification, and compartmentalization. With the advent of fluorescent imaging technologies utilizing fluorescent-linked antibodies and fluorescent protein tags, applications have been developed to monitor transcription factor dynamics. This has allowed the delineation of the regulation of NR compartmentalization, nucleocytoplasmic shuttling, and the characterization of the influences of various receptor interacting proteins.
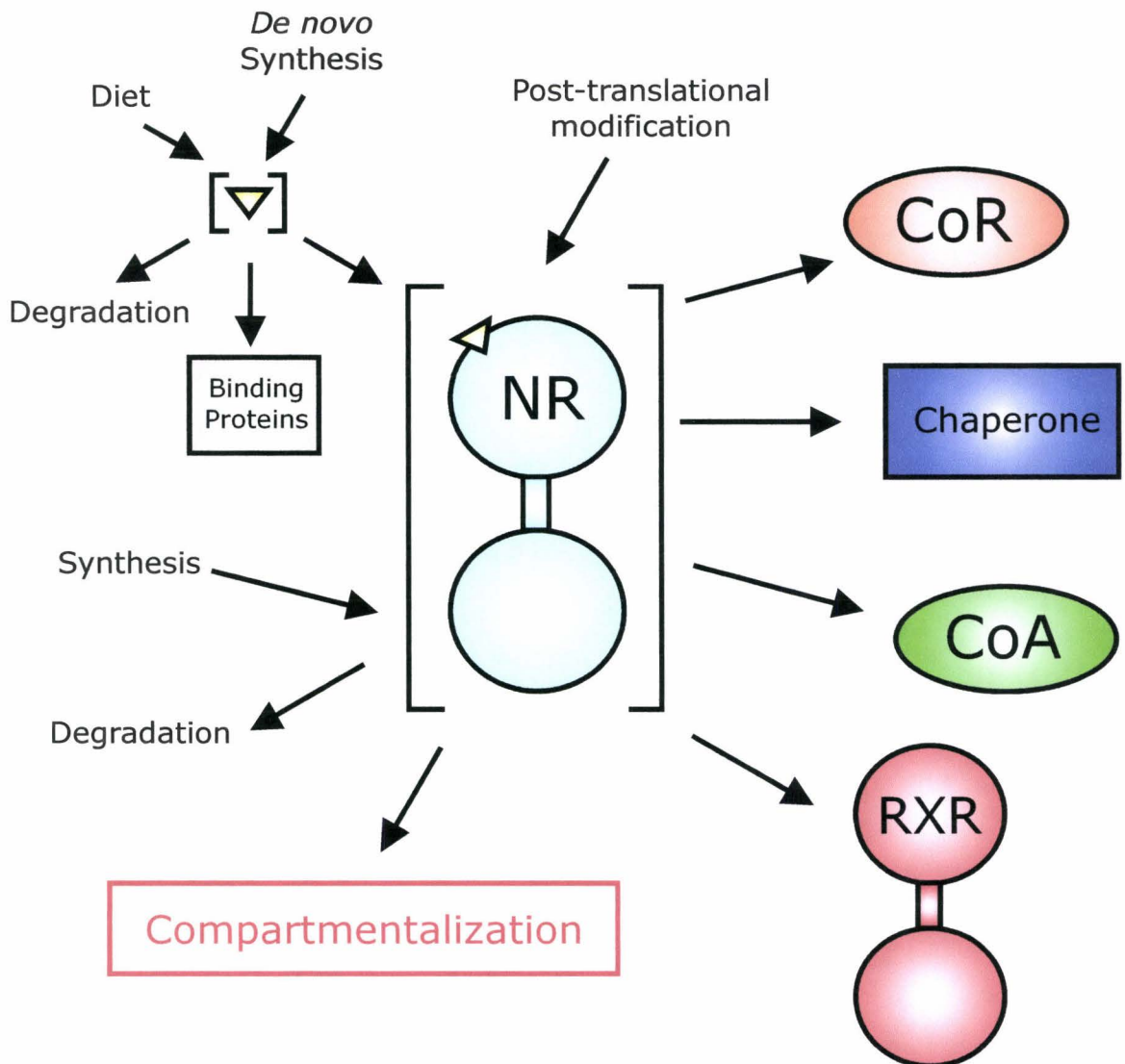
Figure 4. Nuclear receptor regulation.

This is a schematic representation of the possible levels of regulation that a type II nuclear receptor can encounter in a given cell. The ligand concentration is itself influenced by metabolic constraints, as well as any binding proteins that control its availability to interact with the NR. The active NR concentration is regulated by synthesis and degradation pathways, protein-protein interactions, and post-translational modification. Compartmentalization is also thought to play a role in regulation.

▽ *Refers to ligand.*

1.4.1   Compartmentalization:

Compartmentalization is a method of regulation within the cell that establishes regions within the cell where processes can occur more efficiently and limits access of certain components to these regions to control these processes. In essence compartmentalization creates functional units within the cell. Organelles serve this purpose allowing certain conditions to be established to promote certain processes such as the ATP synthesis. Import/Export in to the nucleus is also regulated to allow regulation for processes that occur in the nucleus, such as transcription. In removing or sequestering transcription factors in the cytosol, their action is limited. Also a widely accepted yet not well described model of compartmentalization within the nucleus is theorized to involve the 'nuclear matrix' (Berezney and Jeon 1995). In this theory the nucleus is organized in compartments of activity that involve the cytoskeleton and trafficking elements along with functional subnuclear complexes.

Transcription factors need to get into the nucleus to exert their effects once they are synthesized in the nucleus. Control of their import into the nucleus allows for the regulation of their activity on gene expression. For type I NRs, the mechanisms governing the cytoplasmic/nuclear distribution have been modeled primarily in terms of the conditional interaction of the nuclear localization signals (NLS) with the import/export apparatus present in nuclear pores (Tyagi et al. 1998). In the absence of hormone, these receptors are found in association with a large complex of chaperones in the cytoplasm (Pratt et al. 1992). Interaction of the cognate ligand with these receptors induces a conformational rearrangement that results in dissociation of the complex and loss of many of the associated factors. This reorganization is thought to expose previously masked translocation signals, and the receptors are then transported by the transport machinery. This is observed for the

AR which contains a ligand-dependant bipartite NLS in the DNA-binding domain (Zhou *et al.* 1994) whose functions seems to be also affected by Hsp90 (Georget *et al.* 2002). Further control of AR-activity is provided by the ability to export AR in a ligand dependant manner to limit its activity in the nucleus (Saporita *et al.* 2003).

The nucleus is a highly complex and organized structure containing the genetic information and the components required for DNA replication, transcription, post-transcriptional RNA processing, and DNA repair (de Jong *et al.* 1996; Lamond and Earnshaw 1998; Dundr and Misteli 2001). Despite the knowledge of the intricacy of these processes obtained from *in vitro* studies, the functional and spatial organization of the nucleus and its role in coordinating these processes *in vivo* remains poorly understood. Regulation of gene expression in the nucleus involves a vast array of proteins and protein complexes (Lee and Young 2000; Lemon and Tijan 2000), although for the most part their subnuclear distributions have not been well established. Several subnuclear compartments including nuclear speckles, Cajal and PML bodies, have recently been shown to exhibit transcriptional activity (Carmo-Fonseca 2002; Spector 2003). These observations coincided with the discovery of nuclear foci containing active mRNA synthesis (Jackson *et al.* 1993) or enriched for certain transcription factors, such as HSF granules and OPT domains (Sarge *et al.* 1993; Pombo *et al.* 1998). The focus on the possible effects of subnuclear compartmentalization on the overall organization and temporal behavior of transcription factors is important to the understanding of their overall function *in vivo.*

Replication and transcription have been described to be functionally linked to the nuclear architecture (Jackson *et al.* 1984; Nelson *et al.* 1986). The actual existence of a physical scaffold is often regarded as a controversial issue. A number

of groups support the existence of a nuclear matrix, commonly considered a network of proteins and filaments that form an intranuclear scaffold upon which nuclear processes and components are organized (Nickerson 2001). Others remain unconvinced that a functional nuclear matrix exists *in vivo*, primarily because of the harsh methods used to extract the insoluble nuclear fraction and that the perceived intranuclear organization is an effect of the self-arrangement of nuclear constituents more than the cause of a physical scaffold (Pederson 1998, 2000). Despite the differing view points, researchers have continued to elucidate means to study the nuclear matrix. One of the techniques that could prove important in identifying compartment regions, employs fluorescent imaging technology to monitor proteins of interest and study their movement and interactions in the cells.

The use of these improved cytological methods to examine nuclear constituents and domains will improve defining the relation between nuclear structure and transcriptional regulation, along with their subnuclear and subcellular movements. Utilization of immunocytochemical means to detect brominated RNA indirectly labeled with an antibody allowed the demonstration that active RNA pol II forms between 1000 and 2000 punctate foci within the nucleus (Jackson *et al.* 1993; Wansink *et al.* 1993). Immunocytochemical means were applied to type I NRs, where a group indirectly labeled GR and MR using antibodies, in cultured cells and cells sectioned from mice. They identified that foci, similar in size and appearance were formed by GR (van Steensel *et al.* 1995) and MR (van Steensel *et al.* 1996). These GR or MR foci were able to colocalize with RNA pol II containing foci, however not completely, a large number of GR or MR foci were found that do not colocalize with those foci.

These findings suggested that a large proportion of a given transcription factor might reside in storage domains that are not associated with transcriptionally active genes. Later work supported these results, in 1996 Elefanty *et al.* demonstrated that GATA transcription factors formed discrete domains in the nucleus that did not overlap with RNA pol II/splicing factor foci, while another group showed that other sequence specific transcription factors including Oct-1 and E2F, formed punctuate foci in the nucleus that did not colocalize significantly with RNA pol II transcription domains (Grande *et al.* 1997). The latter study also provided evidence that the general transcription factor TFIIH and the Brahma related gene-1 (BRG1) subunit of the SWI/SNF chromatin remodeling complex were associated to some extent with the RNA pol II foci. This implied the interaction of sequence-specific transcription factors with the transcriptional machinery may be spatially and temporally regulated through sequestration to separate domains or compartments. Oct-1 was later shown to colocalize with the PSE-binding factor (PTF), RNA pol II, TBP, and Sp1 transcription factor to distinct foci, termed OPT domains, in which transcription was active (Pombo *et al.* 1998). Subsequently, the Oct-4 transcription factor was shown to colocalize with RNA pol II and splicing machinery in transcriptionally active oocytes but was sequestered to other compartments in transcriptionally inert oocytes (Parfenov *et al.* 2003). Together these observations lend evidence to the "transcription factory" model, which proposes that RNA synthesis and processing occurs in discrete subnuclear compartments that contain factors required for transcription of a particular gene or genes (Pombo *et al.* 2000; Martin and Pombo 2003).

Early research showed that NRs were associated with the nuclear matrix, but it was not until improved fluorescence microscopy techniques emerged that

subnuclear compartmentalization of the proteins was defined in greater detail. These technologies enabled several groups to visualize GR (Htun *et al.* 1996; van Steensel *et al.* 1996), VDR (Barsony *et al.* 1997), AR (Georget *et al.* 1997), MR (Fejes-Toth *et al.* 1998) and ER (Htun *et al.* 1999) localization in nuclei.

The visual representation of the compartmentalization of NRs has sparked significant interest since GFP technology was employed to create a chimera with the GR, to visualize GR translocation in the presence of ligand in live mouse cells (Htun *et al.* 1996) and the study of the intranuclear dynamics of GR between chromatin and the nucleoplasmic space in live cells (McNally *et al.* 2000). Labeling NRs with GFP allows the ability to monitor protein trafficking in real time and provides important information about NR behavior in the cell. This allows study of compartmentalization of proteins within the cell. GFP chimeras of nuclear receptors have delineated pathways by which some NRs can shuttle between the nucleus and the cytoplasm in a dynamic, hormone- and energy-dependant manner (Baumann *et al.* 1999; Hager *et al.* 2000; Maruvada *et al.* 2003). Important findings have been delineated using this technology. It was found that the A-form of PR was localized in the nucleus in the absence of ligand, while the B-form of PR is predominantly cytoplasmic in a hormone-free cell (Lim *et al.* 1999). Thus, it appears that there are exceptions to the classic model of type I NR cytoplasmic localization. Also using an ERα labeled at the N-terminus with GFP, researchers were able to confirm that ERα is another exception to the classical steroid NRs, where ERα is localized exclusively in the nucleus in the absence and presence of ligand (Htun *et al.* 1999). In this study, they also demonstrated an intranuclear redistribution of ERα from a reticular to a punctuate pattern after stimulation with ligand.

NR antagonists have also been shown to affect the subnuclear distribution of these proteins. For example, studies using the AR fused with GFP showed that while traditional antiandrogenic chemicals or putative antiandrogenic chemicals did not prevent translocation of AR into the nucleus, they did interfere with its normal intranuclear compartmentalization, causing it to adopt a diffuse pattern rather than forming punctuate foci (Tormura *et al.* 2001). These observations, combined with the fact that agonist-bound AR occupies distinct domains within the nucleus, have led to the proposal of an agonist compartment, where nuclear AR resides in complex with other proteins whose interaction with AR is dependant on its agonist-bound confirmation (Black and Paschal 2004). This represents a paradigm for other NRs, since each one has the capacity of binding a variety of agonists or antagonists and interacting with specific binding partners, some of which have been shown to influence the subnuclear distribution of their partner.

By dissecting the MR and fusing them to fluorescent proteins and introducing them to cultured cells, Pearce *et al.* (2002) were able to show that particular regions of the protein were necessary for its proper localization within the nucleus; specifically, deletion of domains containing transactivation activity caused altered subnuclear distribution of MR. Furthermore, DNA-binding MR mutants did not form distinctive intranuclear clusters, however dimerization mutants were able to form clusters. Together, these data suggested that MR subnuclear compartmentalization is both DNA-binding- and transactivation-dependant. Whether these properties are true of other nuclear receptors remains to be elucidated.

The application of this technology to type II NRs has lead to the understanding that the compartmentalization of these receptors is more complex than was previously thought. Using a GFP-TR, it was described that TR is localized in

both the cytoplasm and the nucleus contrary to the classic model for type II NRs (Zhu, *et al.* 1998). In the study it was also determined that there are ligand-dependant translocation determinants in the hinge region of TR, using mutation analysis of a predicted NLS based on the NLS for steroid receptors. Another group demonstrated using GFP-VDR, that VDR also is located in the cytoplasm and undergoes hormone-dependant translocation into the nucleus (Racz and Barsony 1999). They also demonstrated using deletion mutants that the AF-2 domain is involved in the translocation. Another group further characterized a possible sequence in the hinge region of VDR that is responsible for VDR translocation (Michigami *et al.* 1999). In their study, they attached the predicted 20 amino acid sequence from the hinge region to an alkaline phophatase tagged with GFP. Alkaline phosphatase is a cytoplasmic protein that does not normally enter the nucleus. They found that the sequence in hinge region which resembles a bipartite PPXR enables alkaline phosphatase to translocate to the nucleus (Michigami *et al.* 1999). This indicates that the subcellular localization of type II NRs is more complex than previously described by the classical model.

Another regulatory control of NR activity is the nuclear export of NRs from the nucleus to the cytoplasm. AR, GR, PR and TR have been implicated in the rapid shuttling between the nucleus and cytoplasm (Georget *et al.* 1997; Guiochon-Mantel *et al.* 1991; Madan and DeFranco 1993; Baumann *et al.* 2001a; Bunn *et al.* 2001). Studying the nuclear export of GR using part of the GR fused to GFP, allowed the characterization of a possible NES in the DBD (Black *et al.* 2001). Since this NES is identified to be in a highly conserved domain, allows the possibility that nuclear export is a general feature of NRs. It may be that the balance between export and import of NRs is an important mechanism for regulation of NRs, since in the

cytoplasm NRs can be sequestered in chaperones or degraded. Also this may allow for integration of the cytoplasmic signaling pathways with NR-regulated transcription events, or may relate to some unknown cytoplasmic function for NRs that does not involve transcription events.

Intracellular trafficking and subcellular/intranuclear compartmentalization may be a general phenomenon of type II NRs, which could be differentially influenced by ligand binding as described above. Also this can be influenced by interaction with RXR, and/or association with cofactors (Prufer *et al.* 2000; Baumann *et al.* 2001a). Prufer *et al.* using fluorescent protein chimeras for RXR (RXR-BFP) and GFP-VDR were able to demonstrate that RXR influences import of VDR and retention of VDR in the nucleus. This was striking when RXR was able to induce nuclear import of GFP-VDR with a mutated NLS, and rescue the transcriptional activity of VDR for this mutant (Prufer *et al.* 2000). Baumann *et al.* demonstrated also that TRβ1 distribution was also influenced by RXR, through influencing import of a primarily cytoplasmic TRβ1 mutant and retention of TRβ1 in the nucleus (Baumann *et al.* 2001a). Also they found that NCoR also plays a role in maintaining TRβ1 in the nucleus. In using a TRβ1 that does not interact with NCoR and is mainly cytoplasmic in the absence of ligand, they were able to demonstrate that upon addition of T_3 the mutant TRβ1 maintains a 50% cytoplasmic localization while the wild-type displays only 10% cytoplasmic localization (Baumann *et al.* 2001a).

1.5   *Centrosome-Associated Protein 350 (CAP350):*

Utilizing imaging technology has enabled the understanding that type II NRs are not constitutively localized to the nucleus as previously assumed. Rather, these are mobile proteins that continually shuttle between the cytoplasm and nucleus (Barsony

and Prufer 2002; Baumann *et al.* 2001a; Baumann *et al.* 2001b). As well these proteins are regulated into intranuclear compartments. They are thought to exchange between subnuclear macromolecular complexes.

Miyata *et al.* using a yeast two-hybrid screen to identify PPARα interacting proteins discovered an un-described protein (KM3) that specifically binds to PPARα (Miyata *et al.* 1996). The KM3 cDNA was identified to encode amino acids 572-1176 of CAP350, a putative human centrosome-associated protein (GenBank accession number NM_014810.2). CAP350 is a 3117 amino acid protein of unknown function, but is predicted to associate with the centrosome and cytoskeleton because of the presence of a CAP-Gly domain (Saito *et al.* 2004) near its C-terminus (Figure 5). CAP350 also contains two putative LXXLL motifs, an N-terminal LSHLL (contained within the KM3 portion) at amino acids 759-763 and a C-terminal LLDLL at amino acids 2719-2723. The LXXLL motifs are known to be important in mediating protein-protein interactions with NRs as described above (Xu *et al.* 1999; Qi *et al.* 2002). The predicted interaction with cytoskeletal architecture along with putative NR interacting domains has raised the interest that this protein may define a regulatory component of PPAR that involves a compartmentalization mechanism.

To understand the cellular distribution of CAP350, indirect immunofluorescence imaging of a c-myc tagged CAP350 transfected in NIH/3T3 cells showed that CAP350 distributes in the cytoplasm and the nucleus (Patel *et al.* 2005). In the cytoplasmic compartment CAP350 was found in the perinuclear region localized to the centrosome, and localized to branched intermediate filaments. In the nucleus CAP350 is exhibited in distinct nuclear foci (Patel *et al.* 2005). CAP350 has also been shown by another group to form a centrosomal complex that is required for microtubule anchoring (Yan *et al.* 2006). Thus, CAP350 is probably a

multifunctional protein that contains a variety of functional domains, which could serve various roles; however, there is at present little knowledge of its structural and functional properties.

To further understand the association of PPARα with CAP350, the effect of CAP350 on PPARα localization was delineated using immunocytochemical means. CAP350 disrupted PPARα subcellular distribution by altering its intranuclear compartmentalization to the CAP350-defined foci and its intracellular distribution to the cytoplasm (Patel *et al.* 2005). In the nucleus the CAP350-defined foci recruited PPARα, more specifically the CAP350 colocalization with PPARα observed was retained in a truncated N-terminal fragment containing only the N-terminal LXXLL. This colocalization was lost when the same N-terminal CAP350 fragment with a mutated LXXLL was used, indicating a particular role for this motif (Patel *et al.* 2005). Another striking feature was the presence of PPARα in the cytoplasm colocalized to the CAP350 in the centrosome and to the intermediate filaments (Patel *et al.* 2005). This localization pattern was confirmed in live cells using the chimeras YFP-CAP350 and mRFP-PPARα. The functional significance of this association was examined using a transcriptional assay using a rat hepatoma cell line that is responsive to peroxisome proliferators (Zhang *et al.* 1992; Zhang *et al.* 1993). Transient transfection experiments involving a PPRE-linked reporter gene along with CAP350 showed that there is loss of PPARα-mediated induction with increasing amounts of CAP350. This loss of transactivation was overcome by using the N-terminal CAP350 with the mutated LXXLL motif (Patel *et al.* 2005). These findings implicate CAP350 in a dynamic process that mediates distinct pathways of subcellular compartmentalization of PPARα and which may out of consequence regulate the function of this NR within the cell.

CAP350 NR1	A	G	T	A	G	S	L	**L**	S	H	**L**	**L**	S	L	E	H	V	G	I
CAP350 NR2	S	E	K	L	C	T	P	**L**	L	D	**L**	**L**	T	R	E	K	N	Q	L
SRC-1 NR1	Y	S	Q	T	S	H	K	**L**	V	Q	**L**	**L**	T	T	T	A	E	Q	Q
SRC-1 NR2	L	T	E	R	H	K	I	**L**	H	R	**L**	**L**	Q	E	G	S	P	S	D
SRC-1 NR3	E	S	K	D	H	Q	L	**L**	R	Y	**L**	**L**	D	K	D	E	K	D	L
SRC-1 NR4	Q	A	Q	Q	K	S	L	**L**	Q	Q	**L**	**L**	T	E					

CAP350 NR1 A G T A G S L **L** S H **L** **L** S L E H V G I
CAP350 NR2 S E K L C T P **L** L D **L** **L** T R E K N Q L

SRC-1 NR1 Y S Q T S H K **L** V Q **L** **L** T T T A E Q Q
SRC-1 NR2 L T E R H K I **L** H R **L** **L** Q E G S P S D
SRC-1 NR3 E S K D H Q L **L** R Y **L** **L** D K D E K D L
SRC-1 NR4 Q A Q Q K S L **L** Q Q **L** **L** T E

SRC-2 NR1 D S K G Q T K **L** L Q **L** **L** T T K S D Q M
SRC-2 NR2 L K E K H K I **L** H R **L** **L** Q D S S S P V
SRC-2 NR3 K K K E N A L **L** R Y **L** **L** D K D D T K D

SRC-3 NR1 E S K G H K K **L** L Q **L** **L** T C S S D D R
SRC-3 NR2 L Q E K H R I **L** H K **L** **L** Q N G N S P A
SRC-3 NR3 K K E N N A L **L** R Y **L** **L** D R D D P S D

TRBP V T L T S P L **L** V N **L** **L** Q S D I S A G

TRAP220 NR1 K V S Q N P I **L** T S **L** **L** Q I T G N G G
TRAP220 NR2 N T K N H P M **L** M N **L** **L** K D N P A G D

PGC-1α E A E E P S L **L** K K **L** **L** L A P A N T Q

Figure 5. Centrosome-associated protein 350 (CAP350).

A schematic representation of CAP350 is shown. The LXXLL motif are shown by the red bars, the KM3 fragment is shown in grey, and the CAP-Gly domain in black. The LXXLL motif and its surrounding sequence is compared with other LXXLL motif from various co-activators.

1.6   Project Rationale:

The regulation of PPARα seems to have another level of control due to the discovery that PPARα induction can be limited by CAP350; a large multifunctional protein that can redistribute PPARα into intranuclear site in the nucleus that are not associated with transcription, and can influence the sequestration of PPARα in the cytoplasm. PPARα is similar to another type II NR, LXRα, in that both are metabolic regulators, both interact with RXRα, and are interrelated by exhibiting cross-talk in their signaling (Yokishawa *et al.* 2003; Ide *et al.* 2003), and both are important in lipid metabolism and implicated in the development of arthersoclerosis (Li and Glass 2004). Thus the paradigm of CAP350 inhibition of NR activity can also be true for other NRs.

A similar behavior as that of PPARα with CAP350 is hypothesized with LXRα. The compartmentalization role of CAP350 may be more toward a general mechanism which is employed to regulate type II NRs in general. The LXXLL motif contained within CAP350 is a known general NR interacting motif for various coactivators. Thus interaction between LXRα and CAP350 is postulated. The inhibitory effects on the transactivation may also extend to LXRα activity. In order to further study NR localization in the cell, fluorescence imaging technology will be utilized to monitor molecular interactions between LXRα and CAP350. NR chimeras were constructed in order to monitor protein localization in the live cells. The mRFP-PPARα used in the original CAP350 study, mRFP-LXRα the focus of this report, eGFP-RXRα and mRFP-RXRα were constructed and were characterized. Using these together with available YFP-CAP350 constructs (Patel *et al.* 2005), would enable the determination whether any important information could be gathered on the compartmentalization of these NRs as another possible method of regulation of NR activity. This will help explain

whether the observed inhibition of PPAR activity is unique for PPAR or perhaps general for type II NRs.

MATERIALS AND METHODS

2.1   *Chemicals and Reagents:*

The chemicals and reagents used to carry out this research and their origins are listed below:

Acrylamide	Bioshop
bis-Acrylamide	Bioshop
Agarose (electrophoresis grade)	Life Technologies
Agar	Bioshop
Ammonium persulphate	Sigma
Ampicillin	Sigma
BioRad protein assay reagent	BioRad
Bovine calf serum	Gibco
Bovine serum albumin (BSA), 100X	New England Biolabs
Calcium chloride dihydrate ($CaCl_2 \cdot 2H_2O$)	BDH
Charcoal, dextran-coated	Sigma
Deoxynucleotide triphosphates (dNTPs)	Invitrogen
Dimethylsulphoxide (DMSO)	Sigma
Dulbeco's modified Eagle's medium (DMEM)	Gibco
DMEM, phenol minus	Hyclone
ECL detection kit	Amersham
EDTA (ethylene diamine tetraacetate)	Merck
Ethidium bromide	Sigma
ExGen500	Fermentas
Fetal bovine serum (FBS)	Sigma

FuGENE6	Roche
Glutathione sepharose 4B beads	Amersham
Glycerol	Caledon
Hepes	Bioshop
Hoescht 33245 dye	Sigma
22-R-hydroxycholesterol	Sigma
Isopropanpol	ACP chemicals
Isopropyl-β-D-thiogalactopyranoside (IPTG)	Sigma
Kanamycin	Sigma
L-Glutamine	Gibco
Lipofectamine	Invitrogen
Luciferin	Biosynth
L-^{35}S-methionine (1151 Ci/mmol)	Perkin Elmer
Magnesium chloride (MgCl$_2$)	Merck
Magnesium sulphate (MgSO$_4$)	EMD
Eagle's Minimum Essential medium F15 (MEM-F15)	Gibco
2-mercaptoethanol	EM Science
Molecular Weight Standards	
1 Kb Plus DNA ladder	Invitrogen
Prestained SDS-PAGE standards	Invitroen
^{14}C-labelled protein maker	Sigma
MOPS	Sigma
Milk, non-fat powdered	Carnation
Mini-C protease inhibitor	Roche
Nitrocellulose	Amersham

o-Nitrophenyl-β-D-galactopyranoside (ONPG)	Sigma
Nonidet P-40 (NP-40)	Sigma
Potassium acetate (KCHO)	EMD
Potassium Chloride (KCl)	BDH
Penicillin (5000 U/mL)/Streptomycin (5000 U/mL)	Gibco
Qiagen-tip 500 plasmid maxi-kit	Qiagen
QiaexII kit	Qiagen
Reporter lysis buffer, 5X	Promega
Sodium acetate (NaCHO)	BDH
Sodium carbonate (Na$_2$CO$_3$)	EM Science
Sodium chloride (NaCl)	Bioshop
Sodium dodecyl sulphate (SDS)	Bioshop
Sodium hydroxide (NaOH)	BDH
Sodium phosphate	EM Science
Sodium pyruvate	Invitrogen
TNE (Fluorescence Assay Buffer,10X)	Sigma
TO-901317	Sigma
Tris	Bioshop
Triton X-100 (TX-100)	Sigma

2.2   *Enzymes:*

*Bam*HI	New England Biolabs (NEB)
*Bam*HI buffer	NEB
Calf intestinal alkaline Phosphatase (CIP)	NEB
*Eco*RI	NEB

EcoRI buffer, 10X   NEB

NEB buffer 1, 10X   NEB

RNase A   NEB

SacI   NEB

T4 DNA Ligase   NEB

T4 DNA ligase buffer, 10X   NEB

T7 RNA polymerase   Promega

ThermoPol Buffer, 10X   NEB

Vent DNA polymerase   NEB

2.3   Oligonucleotides:

Oligonucleotide Sequence(sense strands only)	Purpose
5'–cgcggatccatggtggacacggaaagcc–3' (forward) 5'–cgctggatccaactcagtacatgtccctg–3' (reverse)	hPPARα fusion hPPARα fusion
5'–cgcggatccatgtccttgtggctgggggcc–3' (forward) 5'–cgcggatcctcattcgtgcacatc–3' (reverse)	hLXRα fusion hLXRα fusion
5'–cggaattccatggacaccaaacatttcctgccg–3' (forward) 5'–ccggaattccgctaagtcatttggtgcggcgc–3' (reverse)	hRXRα fusion hRXRα fusion
5'–ctacaagaccgacatcaagc–3' (upstream) 5'–gtgaaatttgtgatgctattg–3' (downstream)	mRFP seq mRFP seq
5'–tcctgctggagttcgtgaccgccgccggga–3' (upstream) 5'–acgatcataatcagccataccacatttgta–3' (downstream)	EGFP seq EGFP seq

2.4   *Plasmids:*

2.4.1   *Commercially-available plasmids:*

1.   pEGFP-C1 (Clontech): a eukaryotic expression vector containing the human cytomegalovirus (CMV) promoter, the enhanced green fluorescent protein gene followed by an MCS to produce N-terminal fusions, and a kanamycin-resistance gene.

2.   pEYFP-C1 (Clontech): a eukaryotic expression vector containing the human CMV promoter, the enhanced yellow fluorescent protein gene followed by an MCS to produce N-terminal fusions, and a kanamycin resistance gene.

3.   pGEX-2TK (Amersham): a bacterial expression vector with a glutathione-S-transferase gene (GST) under the control of a *tac* promoter (chemically inducible) followed by an MCS to produce an N-terminal fusion. The plasmid also contains an ampicllin resistance plasmid, and has a phosphorylation site that is recognized by cAMP-dependant protein kinase (heart muscle) for labeling of fusion products with ^{32}P.

4.   pRC/CMV (Invitrogen): a eukaryotic expression vector containing enhancer-promoter sequences from the gene of human CMV. It also contains a T7 and SP6 promoter flanking either side of the MCS and is ampicillin-resistant

5.   pSG5 (Stratagene): a eukaryotic expression vector containing an SV40 early promoter with a T7 promoter upstream of the multiple cloning site (MCS). The plasmid is also ampicillin-resistant.

2.4.2   Plasmids Constructed by Others:

1. pCMV-Lac-Z: contains the CMV promoter adjacent to the *lacZ* gene (Merck Research Lab; referenced in Berger *et al.* 2000).

2. pEYFP-CAP350: contains a full length wildtype CAP350 cloned to create a YFP N-terminal fusion protein (Patel *et al.* 2005)

3. pEYFP-CAP350$_{1-890}$ (YFP-CAP350$_{1-890}$): contains the wildtype N-terminal 890 amino acid fragment of the CAP350 protein cloned to create an N-terminal fusion with YFP (Patel *et al.* 2005).

4. pEYFP-CAP350A$_{1-890(LSHAA)}$ (YFP-CAP350$_{1-890(LSHAA)}$): contains a mutated N-terminal 890 amino acids of the CAP350 protein cloned to create an N-terminal fusion with YFP. The mutation involved alanine substitutions of leucine residues of the LXXLL motif at positions 762 and 763 and was generated from pEYFP-CAP350$_{1-890}$ by site-directed mutagenesis (Patel *et al.* 2005).

5. pGEX-2TK-CAP350$_{1-890}$ (GST-CAP350$_{1-890}$): contains the wildtype N-terminal 890 amino acid fragment of the CAP350 protein cloned to create an N-terminal fusion with GST (Patel *et al.* 2005).

6. pGEX-2TK-CAP350$_{1-890(LSHAA)}$ (GST-CAP350$_{1-890(LSHAA)}$): contains a mutated N-terminal 890 amino acids of the CAP350 protein cloned to create an N-terminal fusion with GST. The mutation involved alanine substitutions of leucine residues of the LXXLL motif at positions 762 and 763 and was generated from pEYFP-CAP350$_{1-890}$ by site-directed mutagenesis (Patel *et al.* 2005).

7. pmRFP-C1: kind gift from Graczyk, J. (Dr. Truant lab, McMaster University); a eukaryotic expression vector that was made by PCR amplification

of the monomeric red fluorescent protein (mRFP) cDNA (Campbell *et al.* 2002) and insertion into pEGFP-C1 to replace EGFP with mRFP cDNA.

8. pRC/CMV-LXRα: contains a full length human LXRα cloned into MCS of pRC-CMV (Miyata *et al.* 1996).

9. pSG5-PPARα: contains a full length human PPARα cloned into the site of pSG5 (Patel *et al.* 2005).

10. pSG5-RXRα: contains a full length human RXRα cloned into the *Eco*RI site of pSG5 (Marcus *et al.* 1993).

11. pTK-LXRE-*Luc* (LXRE): contains 3 copies of the LXRE-ΔMTV DNA response element cloned into the *Hin*DIII site of TK-*luc* in a tandem repeat (Willy *et al.* 1995).

2.4.3   Plasmids Constructed for this Project:

1. pmRFP-PPARα: contains the N-terminal mRFP fusion protein with human PPARα, cloned using PCR amplification to create *Bam*HI ends on the PPARα cDNA, and insertion into the *Bam*HI site of pmRFP.

2. pmRFP-LXRα: contains the N-terminal mRFP fusion protein with human LXRα, cloned using PCR amplification to create *Bam*HI ends on the LXRα cDNA, and insertion into the *Bam*HI site of pmRFP.

3. pmRFP-RXRα: contains the N-terminal mRFP fusion protein with human RXRα, cloned using PCR amplification to create *Eco*RI ends on the RXRα cDNA, and insertion into the *Eco*RI site of pmRFP.

4.   pEGFP-RXRα: contains the N-terminal EGFP fusion protein with human RXRα, cloned using PCR amplification to create *Eco*RI ends on the RXRα cDNA, and insertion into the *Eco*RI site of pEGFP.

All plasmids constructed herein verified by DNA sequence analysis (MOBIX, McMaster University).

2.5   *Bacterial Strains and Growth Conditions:*

E. coli DH5α (American Type Culture Collection) were used in the growth and preparation of plasmid DNA used in these studies. Bacteria were grown at 37°C in 2YT (1.6% bactotryptone, 1% bacti-yeast, and 0.5% NaCl) that was supplemented with either 100 µg/mL ampicillin or 50 µg/mL kanamycin.

2.6   *Cloning of fluorescent fusion constructs:*

2.6.1   *Preparation of cDNA insert:*

The NR cDNA was amplified from their expression plasmids using PCR with oligonucleotide primers (shown above) that were designed to introduce a restriction site at each end of the cDNA that would enable insertion into the MCS of the fluorescent protein vector. In the case of PPARα, LXRα a *Bam*HI site was used while for and RXRα and *Eco*RI site was used. The PCR reaction was conducted using 30 cycles with 3 segments (Annealing at 94 °C for 30 s; melting at 60 °C for 30 s; synthesis at 72 °C for 2 min) and an extension reaction at 72 °C for 10 min. The enzyme used was Vent DNA polymerase (NEB) which is a high-fidelity thermophillic DNA polymerase.

The cDNA insert was purified from the PCR mix by precipitation in 0.25 M Sodium Acetate. Prior to ligation, the plasmid and insert were digested with appropriate restriction enzyme, dephosphorylated with CIP, purified on 1% agarose gel and extracted from the gel using the QIAEXII kit according to manufacturer's specification (Qiagen). The digested, dephosphorylated and purified plasmid and insert were ligated using T4 DNA ligase.

2.6.2   *Transformation of plasmid DNA into bacteria by heat shock:*

To introduce plasmids into bacteria, wildtype *E. coli* DH5α competent cells were made using Transformation buffer I (0.01 M RbCl, 0.05 M $MnCl_2 \cdot 4H_2O$, 0.03 M KCHO, 0.01 M $CaCl_2 \cdot 2H_2O$, 15%(w/v) glycerol, pH 5.8 with acetic acid) and Transformation buffer II (0.01 M MOPS pH 6.8, 0.013 M RbCl, 0.075 M $CaCl_2 \cdot 2H_2O$, 15%(w/v) glycerol). The heatm shock method was used to introduce potentially ligated plasmids into bacteria, 5 μL of the ligation mixture was incubated with 100 μL of competent cells at 4°C for 40 mins. The vessel was then incubated at 37°C for 30 seconds and then placed back at 4°C for 2 minutes. The cells were then incubated in 500 μL 2YT for 1 hour to permit the expression of the transformed plasmid. Cells were then streaked on 2YT-agar plates supplemented with kanamycin (50 μg/mL) and incubated at 37°C.

2.6.3   *Mini-Prep plasmid DNA purification:*

Potential positive clones are grown in order to extract a small amount of plasmid to check which colony contains the desired plasmid. An alkali-lysis method of extraction is used, in which the plasmid was extracted from 1.5 mL of pelleted bacterial culture, grown overnight at 37°C in 5 mL of 2YT supplemented with 50 μg/mL of kanamycin.

This pellet is resuspended in 200 μL of P1-RNase (50 mM Tris-Cl, 10 mM EDTA, 100 μg/mL RNase A, pH 8). The cell solution is lysed with 400 μL of P2 buffer (0.2 M NaOH and 1% SDS), and the proteins precipitated using 300 μL of 3 M potassium acetate. After pelleting the protein debris, the DNA is precipitated from the supernatant using 1 volume of 95% ethanol. The DNA is pelleted and washed with 70% ethanol. The pellet resuspended with 20 μL of H_2O following drying.

2.6.4   Digest Screen:

The extracted plasmid DNA from multiple potential positive clones, is screened using restriction enzymes to determine the size of and orientation of the insert.

For the mRFP-PPARα the plasmid was digested using *Bam*HI to determine the size of the insert (1428 bp), and the plasmid was digested with *Sac*I to determine the orientation; 913 bp correct, 603 bp incorrect.

For the mRFP-LXRα the plasmid was digested using *Bam*HI to determine the size of the insert (1362 bp), and the plasmid was digested with *Eco*RI to determine the orientation; 1040 bp correct, 384 bp incorrect.

For the mRFP-RXRα the plasmid was digested using *Eco*RI to determine the size of the insert (1401 bp), and the plasmid was digested with *Sac*I to determine the orientation; 188 bp correct, 1239 bp incorrect.

2.6.5   Maxi-Prep plasmid DNA purification:

Once the positive clone was established and the plasmid sequenced (MOBIX, McMaster University) and a large amount of plasmid was prepared. The method used for this involves Qiagen DNA purification columns (anionic silica-gel resin which interacts specifically with double stranded DNA), and an alkaline lysis procedure.

Briefly, a 50 mL starter culture was grown overnight from a single bacterial colony in 2YT and the appropriate antibiotic. The starter culture was used to inoculate 250 mL of 2YT supplemented with the appropriate antibiotic which was grown overnight. This culture was harvested and plasmid DNA was extracted and purified on Qiagen-tip 500 using the Qiagen plasmid maxi kit according to the manufacturer's instructions (Qiagen).

2.6.6   DNA quantification by fluorometry:

Plasmid DNA was quantified in a fluorometer (TBS-380 Turner Biosystems). All DNA were measured in 1X TNE solution supplemented with Hoescht 33528 dye relative to a calf thymus DNA standard (1 µg/µL).

2.7   Mammalian Cells growth and culture conditions:

HepG2 (HB-8065, ATCC) is a human hepatocellular carcinoma line. These cells were maintained in Eagle's Minimum Essential medium F15 (MEM-F15) supplemented with 1% non-essential amino acids, 1% sodium pyruvate, 1% penicillin/streptomycin, 1% L-glutamine, and 10% fetal bovine serum; and maintained at 37°C, 5% CO_2 and 99.9% humidity.

NIH/3T3 (CRL-1658 , ATCC) is a mouse embryonic fibroblast line. These cells were obtained from Dr. R. Truant's lab (McMaster University). NIH/3T3 (3T3) cells were maintained in Dulbeco's modified Eagle's medium (DMEM) supplemented with 1% penicillin/streptomycin, 1% L-glutamine, and 10% bovine calf serum; and maintained at 37°C, 5% CO_2 and 99.9% humidity.

2.8 *Western Blots Analysis:*

2.8.1 *Transfections to extract proteins for western blot analysis:*

Transient transfections were carried out to overexpress protein in mammalian cells. 3×10^5 NIH/3T3 cells were prepared on 6-well plates, while 3×10^6 HepG2 cells were plated on 6-well plates, prepared 16h prior to transfection. These transient transfections involved Lipofectamine transfection reagent (Invitrogen) for NIH/3T3 and FuGENE6 transfection reagent (Roche) for HepG2 cells, were carried out according to the manufacturer's instructions. Using Lipofectamine, briefly, 1 µg of the appropriate plasmid and 4 µL of Lipofectamine was used to make the Lipofectamine:DNA precipitate. Using FuGENE 2 µg of plasmid and 3 µL of FuGENE6 was used to make the FuGENE6:DNA precipitate. 48h post-transfection, 400 µL of 1X reporter lysis buffer (RLB; Promega) supplemented with mini-C protease inhibitors (Roche) was used to prepare the cell extracts. First the cells were washed once with 1X PBS, after removal of the 1X PBS, 1X RLB was added and the cells were scraped using a cell lifter. The cells were collected in a clean eppendorf tube, and the contents vortexed, and centrifuged at 12000 rpm at 4°C to collect the supernatant.

2.8.2 *Western blot:*

The supernatants were measured for protein content using the Bradford protein assay (BioRad) and equal amounts of protein was run on SDS-PAGE. Following transfer onto nitrocellulose membrane, conducted according to manufacturer's specifications (Amersham), the membrane was washed and probed with an appropriate primary antibody. Following a washing step to remove the excess primary antibody, an appropriate horse radish peroxidase conjugated secondary antibody was used to detect the primary antibody on the membrane. Following

another washing step to remove the secondary antibody, detection was carried using a detection kit according to manufacturer's specification (Amersham) was used to allow detection of the complex by exposure on an X-OMAT blue film (Kodak).

2.8.3   Antibodies:

Antibodies	Catalog #	Company	Dilution
Anti-PPARα	(H-98) Sc-9000 (Rabbit)	Santa Cruz	1/200
Anti-RXRα	(D-20) Sc-553 (Rabbit)	Santa Cruz	1/200
Anti-LXRα	2ZK8607L (mouse)	Perseus Proteomics	1/1000
Anti-eGFP	(Rabbit)	Affinity purified	1/2500
Anti-Rabbit HRP conjugated	NA934V	Amersham	1/5000
Anti-Mouse HRP conjugated	NA931	Amersham	1/5000

2.9   Transfection for functional study:

2.9.1   Transient transfection function study:

Transient transfection experiments involving HEPG2 cells were conducted using FuGENE 6 transfection reagent (Roche). The HEPG2 cells (3×10^6 cells/well in 6-well plates) were transfected with 3 μL of FuGENE 6, 1 μg reporter, 0.8 μg of the appropriate nuclear receptor combination, and 0.2 μg of pCMV-*LacZ*. These experiments included controls which replaced the nuclear receptors with empty vectors as indicated. At 5h the media was replaced with normal growth media and at 24h post-transfection, the media was replaced with the appropriate ligand-containing medium. Where indicated, TO-901317 (Sigma) was added to a final concentration of 1 μM from a stock solution prepared in DMSO; and 22-R-hydroxycholesterol was added to final concentration of 10 μM in 95% ethanol. Control cells received equal

amounts of vehicle. At 48h the cells are harvested by washing once in 1X PBS and lysing the cells in 400 μL 1X RLB (Promega). The cells were lifted into eppendorf tubes, and following vortexing, were centrifuged and the supernatant used for further analysis.

2.9.2   *Luciferase assay and β-galactosidase assay:*

The luciferase activity of the supernatants was measured using a Lumat LB 9507 (Berthold) according to the manufacturer's protocol. 20 μL of supernatant was used for measuring, to which was added 100 μL of luciferase assay buffer (470 μM firefly luciferin, 270 μM Coenzyme A, 530 μM ATP, 33.3 mM DTT, 20 mM Tricine, 1.07 mM $(MgCO_3)_4Mg(OH)_2 \cdot 5H_2O$, 2.67 mM $MgSO_4$, 0.1 mM EDTA). The luminometer measures luciferase activity based on light emission at 562 nm, and expresses this activity in relative light units (RLU).

The protein content of each sample was measured using both a Bradford Assay and β-gal assay. The Bradford assay involved taking 20 μL of lysate and adding to it 200 μL of 1X BioRad protein assay reagent (BioRad) and measuring the OD at 595 nm in a plate reader (Spectra max plus 384, Molecular Devices). Assessment of β-galactosidase activity was performed using a β-galactosidase assay (Ausubel, *et al*, 1994). 20 μL of lysate was added to 400 μL of β-galactosidase buffer (10 mM KCl, 1 mM $MgSO_4$, 100 mM sodium phosphate, 50 mM 2-mercaptoethanol, pH 7.5). To this was added 150 μL ONPG (4 mg/mL) dissolved in β-galactosidase buffer and the resultant mixture was incubated at 37°C until the solution turned to a yellow color determined to fit within a linear range of color detection for this experiment. The reaction was terminated using 200 μL of 1M $NaCO_3$ and 50 μL

isopropanol. The amount of product (*o*-nitrophenol) made in this reaction was detected spectrally at 420 nm (Cary 300 Bio UV spectrophotometer, Varian).

Luciferase activity was normalized to protein content and β-galactosidase activity by dividing the RLU by OD_{595} and OD_{420}. The average and standard deviations were calculated for each experiment by using values generated from three independent transfections for each test condition.

2.10   *GST-binding assay:*

2.10.1   Bacterial strains, growth conditions, and protein extraction:

GST-CAP350$_{1-890}$- and GST-CAP350$_{1-890(LSHAA)}$-transformed BL-21 cells (Patel *et al.* 2005) were used to overexpress the desired protein. Wildtype GST protein was overexpressed from a transformed DH5α strain. A 50 mL starter culture was grown overnight in 2YT supplemented with 100 µg/mL ampicillin at 37°C with agitation. The 50 mL culture was used to inoculate 500 mL of 2YT supplemented with 2% glucose and 100 µg/mL ampicillin. This was grown at 30°C with agitation for approximately 1-2 hrs until the OD_{600} reached between 0.6 and 1. After which the cells were induced with 0.1 mM IPTG for 1 hr.

2.10.2   Protein extraction:

The cells were pelleted and resuspended in 20 mL NETN (0.5% NP40, 1 mM EDTA, 20 mM Tris-Cl, 100 mM NaCl, pH 8.0) supplemented with mini-C protease inhibitors (Promega). The cells were lysed using a sonicator, 10X for 20 secs at 4°C, while keeping the cells at 4°C for 2 mins in between repetitions. The cells were centrifuged at 10000 rpm and store the supernatant in aliquots at -70°C.

2.10.3 In vitro translation and labeling with ^{35}S-Met:

In vitro transcription and translation were carried out using the TNT coupled system (Promega). This system allows for simultaneous transcription and translation of cDNAs within the same reaction mixture. The PPARα reaction mixture comprised of 25 µL TNT rabbit reticulocyte lysate, 2 µL of TNT reaction buffer, 1 µL T7 RNA polymerase, 2 µL of 1 mM amino acid mixture minus Met, 1 µL of RNAsin ribonuclease inhibitor (400 U/µL), 2 µg of cDNA-containing plasmid DNA, 6 µL ^{35}S-labelled Met and sterile water to a final volume of 50 µL. The LXRα reaction mixture comprised of 27.5 µL TNT rabbit reticulocyte lysate, 2 µL of TNT reaction buffer, 1 µL T7 RNA polymerase, 2 µL of 1 mM amino acid mixture minus Met, 1 µL of RNAsin ribonuclease inhibitor (400 U/µL), 1 µg of cDNA-containing plasmid DNA, 6 µL ^{35}S-labelled Met and sterile water to a final volume of 50 µL. The mixture was incubated at 30°C for 1.5 hrs, and the translated product analyzed by SDS-PAGE.

2.10.4 GST-binding:

The extracted protein was immobilized using Glutathione sepharose 4B beads (Amersham). 50 µL of beads were equilibrated with NETN buffer, and incubated with 1 mL of protein extract for 1.5 hr at 4°C. The beads were then washed twice with NETN buffer and once with 1X PBS. The beads were then equilibrated with IPAB buffer (150 mM KCl, 0.1% TX-100, 0.1% NP40, 5 mM MgCl$_2$, 20 mM Hepes, pH 7.9) supplemented with 0.02 mg/mL BSA, and mini-c protease inhibitors (Promega). 5 µL of the *in vitro* translated NRs labeled with ^{35}S-Met were incubated with immobilized protein in a 250 µL reaction for 2 hrs at 4°C. The immobilized protein was then washed 8 times with IPAB buffer at 25°C.

The immobilized protein complex bound to the desired receptor was then denatured using 6X SDS loading buffer and boiling. The beads were destroyed by a high speed spin and the protein was analyzed on 10% SDS-PAGE, which was dried and exposed on a storage phosphor screen and developed in a phosphor imager (Typhoon, Amersham Pharmacia biotech).

2.11   Imaging:

NIH/3T3 cells were used for all the imaging studies. The cells for imaging were grown in 35-mm plates that were altered to have a glass-cover-slip bottom to ensure improved visualization in the microscope. These plates were sterilized by UV-exposure while immersed in 70% ethanol for at least 8 hrs. The plates are allowed to dry while exposed to UV, and rinsed three times with 1X PBS prior to use. 3×10^5 cells were plated on the 35-mm glass-cover slip plates and grown overnight. For imaging the cells were transfected using ExGen 500 transfection reagent (Fermentas), according to the manufacturer's specifications. The cells were transfected with 3 µg of the appropriate DNA combination and 10 µL ExGen 500. The cells are grown for 24h or 48h prior to viewing in the microscope. To delineate the location of the nucleus, DNA was stained with Hoescht dye which was added to the media 20 min prior to the experiment, and washed out with new media.

Live-cell fluorescence microscopy was conducted with a Nikon TE200 inverted microscope equipped with a 175W xenon arc lamp (Sutter Instruments LB-LS/17), using Nikon 100X plan apochromat objective (numerical apertures 1.3). Filter sets (Chroma) denoting bandpass excitation and emission filters for each fluorescent protein or dye used are as follows.

Fluorescent protein or dye	Set	Excitation	Emission
mRFP	31004	D560/50x	D630/60m
eYFP	31040	D480/30x	D535/40m
eGFP	41017	D470/40x	D525/50x
Hoescht dye	31000	D360/40x	D460/50m

Images were collected using a monochrome camera, which captured images in each channel separately using a Hamamatsu Orca high resolution digital camera and controller (model C4742-95 Hamamatsu Photonics). Control of instruments, merging and pseudocoloring of the unbinned mages was done using Simple PCI version 5.2.0.2404 (Compix) software. LSM 510 image browser (Carl Zeiss), and CorelDRAW graphics suite 12 (Corel Corporation) was used to sharpen and adjust brightness and contrast of the images.

RESULTS

3.1   *Characterization of fluorescent protein constructs*

In order to study the localization of nuclear receptors in the live cell, fluorescent protein chimeras with PPARα, LXRα, and RXRα were constructed. To determine the utility of these constructs as models for the wildtype receptors, the expression of the construct was examined by western blot, and visualized by fluorescent microscopy. The retention of functional ability of the construct to transactivate at an HRE reporter gene, in comparison to wildtype was also examined.

3.1.1   *mRFP-hPPARα characterization:*

An N-terminal mRFP fusion protein was constructed by inserting the human PPARα cDNA into the *Bam*HI site of the MCS of pmRFP. The plasmid was confirmed by sequencing (MOBIX, McMaster University) and encodes for an N-terminal fusion protein with human PPARα (schematic representation shown in figure 6A). In order to determine whether the mRFP-hPPARα construct could be used as a model for studying hPPARα localization in a cell, its expression was characterized. The mRFP-hPPARα fusion protein and hPPARα were over-expressed in mouse embryonic fibroblasts (NIH/3T3) and following extraction, western blot analysis was performed using anti-PPARα antibody (Santa Cruz) with the result shown in figure 6B. Over-expressed hPPARα is detected at an approximate size of 55 kDa as expected (Bordji *et al.* 2000). The mRFP-hPPARα fusion protein is expected to be approximately 85 kDa which includes the mRFP moiety being 30 kDa (Clontech). The western blot analysis confirms the presence of an ~90 kDa mRFP-PPARα. The intensity of the bands are similar and indicate that the expression level of hPPARα is similar to the

level shown by the mRFP-PPARα. This indicates that the mRFP protein is expressed with hPPARα as a fusion protein in NIH/3T3 cells.

To determine if the construct can be utilized for live cell fluorescent analysis, it was transiently transfected into NIH/3T3 cells and viewed under fluorescent microscope. Figure 6C shows a representative cell that is transfected with mRFP-PPARα and stained with Hoescht. The Hoescht stains the DNA to outline the boundary of the nucleus. The construct gives a red signal that is detected after approximately 12 hours and is localized predominantly in the nucleus and is not detected in the nucleoli, which is expected for PPARα. The ability of this construct to retain its transactivation ability using a PPRE luciferase linked reporter plasmid was not compared to that of PPARα. However this construct was used in the CAP350 localization study that determined that CAP350 redirects the intranuclear and intracellular distribution of PPARα to inhibit PPARα activity (Patel *et al*. 2005).
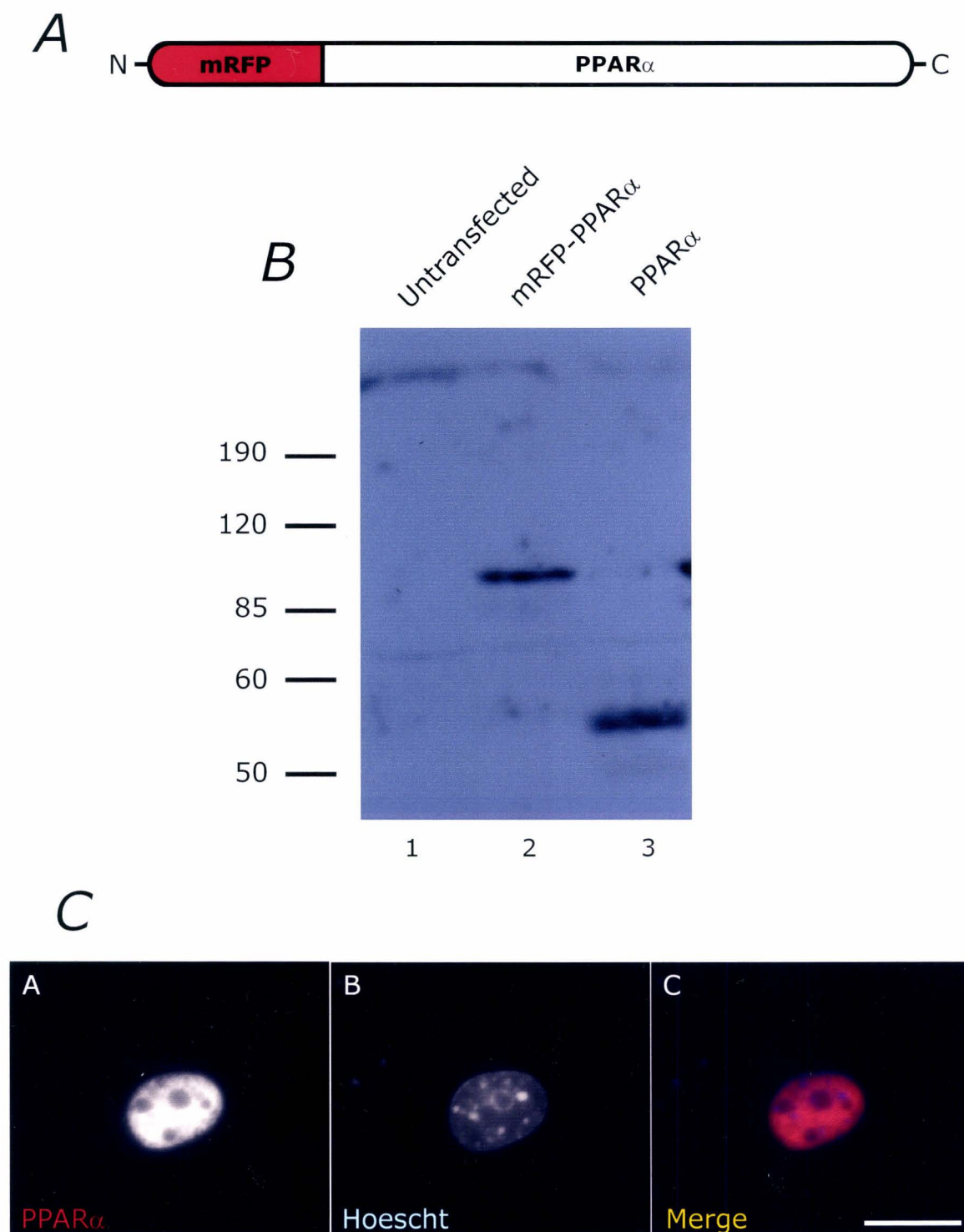
Figure 6. Characterization of mRFP-PPARα construct.

Figure 6. Characterization of mRFP-hPPARα construct.

A, Shematic representation of the mRFP-PPARα construct showing the position of the mRFP (in red) at the N-terminal.

B, mRFP-PPARα expresses to a smilar level as wildtype PPARα in NIH/3T3 cells, and expresses to a size of approximately 90 kDa indicating the presence of a ~30 kDa mRFP tag. 1 µg mRFP-hPPARα and hPPARα were transiently transfected using Lipofectamine transfection reagent in NIH/3T3 cells and the protein was extracted using 1X RLB (Promega) supplemented with mini-C protease inhibitors (Roche). Equal amount of protein extract was run on 10% SDS-PAGE as determined by Bradford protein assay and transferred onto nitrocellulose membrane according to manufacturer's specifications (Amersham). A rabbit anti-PPARα antibody (Santa Cruz) diluted 1/200 in 1% blocking solution. Lane 1. Untransfected cell extract; Lane 2. MRFP-PPARα transfected cell extract; Lane 3. PPARα transfected cell extract. Molecular masses are labeled in kDa.

C, Representative live-fluorescence image of mRFP-PPARα transfected in NIH/3T3 cells. mRFP-PPARα expression is predominantly nuclear in NIH/3T3 cells, while no expression is detected in the nucleoli (Panels A-C). 1 µg of mRFP-PPARα was transfected into NIH/3T3 cells using ExGen500 transfection reagent (Fermentas). 24h post-transfection the cells were viewed under fluorescent microscope. Panel A, shows the mRFP-PPARα viewed in the red channel; Panel B shows the Hoescht staining of DNA to represent the nucleus viewed in the blue channel; Panel C is the merged image in which shows that PPARα expression is predominantly nuclear. Bar represents approximately 10 µm.

3.1.2 mRFP-hLXRα characterization:

An N-terminal mRFP fusion protein was constructed by inserting human LXRα cDNA into the BamHI site of the MCS of pmRFP. The plasmid was sequenced (MOBIX, McMaster University) and encodes an N-terminal fusion protein with human LXRα (schematic representation shown in figure 7A). In order to determine whether the mRFP-LXRα construct could be used as a model for studying LXRα localization in a cell, its expression and functional ability was characterized. The mRFP-LXRα and LXRα plasmids were over-expressed in hepatocellular carcinoma cells (HepG2) and following extraction of the protein, western blot analysis was performed using a mouse monoclonal antibody directed toward hLXRα (Watanabe et al. 2003; Perseus Proteomics). 2 μg of hLXRα and mRFP-hLXRα were transiently transfected in HepG2 cells. Protein extract was obtained 48 hrs post-transfection and equal amounts run on 10% SDS-PAGE. Figure 7B shows that hLXRα was detected at ~50 kDa, and mRFP-LXRα at ~85 kDa, indicating the presence of the mRFP moiety. The intensity of the bands is similar and indicates that the expression level of mRFP-LXRα is comparable to the level shown by LXRα. Thus their expression in HepG2 cells appears to be similar and produces the desired protein.

To determine if the mRFP-LXRα construct can be utilized for live cell fluorescent analysis, it was transiently transfected into NIH/3T3 cells and viewed under fluorescent microscope. Figure 7C shows a representative cell transfected with the construct. mRFP-LXRα is monitored in the red channel and is detected post-transfection after approximately 12 hrs. A predominantly diffuse nuclear localization is exhibited by mRFP-LXRα and is not detected in the nucleoli, which is expected for LXRα.

The ability of mRFP-hLXRα to mediate the induction of an LXRE-linked luciferase reporter gene is compared with that of the wildtype hLXRα to understand whether any functional differences exist as a result of the fusion with mRFP. This transient transfection assay involves the cotransfection of LXRα, an LXRE-luciferase reporter plasmid, and pCMV-*lacZ* to control for transfection efficiency. 24 hrs following transfection into HepG2 cells, the cells were treated with either 1 µM TO-901317 dissolved in DMSO (Sigma) or DMSO vehicle. Following extraction the luciferase activity was measured, along with the protein content and β-galactosidase activity. The pattern of induction for the mRFP-LXRα construct was determined to be similar to that seen for LXRα (Figure 8). There is a slight decrease in ligand independent activation from 11-fold for LXRα to 10-fold for mRFP-LXRα compared to baseline. The ligand dependant activation also shows a decrease from 27-fold for LXRα to 22-fold for mRFP-LXRα compared to baseline. Thus the transactivation ability and ligand dependency of LXRα function is retained in the mRFP-LXRα construct but decreases slightly with the addition of the mRFP moiety. Along with the ability to view this construct in the live cell fluorescence microscope and the appropriate expression compared to LXRα, the mRFP-LXRα can be used as a model to study the cellular localization of LXRα.
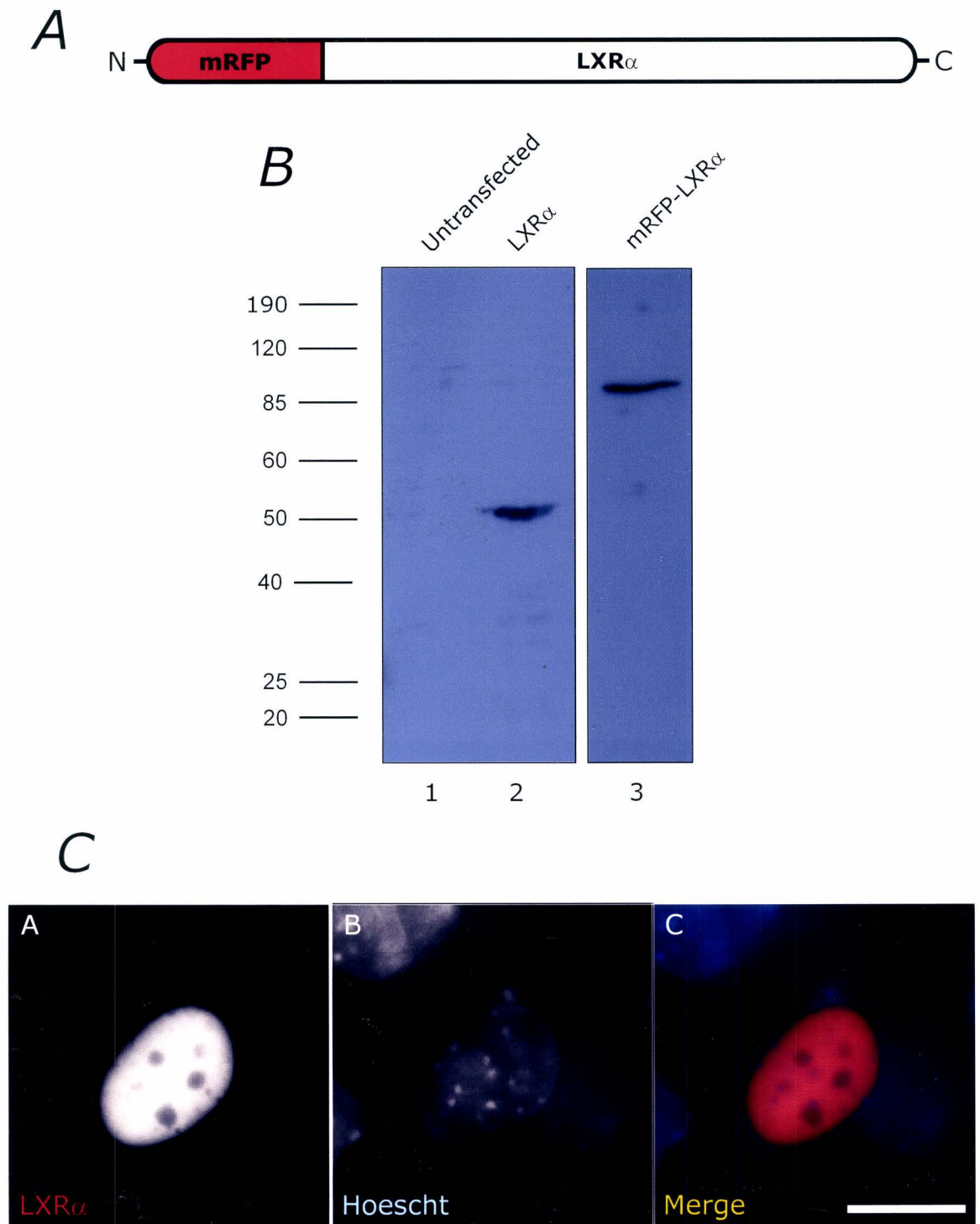
Figure 7. Characterization of mRFP-LXRα **construct.**

Figure 7. Characterization of mRFP-LXR construct.

A, Shematic representation of the mRFP-LXRα construct showing the position of the mRFP (in red) at the N-terminal.

B, mRFP-LXRα expresses to a similar level as wildtype LXRα in HepG2 cells, and expresses to the predicted size of ~85 kDa that indicates the presence of the mRFP tag. 2 μg of mRFP-LXRα and LXRα were transiently transfected using FuGENE6 transfection reagent (Roche) in HepG2 cells and the protein was extracted using 1X RLB (Promega) supplemented win mini-C protease inhibitors (Roche). Equal amounts of protein extract as determined by Bradford assay (BioRad) was run on 10% SDS-PAGE and transferred onto nitrocellulose membrane according to manufacturer's specifications (Amersham). A mouse anti-LXRα monoclonal antibody (Perseus Proteomics) diluted 1/1000 in 1% blocking solution. Lane 1. Untransfected cell extract; Lane 2. hLXRα transfected cell extract; Lane 3. mRFP-LXRα transfected cell extract. Molecular masses are labeled in kDa.

C, Representative live-cell fluorescence image of mRFP-LXRα expressed in NIH/3T3 cells. mRFP-LXRα displays a predominantly nuclear localization, while no expression is detected in the nucleoli (Panels A-C). 1 μg of mRFP-LXRα was transiently transfected into NIH/3T3 cells using ExGen500 transfection reagent (Fermentas). 24h post-transfection the cells were viewed under fluorescent microscope. Panel A, shows the mRFP-LXRα viewed in the red channel; Panel B, shows the Hoescht staining of DNA to represent the boundary of the nucleus viewed in the blue channel; Panel, C. is the merged image which shows that LXRα expression is predominantly nuclear. Bar represents approximately 10 μm.

pSG5	+	+	+	+
pRC-CMV	+			
mRFP		+		
LXRα			+	
mRFP-LXRα				+
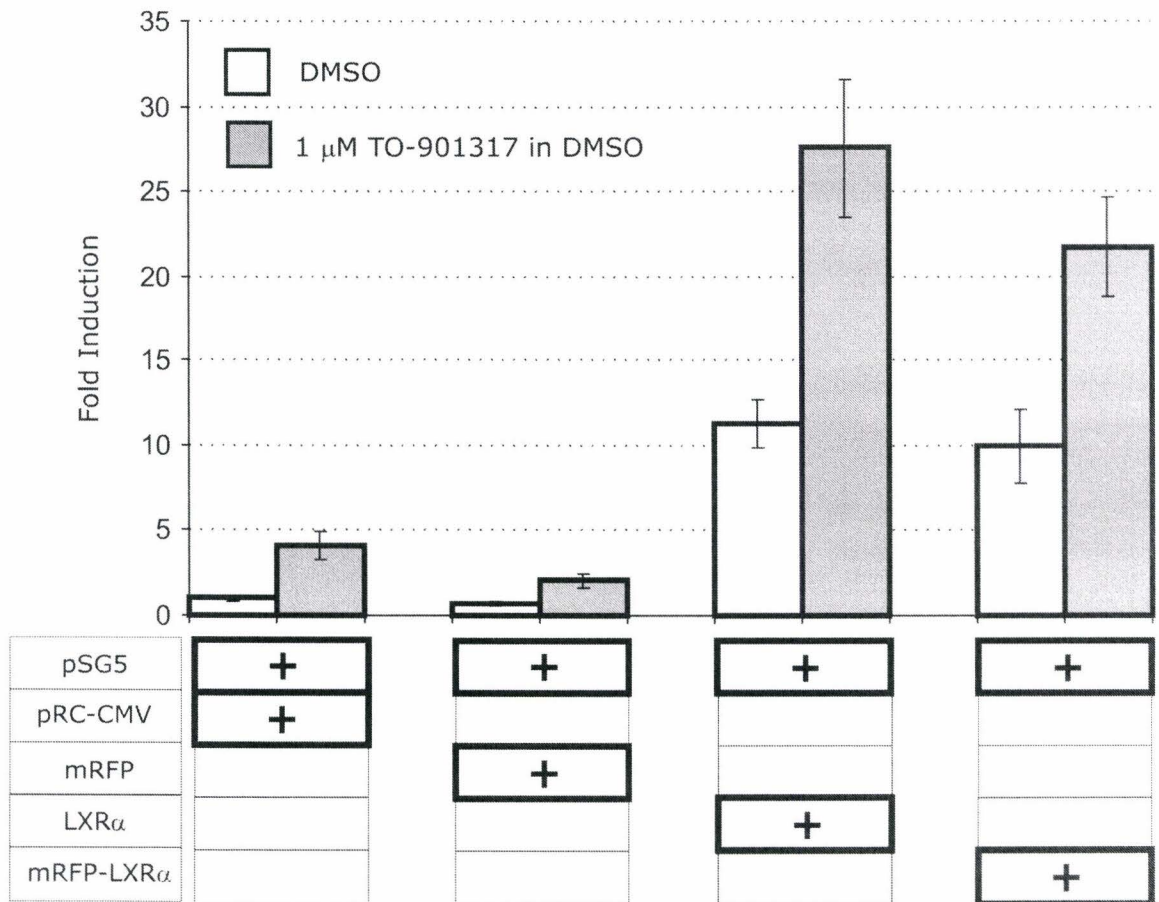
Figure 8. mRFP-LXRα **retains LXR**α **function.**

Figure 8. mRFP-LXR*α* retains LXR*α* function.

Transient transfection assays are used to compare the transcriptional activity of mRFP-LXRα to that of LXRα at an LXRE-luciferase reporter. This shows that the mRFP-LXRα retains the transactivation ability and ligand dependence of LXRα function. HepG2 cells were transfected using FuGENE (Roche) transfection reagent with the appropriate DNA combinations as above. Breifly, 1 μg of of LXRE luciferase reporter plasmid, along with 0.4 μg NR, and 0.2 μg pCMV-lacZ were cotransfected. The experiment was performed in triplicate in the presence or absence of 1 μM TO-901317 in DMSO. The lysates were assayed for luciferase activity in relative light units (RLU) and normalized for protein content using β-galactosidase and Bradford assay (BioRad). The data shown is the average of the 3 independent trials each involving triplicates of each case.

3.1.3   eGFP-hRXRα characterization:

An N-terminal eGFP fusion protein was constructed by inserting human RXRα cDNA into the *Eco*RI site of the MCS of pEGFP-C1. The plasmid was sequenced (MOBIX, McMaster University) and encodes for an N-terminal fusion protein with human RXRα (schematic representation shown in figure 9A). In order to determine whether the eGFP-RXRα construct could be used as a model for studying RXRα localization in a cell, its expression and functional ability was characterized. eGFP-RXRα and RXRα were over-expressed in NIH/3T3 cells and compared using western blot analysis involving an anti-RXRα antibody (Santa Cruz). eGFP-RXRα contains the RXRα moiety and is approximately 85 kDa (figure 9B), while the wildtype hRXRα protein was detected at 55 kDa as expected (Murata *et al.* 1998). The RXRα and eGFP-hRXRα are also detected to be expressed to similar levels. Using an anti-eGFP antibody the eGFP moiety is detected in the eGFP-RXRα construct and displays a size of approximately 85 kDa (figure 9C), while the over-expressed native eGFP is detected as a 30 kDa protein as expected (Tsien R., 1998). Therefore, these results indicate that the eGFP protein is expressed with hRXRα as a fusion protein in NIH/3T3 cells with the approximate mass of 85 kDa.

The eGFP-RXRα construct can be utilized for live cell fluorescent analysis following transient transfection into NIH/3T3 cells and viewing under fluorescent microscope. Figure 9D shows a representative cell transfected with the construct. eGFP-RXRα can be monitored in the green channel, detected at approximately 18 hrs post-transfection. eGFP-RXRα is localized predominantly in the nucleus in a diffuse distribution and is not detected in the nucleoli, which is expected for RXRα.

The ability of eGFP-RXRα to mediate induction with LXRα at an LXRE-luciferase receptor was compared to that of wildtype RXRα, to understand whether

any functional differences exist as a result of the fusion with eGFP. This transient transfection assay involves the cotransfection of LXRα, RXRα, an LXRE-luciferase reporter plasmid, and pCMV-*lacZ* to control for transfection efficiency. 24 hrs following transfection into HepG2 cells, the cells were treated with either 10 μM 22-R-hydroxycholesterol (Sigma) dissolved in 95% ethanol or vehicle. Following extraction the luciferase activity was measured, along with the protein content and β-galactosidase activity. The pattern of induction for the eGFP-RXRα construct was determined to be similar to that for observed RXRα (Figure 10). The induction levels are decreased relative to the wildtype RXRα, an approximately 20-fold induction of LXR activity independent of ligand is observed in the presence of RXRα, while only a 7-fold induction is observed in the presence of eGFP-RXRα. In the presence of ligand, a 30-fold increase LXR activity in the presence of RXRα, while a 15-fold increase is observed for the eGFP-RXRα. Therefore the addition of the eGFP moiety to hRXRα decreased the overall activity at this LXRE approximately 3-fold compared to hLXRα; however the pattern of induction in the presence and absence of 22R-OH-CH is very similar. Indicating that the addition of the eGFP maintains the ability of hRXRα to increase LXR-activity at an LXRE, and maintain responsiveness of LXRα to 22-R-hydroxycholesterol. Thus the eGFP-RXRα construct can be used as model to study the cellular localization for RXRα.
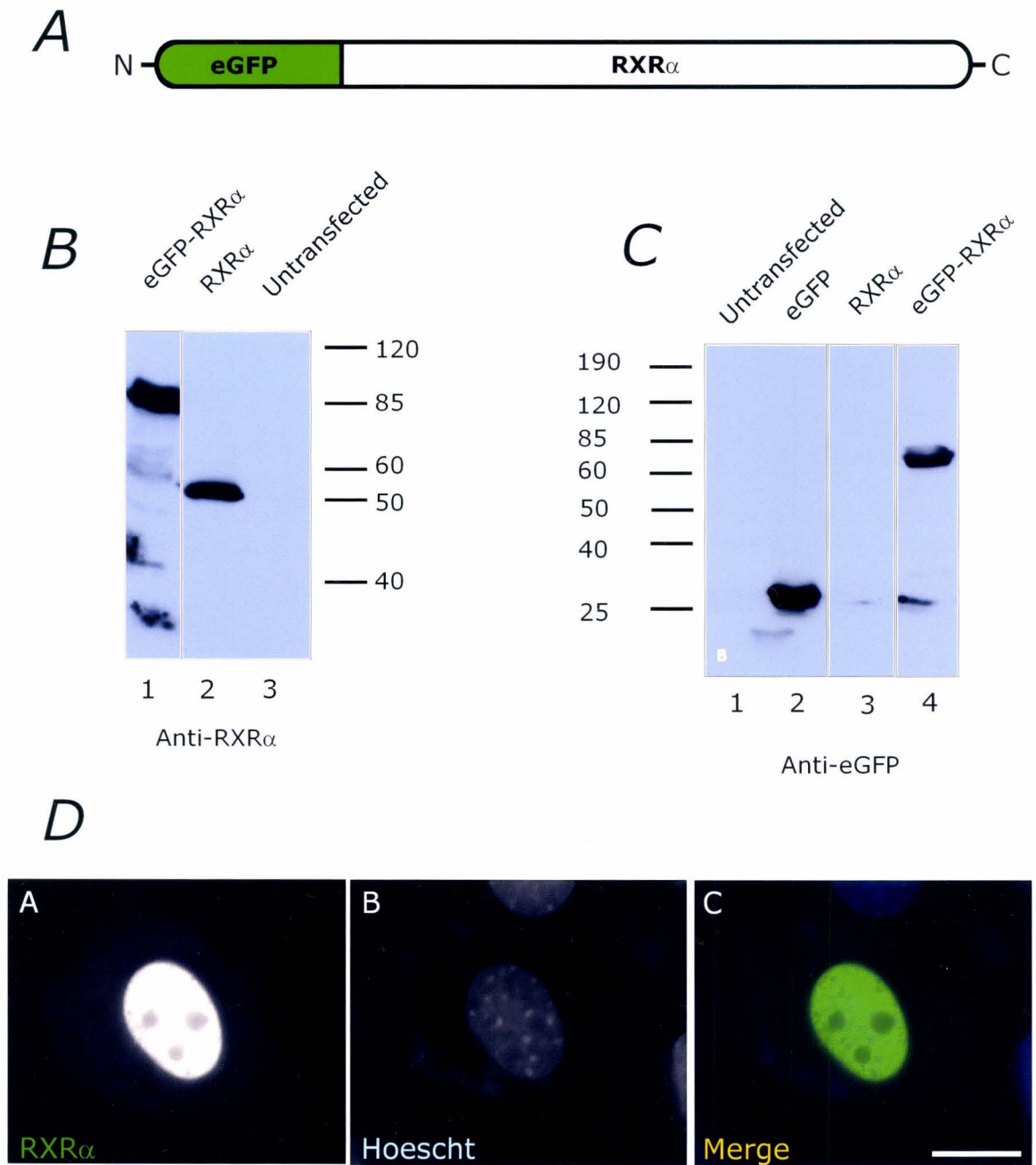
Figure 9. Characterization of eGFP-RXRα construct.

Figure 9. Characterization of eGFP-RXRα construct.

A, Shematic representation of the eGFP-RXRα construct showing the position of the eGFP (in green) at the N-terminal.

B-C, eGFPLXRα expresses to a similar level as wildtype RXRα in NIH/3T3 cells, and expresses to the predicted size of ~85 kDa that indicates the presence of the eGFP tag. 1 μg of eGFP-RXRα, eGFP and RXRα were transiently transfected in NIH/3T3 cells and the protein was extracted using 1X RLB (Promega) and supplemented with mini-C protease inhibitors (Roche). Equal amounts of protein extract, as determined by Bradford assay (BioRad), was run on 7.5% SDS-PAGE and transferred onto nitrocellulose membrane according to manufacturer's specifications (Amersham). Molecular masses are labeled in kDa.

B, a rabbit anti-RXRα antibody (Santa Cruz) diluted 1/200 in 1% blocking solution was used for detection. Lane 1, eGFP-RXRα transfected cell extract; Lane 2, RXRα transfected cell extract; Lane 3, Untransfected cell extract.

C, a rabbit anti-GFP antibody (affinity purified) diluted 1/2500 in 1% blocking solution was used for detection. Lane 1. Untransfected cell extract; Lane 2. eGFP transfected cell extract; Lane 3, RXRα transfected cell extract; Lane 4. EGFP-RXRα transfected cell extract.

D, representative live-cell fluorescence image of eGFP-RXRα expressed in NIH/3T3 cells. EGFP-RXRα displays predominantly nuclear localization, while no expression is evident in the nucleoli (Panels A-C). 1 μg of eGFP-RXRα was transiently transfected into NIH/3T3 cells using ExGen500 transfection reagnt (Fermentas). 24h post-transfection the cells were viewed using fluorescent microsope. Panel A, shows the eGFP-RXRα viewed in the green channel; Panel B, shows the Hoescht staining of DNA to represent the boundary of the nucleus viewed in the blue

channel; Panel C, is the merged image which shows that RXRα is contained within the nuclear boundary and is this predominantly nuclear. Bar represents approximately 10 µm.
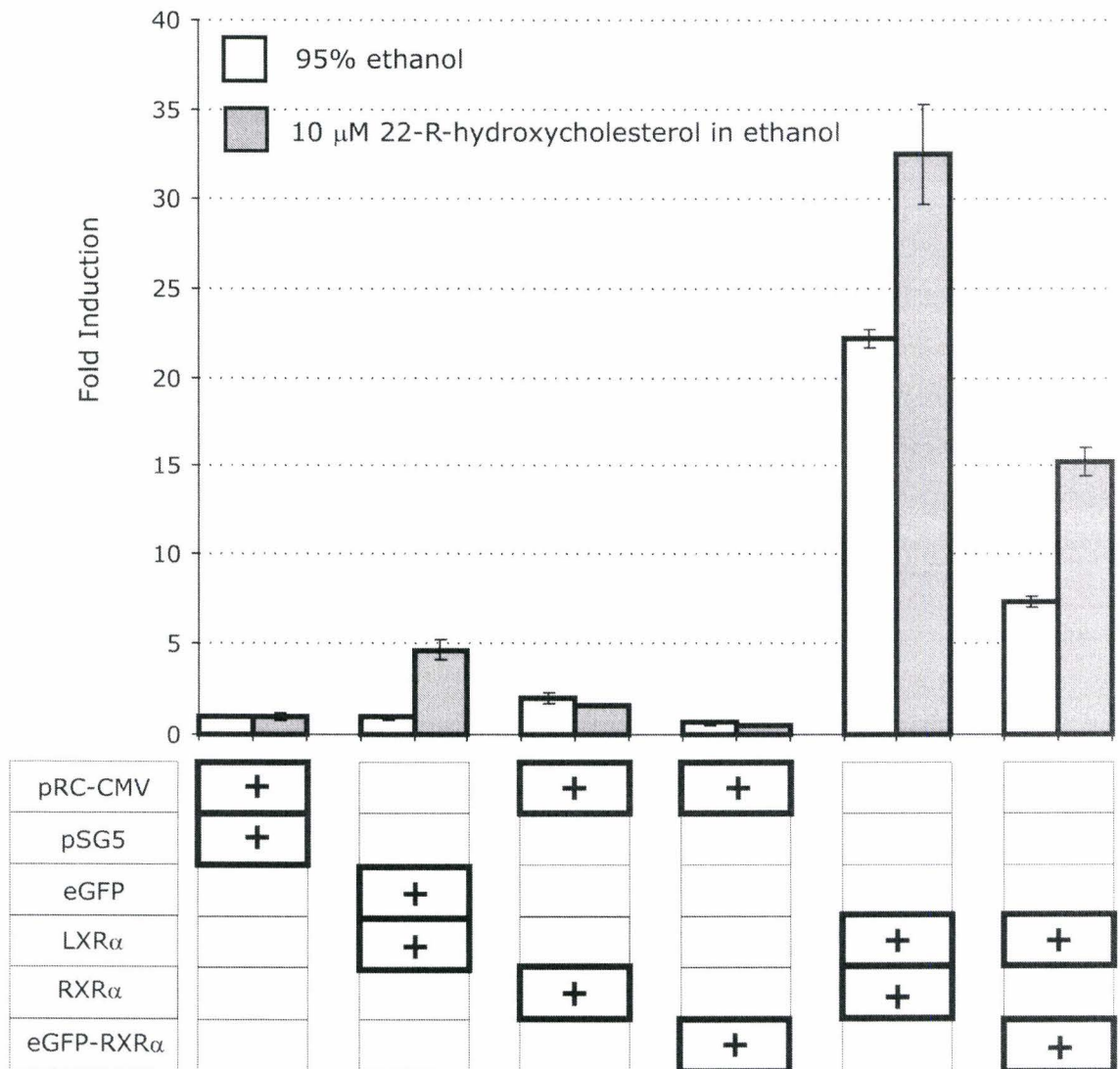
Figure 10. EGFP-RXRα **retains function.**

Figure 10. eGFP-RXRα retains RXRα function.

Transient transfection assays are used to compare the transcriptional activity of eGFP-RXRα to that of RXRα at an LXRE-luciferase reporter. The transcription induction pattern influence by eGFP-RXR is similar but lower than the pattern exhibited by RXRα. EGFP-RXRα also maintain the ligand inducibility of LXRα also to a lower level than RXRα. This shows that eGFP-RXRα retains the function of RXRα despite the presence of the eGFP moiety and the lower induction levels. HepG2 cells were transfected with the appropriate DNA combinations as above. Briefly, 1 µg of LXRE luciferase reporter plasmid, along with 0.4 µg NR combination, and 0.2 µg pCMV-lacZ were cotransfected. The experiment was performed in triplicate in the presence or absence of 10 µM 22-R-hydroxycholesterol in 95% ethanol. The lysates were assayed for luciferase activity in relative light units (RLU) and normalized for protein content using β-galactosidase and Bradford assay (BioRad). The data shown is the average of the 1 independent trial involving triplicates of each case.

3.1.4   mRFP-hRXRα characterization:

An N-terminal mRFP fusion protein was constructed by inserting human RXRα cDNA into the *Eco*RI site of the MCS of pmRFP. The plasmid was sequenced (MOBIX, McMaster University) and encodes for an N-terminal fusion protein with human RXRα (schematic representation shown in figure 11A). In order to determine whether the mRFP-RXRα construct could be used as a model for studying RXRα localization in a cell, its expression and functional ability was characterized. mRFP-RXRα and RXRα were over-expressed in NIH/3T3 cells and compared following western blot analysis involving an anti-RXRα antibody (Santa Cruz). mRFP-RXRα contains the RXRα moiety and is approximately 90 kDa (Figure 11B, while hRXRα was detected at 55 kDa as expected (Murata *et al.* 1998). The RXRα is expressed to a slightly higher level than the mRFP-RXRα. Therefore, these results indicate that the mRFP protein is expressed with hRXRα as a fusion protein in NIH/3T3 cells with the approximate mass of 80 kDa.

The mRFP-RXRα construct can be utilized for live cell fluorescent analysis following transient transfection into NIH/3T3 cells and viewing under fluorescent microscope. Figure 11C shows a representative cell transfected with the construct. mRFP-RXRα can be monitored in the red channel and is localized predominantly in the nucleus with a diffuse distribution and is not detected in the nucleoli, as is expected for RXRα. Thus the mRFP-hRXRα construct can be employed to monitor hRXRα *in vivo*. However, the effect of the mRFP moiety on the function with respect to hRXRα, has not been determined and is expected to be similar to the function shown by eGFP-RXRα above.
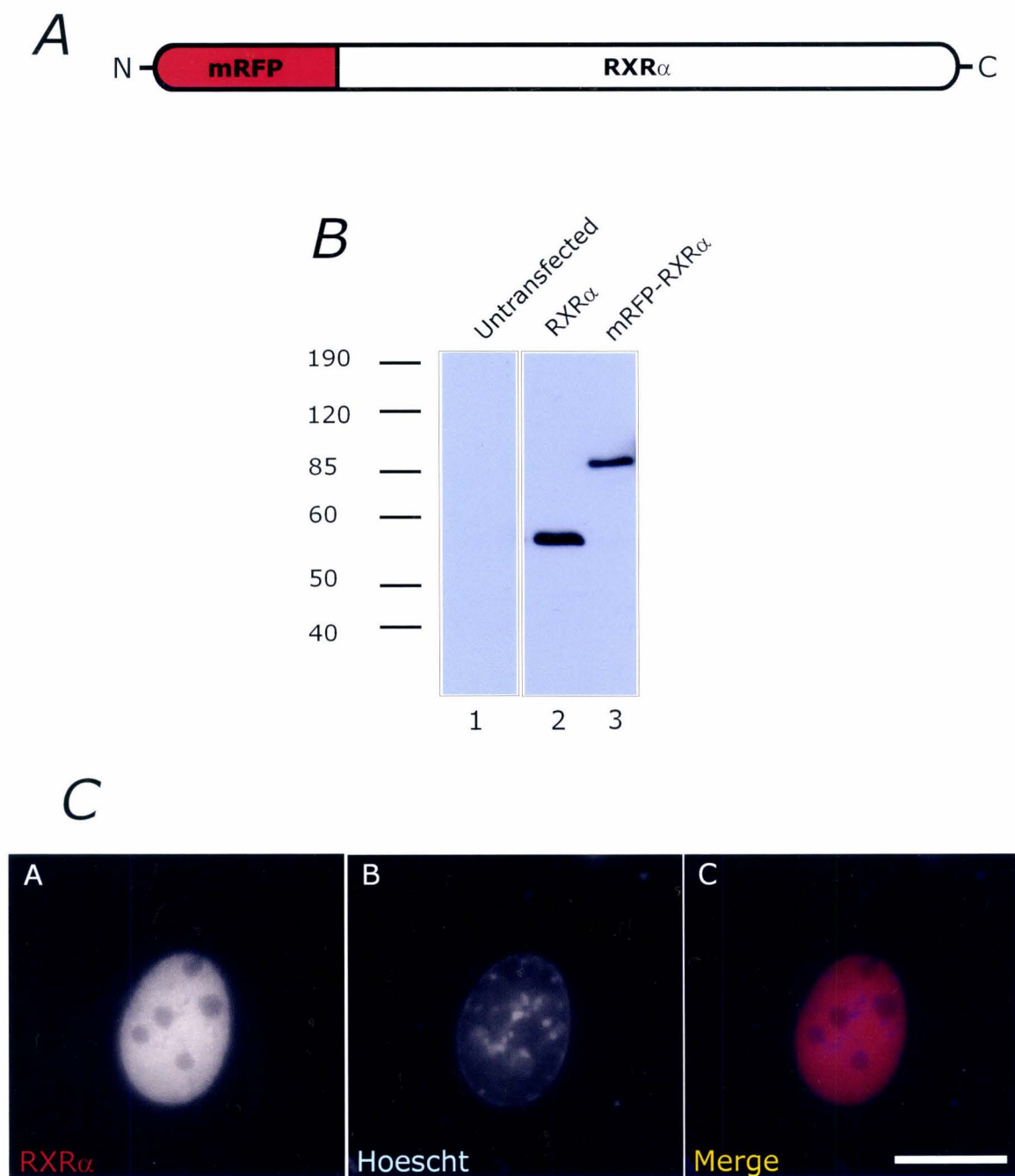
Figure 11. Characterization of mRFP-RXRα construct.

Figure 11. Characterization of mRFP-RXRα construct.

A, Shematic representation of the mRFP-RXRα construct showing the position of the mRFP (in red) at the N-terminal.

B, mRFP-RXRα expresses to a slightly lower level than the wildtype RXRα in NIH/3T3, and expresses to the predicted size of ~90 kDa that indicates the presence of the mRFP tag. 1 μg of mRFP-RXRα, and RXRα were transiently transfected in NIH/3T3 cells and the protein was extracted using 1X RLB (Promega) supplemented with mini-C protease inibitor (Roche). Equal amounts of protein extract, as determined by Bradford assay (BioRad), was run on 7.5% SDS-PAGE and transferred onto nitrocellulose membrane according to manufacturer's specifications (Amersham). A rabbit anti-RXRα antibody (Santa Cruz) diluted 1/200 in 1% blocking solution was used for detections. Lane 1, untransfected cell extract. Lane 2, RXRα transfected cell extract; Lane 3, mRFP-RXRα transfected cell extract. Molecular masses are labeled in kDa.

C, representative live-cell fluorescence image of mRFP-RXRα expressed in NIH/3T3 cells. mRFP-RXRα displays a predominantly nuclear localization, while no expression is detected in the nucleoli (Panels A-C). 1 μg of mRFP-RXRα was transiently transfected into NIH/3T3 cells using ExGen5000 transfection reagent (Fermentas). 24h post-transfection the cells were viewed using fluorescent microscope. Panel A, shows the mRFP-RXRα viewed in the red channel; Panel B, shows the Hoescht staining of DNA to represent the boundary of the nucleus viewed in the blue channe; Panel C, is the merged image which shows that RXRα is contained within the nuclear boundary and is predominantly nuclear. The bar represents approximately 10 μm.

3.2   CAP350$_{1-890}$ interacts with nuclear receptors

CAP350 was identified in a yeast 2-hybrid experiment to interact with PPARα. The protein sequence indicates the presence of an LXXLL motif that is known to interact with transcription factors. The protein sequence also indicates the presence of a CAP-Gly domain which indicates possible cytoskeletal interaction ability, leading to the idea that CAP350 may have a function in the organizational or subcellular compartmentalization of nuclear receptors. To determine if the LXXLL motif of CAP350 can interact with LXRα a GST-binding experiment was designed, and showed that an N-terminal fragment can interact with PPARα (Patel *et al.* 2005). The GST-fusion N-terminal fragment of CAP350 (GST-CAP350), was over-expressed in bacteria and extracted using sonication. Using this procedure to extract the protein is known to produce extensive breakdown products. The extracted protein was immobilized on glutathione sepharose 4B beads (Amersham) and the content of the immobilized protein was analyzed on 10% SDS-PAGE with the result shown in Appendix 1. This confirms the expression and immobilization of the GST-CAP350 constructs, and shows the presence of breakdown products. This protein was then used for pull-down assays with *in vitro* translated NRs.

3.2.1   CAP350$_{1-890}$ and CAP350$_{1-890(LSHAA)}$ interacts with hPPARα:

It was previously shown that the N-terminal fragment of CAP350 (GST-CAP350$_{1-890}$) can interact with PPARα as determined in a GST-pull down assay employing a bacterially synthesized GST-CAP350$_{1-890}$ (CAP350$_{1-890}$) and *in vitro* synthesized PPARα radiolabeled with L-[^{35}S]Met (Patel *et al.* 2005). This experiment was repeated to confirm the result. In this experiment GST-CAP350$_{1-890}$ and GST-CAP350$_{1-890(LSHAA)}$ were immobilized on glutatione sepharose 4B beads (Amersham), and incubated with

in vitro translated and L-[^{35}S]Met-labelled PPARα. Following the incubation a series of washes to collect unbound material was conducted followed by denaturation to release the bound protein complexes. This was analyzed on 10% SDS-PAGE. It was confirmed that PPARα interacts *in vitro* with the N-terminal CAP350 (Figure 12), and that mutation of the LXXLL motif from LSHLL to LSHAA does not seem to affect this interaction *in vitro*. Using a Phosphor Imager (Typhoon, GE Healthcare) for quantification of the bands the data shows that approximately 1% of the input L[^{35}S]Met-PPARα interacts with each CAP350$_{1-890}$ construct *in vitro*.
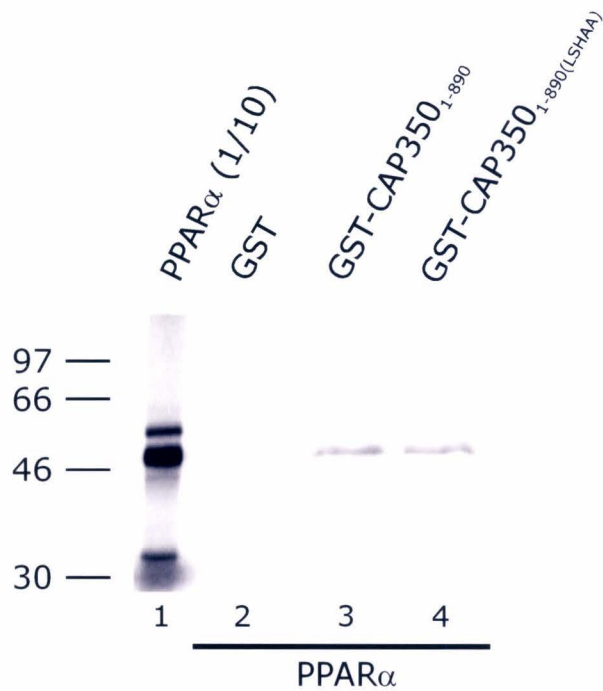
Band	Percent of Input
GST	0.06
GST-CAP350$_{1\text{-}890}$	1.1
GST-CAP350$_{1\text{-}890(LSHAA)}$	1.1

Figure 12. hPPARα interacts with CAP350$_{1\text{-}890}$ *in vitro*.

Figure 12. PPARα interacts with CAP350$_{1-890}$ in vitro.

PPARα interacts with CAP350$_{1-890}$ and CAP350$_{1-890(LSHAA)}$ in vitro. Bacterial synthesized CAP350$_{1-890}$ and CAP350$_{1-890(LSHAA)}$ was immobilized on glutathione sepharose 4B beads (Amersham) and incubated in vitro synthesized L-[^{35}S]Met-labelled PPARα. Bound radiolabeled proteins were analyzed on 10% SDS-PAGE. The gel was dried and exposed to a storage phosphor screen and analyzed using a Phosphor Imager (Typhoon; GE Healthcare). Shown is this scan with quantification for the intensity of the major bands Lane 1, 10% of the L-[^{35}S]Met-labelled PPARα input in each reaction; Lane 2, GST control reaction; Lane 3, GST-CAP350$_{1-890}$ reaction; Lane 4, GST-CAP350$_{1-890(LSHAA)}$. The quantification is represented in percent with respect to the amount of L-[^{35}S]Met-labelled PPARα input.

3.2.2   *CAP350$_{1-890}$ and CAP350$_{1-890(LSHAA)}$ interacts with hLXRα:*

A similar experiment was designed to determine if CAP350 can also interact with LXRα in the same manner as with PPARα. In this experiment GST-CAP350$_{1-890}$ and GST-CAP350$_{1-890(LSHAA)}$ were immobilized on glutatione sepharose 4B beads (Amersham), and incubated with *in vitro* translated and L-[^{35}S]Met-labelled LXRα. Following the incubation a series of washes were conducted to collect unbound protein. The protein-bead complexes were denatured to release the bound protein and were analyzed on SDS-PAGE. It was found that LXRα interacts *in vitro* with the N-terminal CAP350 fragments (Figure 13), and that the mutation of the LXXLL motif from LSHLL to LSHAA does not seem to affect this interaction *in vitro*. The bands were quantified using a Phosphor Imager (Typhoon, GE Healthcare) and the data shows that approximately 0.7% of the LXRα input interacts with each CAP350 construct. This interaction appears similar to that observed for PPARα and the CAP350 N-terminal fragment *in vitro*.
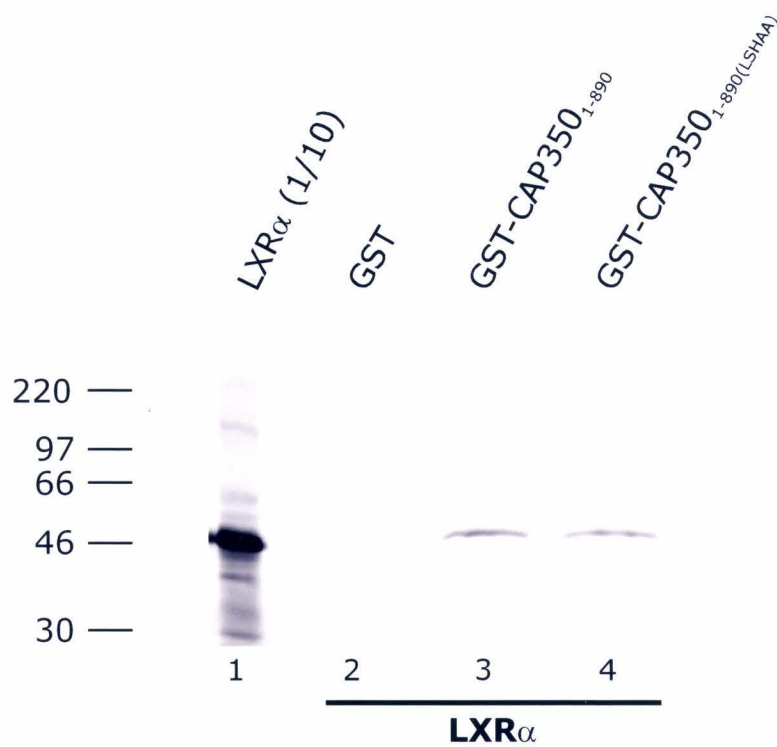
Band	Percent of Input
GST	0.01
GST-CAP350$_{1\text{-}890}$	0.8
GST-CAP350$_{1\text{-}890(LSHAA)}$	0.6

Figure 13. hLXRα **interacts with CAP350$_{1\text{-}890}$** *in vitro.*

Figure 13. hLXRα interacts with CAP350$_{1-890}$ in vitro.

LXRα interacts with CAP350$_{1-890}$ and CAP350$_{1-890(LSHAA)}$ in vitro. Bacterial synthesized CAP350$_{1-890}$ and CAP350$_{1-890(LSHAA)}$ was immobilized on glutathione sepharose 4B beads (Amersham) and incubated in vitro synthesized L-[^{35}S]Met-labelled LXRα. Bound radiolabeled proteins were analyzed on 10% SDS-PAGE. The gel was dried and exposed to a storage phosphor screen and analyzed using a Phosphor Imager (Typhoon, GE Healthcare). Shown is this scan with quantification for the intensity of the major bands Lane 1, 10% of the L-[^{35}S]Met-labelled LXRα input in each reaction; Lane 2, GST control reaction; Lane 3, GST-CAP350$_{1-890}$ reaction; Lane 4, GST-CAP350$_{1-890(LSHAA)}$. The quantification is represented in percent with respect to the amount of L-[^{35}S]Met-labelled LXRα input.

3.3 *LXRα colocalizes with CAP350*

Live cell fluorescence studies of CAP350 showed that it is present in the cytoplasm and the nucleus. In the nucleus it aggregates in distinct foci, while in the cytoplasm it localizes to the centrosome and intermediate filaments (Patel *et al.* 2005). Furthermore, in studying its predicted effects on NR localization, PPARα localization was redirected to the subnuclear foci defined by CAP350 and in the cytoplasm to the centrosome and the intermediate filaments defined by CAP350 (Patel *et al.* 2005). This indicates that CAP350 is involved in the compartmentalization and subcellular localization of PPARα. Above it was shown that CAP350 and LXRα interact *in vitro* similar to PPARα, thus it is predicted that CAP350 may influence LXR localization in similar manner. Using the mRFP-LXRα described above with the previously constructed YFP-CAP350 constructs (Patel *et al.* 2005), live cell fluorescence analysis of LXRα and CAP350 indicates that hLXRα localization is affected by CAP350.

3.3.1 *YFP-CAP350 constructs:*

The expression characteristics of YFP-CAP350 constructs are described following as viewed in NIH/3T3 cells. There are 3 YFP-CAP350 constructs: a full length CAP350 protein fused to YFP (YFP-CAP350), a truncated CAP350 (YFP-CAP350$_{1-890}$), a mutated version of the truncated (YFP-CAP350$_{1-890(LSHAA)}$). Each construct was individually transfected into NIH/3T3 cells and viewed under fluorescence microscope at 24h and 48h post-transfection. Their localization, number of visible foci, and interaction with intermediate filaments were noted. In order to understand and determine differences in expression, counts are used to assess 3 characteristics; the percentage of cells that display expression of CAP350 in the nucleus or cytoplasm, the number of nuclear foci formed, and the percentage that colocalize with filaments.

For the number of foci formed by each construct, the mean # of foci was determined.

3.3.1.1   YFP-CAP350 characteristics:

YFP-CAP350 over-expressed in NIH/3T3 cells has a nuclear localization to foci which are evident at 24h post-transfection (Figure 14 Panels A-C). At 24h the predominant localization of CAP350 is in nuclear foci, with a mean of 7 foci per cell (Table 1). In 93% of the cells there is detectable expression of CAP350 in both the cytoplasmic and nuclear compartments. With 77% of those cells expressing cytoplasmic CAP350, exhibiting localization to specific filamentous structures. At 48h post-transfection, expression of CAP350 is evident in both the nucleus and cytoplasm (Figure 14 Panels D-F), with 98% of the cells show detectable expression of CAP350 in both the cytoplasmic and nuclear compartments (Table 1). 73% of the cells expressing CAP350 in the cytoplasm exhibit localization to specific branched intermediate filament network. In the nucleus, CAP350 aggregates in nuclear foci which at 48h have a mean of 11 foci per cell. There is no overall change in intracellular distribution of CAP350 due to increase expression time, other than an increase in expression levels. These findings are consistent with those previously reported (Patel *et al.* 2005).
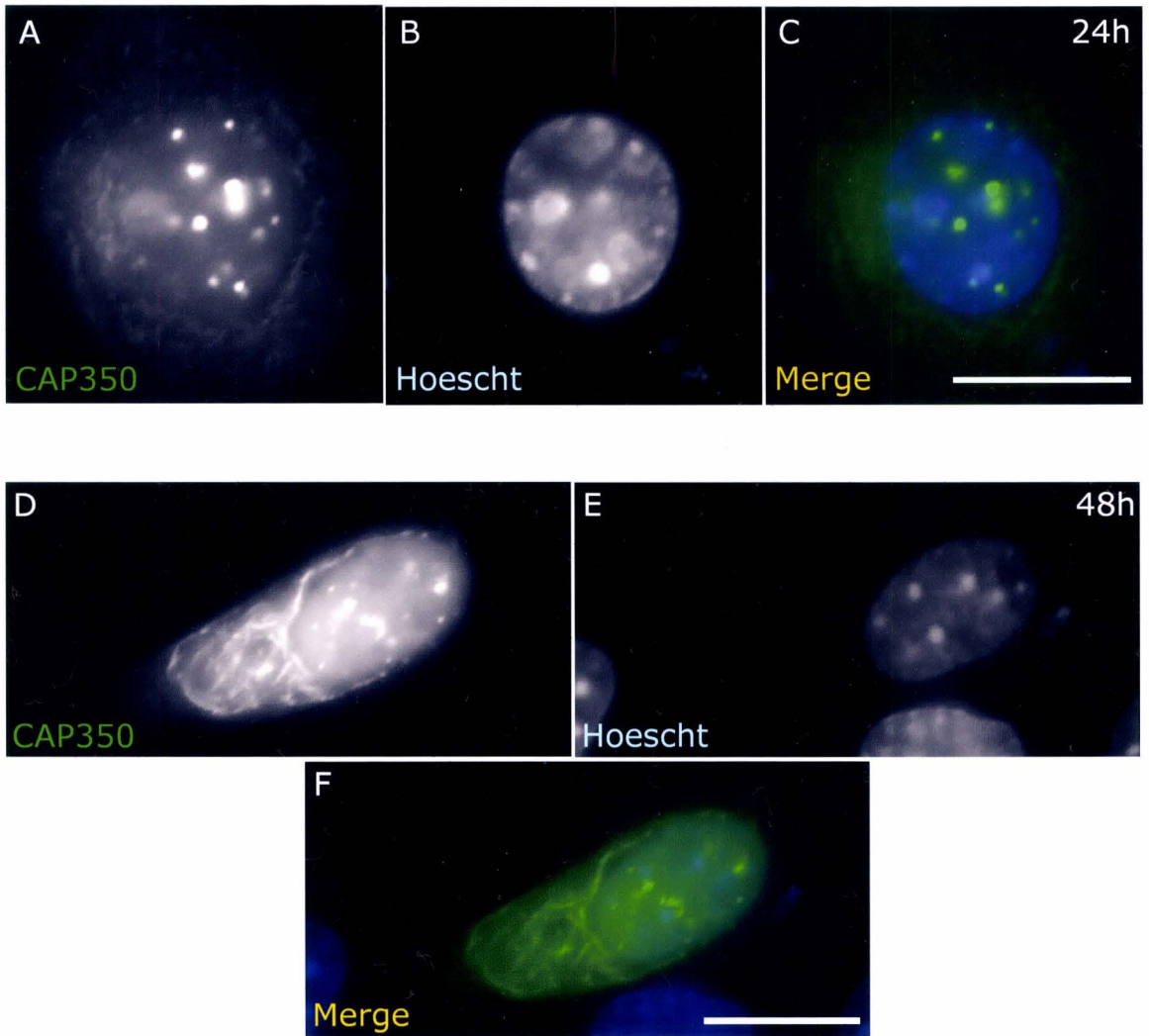
Figure 14. CAP350 viewed at 24h and 48h post-transfection.

Figure 14. CAP350 expression viewed at 24h and 48h post-transfection.

YFP-CAP350 exhibits expression in the nucleus and in the cytoplasm in NIH/3T3 cells. Representative live-cell fluorescence images of YFP-CAP350 expressed in NIH/3T3 cells at 24h (Panels A-C) and 48h (Panels D-F) post-transfection. 2 μg of YFP-CAP350 was transiently transfected using ExGen500 in NIH/3T3 cells. CAP350 shows a nuclear localization in foci and cytoplasmic localization to filaments at both 24h and 48h post-transfection. The scale is approximately 10 μm.

Panels A-C, show YFP-CAP350 expression at 24h in NIH/3T3 cells. Panel A, represents CAP350 viewed in the green channel; Panel B, represents hoescht staining of the DNA to indicate the location of the nucleus as viewed in the blue channel; Panel C, shows the merged image indicating that the foci are contained in the nucleus and that CAP350 expression is observed in the cytoplasm.

Panels D-F, show YFP-CAP350 expression at 48h. Panel D, represents CAP350 as viewed in the green channel. Panel E, represents hoescht staining of the DNA to indicate the boundary of the nucleus as viewed in the blue channel. Panel F, shows the merged image indicating that the foci are contained in the nucleus and that CAP350 expression is observed in the cytoplasm.

Table 1

	time point (h)	# of Cells	Cytoplasmic Only (% of Cells)	Nuclear Only (% of Cells)	Both (% of Cells)	# of CAP350 foci per nucleus	Filaments (% of Cells)
CAP350	24	96	1.04	5.21	93.75	7.03 +/- 3.25	77.08
	48	93	0	1.08	98.9	10.88 +/- 5.65	73.1
CAP350$_{1-890}$	24	81	3.7	93.83	2.47	18.68 +/- 8.48	1.23
	48	59	3.39	91.53	5.08	17.71 +/- 6.137	5.08
CAP350$_{1-890(LSHAA)}$	24	90	5.55	94.44	0	11.52 +/- 5.08	3.33
	48	80	3.75	96.25	0	23.7 +/- 13.02	3.75

3.3.1.2   YFP-CAP350$_{1-890}$ characteristics:

YFP-CAP350$_{1-890}$ over-expressed in NIH/3T3 cells has a predominantly nuclear localization to CAP350-defined foci which are evident at 24h post-transfection (Figure 15 Panels A-C). At 24h the predominant localization of CAP350$_{1-890}$ is in nuclear foci with a mean of 19 foci per cell (Table 1). In 93% of cells, CAP350$_{1-890}$ exhibits localization only in the nucleus. With only about 1% of the cells that show cytoplasmic localization exhibiting localization to filaments. At 48h post-transfection, expression of CAP350$_{1-890}$ is predominantly nuclear (Figure 15 Panels D-F). In 91% of the cells, CAP350$_{1-890}$ exhibits localization only in the nucleus, with a mean of 17 foci per cell (Table 1), with about 5% of the cells showing cytoplasmic localization to filaments. Indicating the truncation causes CAP350 to lose the ability to localize to the centrosome and intermediate filaments which is as expected due to the loss of the CAP-Gly domain. The ability of CAP350 to aggregate into nuclear foci is retained in the CAP350$_{1-890}$ construct and can be utilized in further studies. There is no overall change in intracellular distribution of CAP350$_{1-890}$ due to increased expression time.
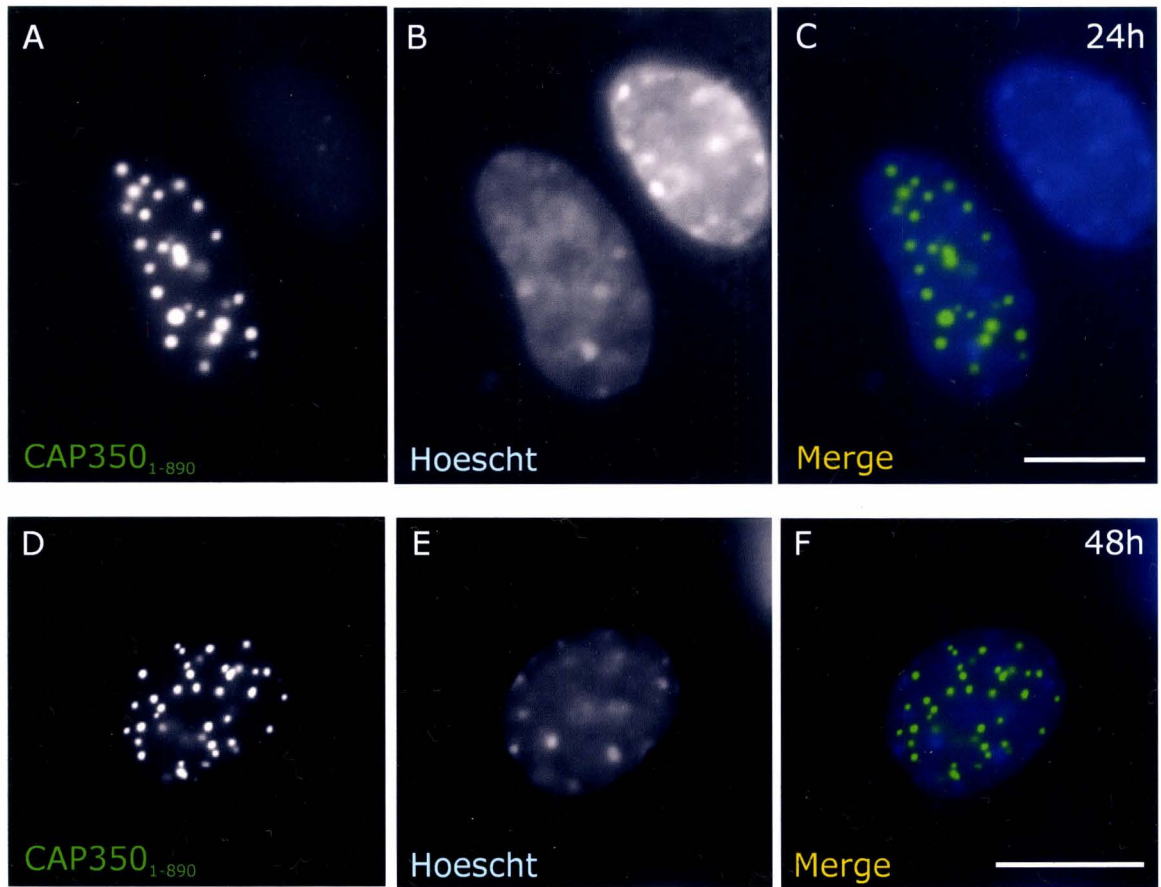
Figure 15. CAP350$_{1-890}$ expression viewed 24h and 48h post-transfection.

Figure 15. CAP350$_{1-890}$ expression viewed 24h and 48h post-transfection.

YFP-CAP350$_{1-890}$ exhibits expression in the nucleus with no expression in the cytoplasm in NIH/3T3 cells. Representative live-cell fluorescence images of YFP-CAP350$_{1-890}$ expressed in NIH/3T3 cells at 24h (Panel A-C) and 48h post-transfection (Panels D-F). 1 µg of YFP-CAP350$_{1-890}$ was transiently transfected using ExGen500 in NIH/3T3 cells. CAP350$_{1-890}$ shows a nuclear localization in foci and no cytoplasmic localization at both 24h and 48h post-transfection. The bar represents the scale at approximately 10 µm.

Panels A-C, shows YFP-CAP350$_{1-890}$ expression at 24h. Panel A, represents CAP350$_{1-890}$ as viewed in the green channel. Panel B, represents hoescht staining of the DNA to indicate the boundary of the nucleus as viewed in the blue channel. Panel C, shows the merged image indicating that the foci are contained in the nucleus and that CAP350$_{1-890}$ expression is not observed in the cytoplasm.

Panels D-F, shows YFP-CAP350$_{1-890}$ expression at 48h. Panel D, represents CAP350$_{1-890}$ as viewed in the green channel. Panel E, represents hoescht staining of the DNA to indicate the boundary of the nucleus as viewed in the blue channel. Panel F, shows the merged image indicating that the foci are contained in the nucleus and that CAP350$_{1-890}$ expression is not observed in the cytoplasm.

3.3.1.3   *YFP-CAP350$_{1-890(LSHAA)}$ characteristics:*

YFP-CAP350$_{1-890(LSHAA)}$ over-expressed in NIH/3T3 cells has a predominantly nuclear localization to CAP350-defined foci which are evident at 24h post-transfection (Figure 16 Panels A-C). At 24h the predominant localization of CAP350$_{1-890(LSHAA)}$ is in nuclear foci with a mean of 11 foci per cell (Table 1). In 95% of cells, CAP350$_{1-890}$ exhibits localization only in the nucleus. With only about 3% of the cells that show cytoplasmic localization exhibiting localization to filaments. At 48h post-transfection, expression of CAP350$_{1-890(LSHAA)}$ is predominantly nuclear (Figure 16 Panels D-F). In 96% of the cells, CAP350$_{1-890(LSHAA)}$ exhibits localization only in the nucleus, with a mean of 24 foci per cell (Table 1), with about 3% of the cells showing cytoplasmic localization to filaments. Indicating the truncation causes the lack of the CAP350 ability to localize to the centrosome and intermediate filaments as expected due to the loss of the CAP-Gly domain. The ability of CAP350 to aggregate into nuclear foci is retained in the CAP350$_{1-890(LSHAA)}$ construct despite the mutation and can be utilized in further studies. There does not seem to be any change to the intracellular distribution pattern compared with CAP350$_{1-890}$ due to the mutation of the LXXLL motif.

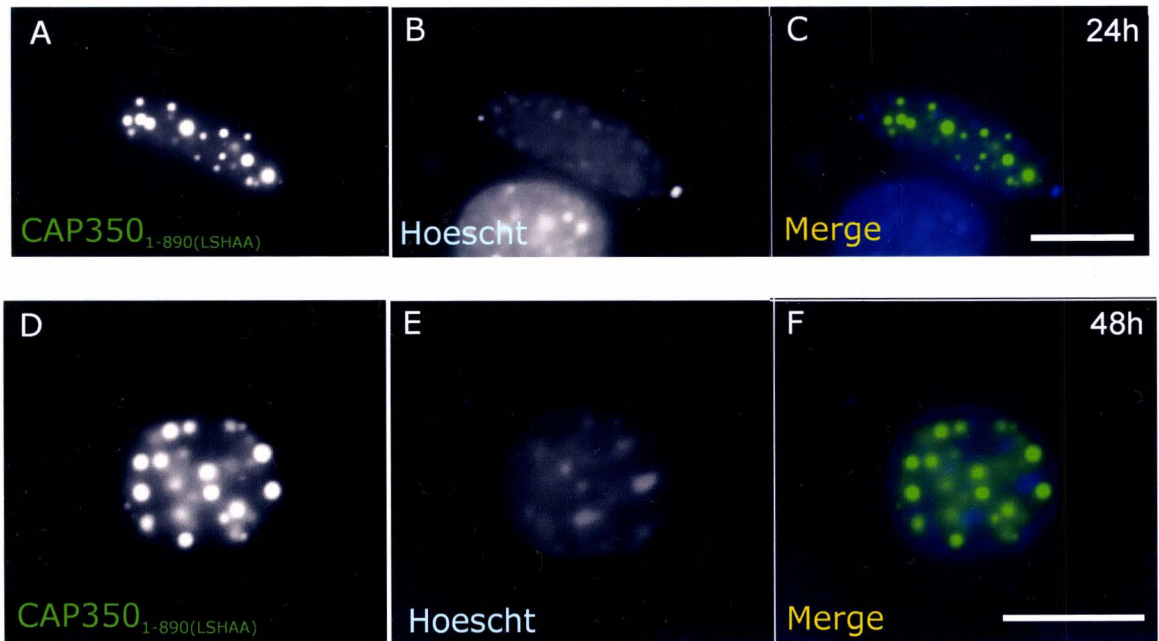**Figure 16. CAP350$_{1-890(LSHAA)}$ viewed at 24h and 48h post-transfection.**

Figure 16. CAP350$_{1-890(LSHAA)}$ expression viewed 24h and 48h post-transfection.

YFP-CAP350$_{1-890(LSHAA)}$ exhibits expression in the nucleus with no expression in the cytoplasm in NIH/3T3 cells. Representative live-cell fluorescence images of YFP-CAP350$_{1-890(LSHAA)}$ expressed in NIH/3T3 cells at 24h (Panel A-C) and 48h post-transfection (Panels D-F). 1 µg of YFP-CAP350$_{1-890(LSHAA)}$ was transiently transfected using ExGen500 in NIH/3T3 cells. CAP350$_{1-890(LSHAA)}$ shows a nuclear localization in foci and no cytoplasmic localization at both 24h and 48h post-transfection. The bar represents the scale at approximately 10 µm.

Panels A-C, shows YFP-CAP350$_{1-890(LSHAA)}$ expression at 24h. Panel A, represents CAP350$_{1-890(LSHAA)}$ as viewed in the green channel. Panel B, represents hoescht staining of the DNA to indicate the boundary of the nucleus as viewed in the blue channel. Panel C, shows the merged image indicating that the foci are contained in the nucleus and that CAP350$_{1-890(LSHAA)}$ expression is not observed in the cytoplasm.

Panels D-F, shows YFP-CAP350$_{1-890(LSHAA)}$ expression at 48h. Panel D, represents CAP350$_{1-890(LSHAA)}$ as viewed in the green channel. Panel E, represents hoescht staining of the DNA to indicate the boundary of the nucleus as viewed in the blue channel. Panel F, shows the merged image indicating that the foci are contained in the nucleus and that CAP350$_{1-890(LSHAA)}$ expression is not observed in the cytoplasm.

3.3.2   LXRα colocalizes with CAP350 at 24h and 48h:

Utilizing the YFP-CAP350 construct in transient cotransfection studies with mRFP-LXRα will allow observation under fluorescence microscope of LXRα and CAP350 in live NIH/3T3 cells. At 24h post-transfection, colocalization between LXRα and CAP350 is evident in the nucleus (Figure 17 Panel A-D). LXRα incompletely redistributes from a diffuse nuclear pattern to one that exhibits nuclear foci in the presence of CAP350. LXRα colocalizes to the CAP350-defined foci with mean of 3 and 5 respectively at 24h (Table 2). This indicates that slightly more foci represent CAP350 than LXR within a nucleus. In 98% of the cells, CAP350 is cytoplasmic while only 4.5% of cells show LXRα in the cytoplasmic and none of those display recruitment to the branched filamentous structures that CAP350 localizes to. This indicates that CAP350 expresses in cytoplasm and localizes to intermediate filaments but does not influence the shuttling of LXRα out of the nucleus. However, nuclear CAP350 is able to recruit LXRα to the CAP350-defined foci in the nucleus. At 48h post-transfection, colocalization between LXRα and CAP350 is evident in the nucleus (Figure 17 E-H). LXRα is recruited to CAP350-defined foci with a mean of 2.37 and 6.27 respectively (Table 2). In all the cells that were looked at, CAP350 displayed cytoplasmic distribution with none of the cells showing LXRα cytoplasmic localization. This indicates that CAP350 shows expression in cytoplasm to intermediate filaments (70%) but fails to influence the shuttling of LXRα out of the nucleus. However, CAP350 is able to recruit LXRα into CAP350-defined foci in the nucleus. These results show that LXRα intranuclear distribution can be altered by CAP350 to discrete foci, in a similar manner to that of PPARα. However, CAP350 does not influence the shuttling of LXRα.
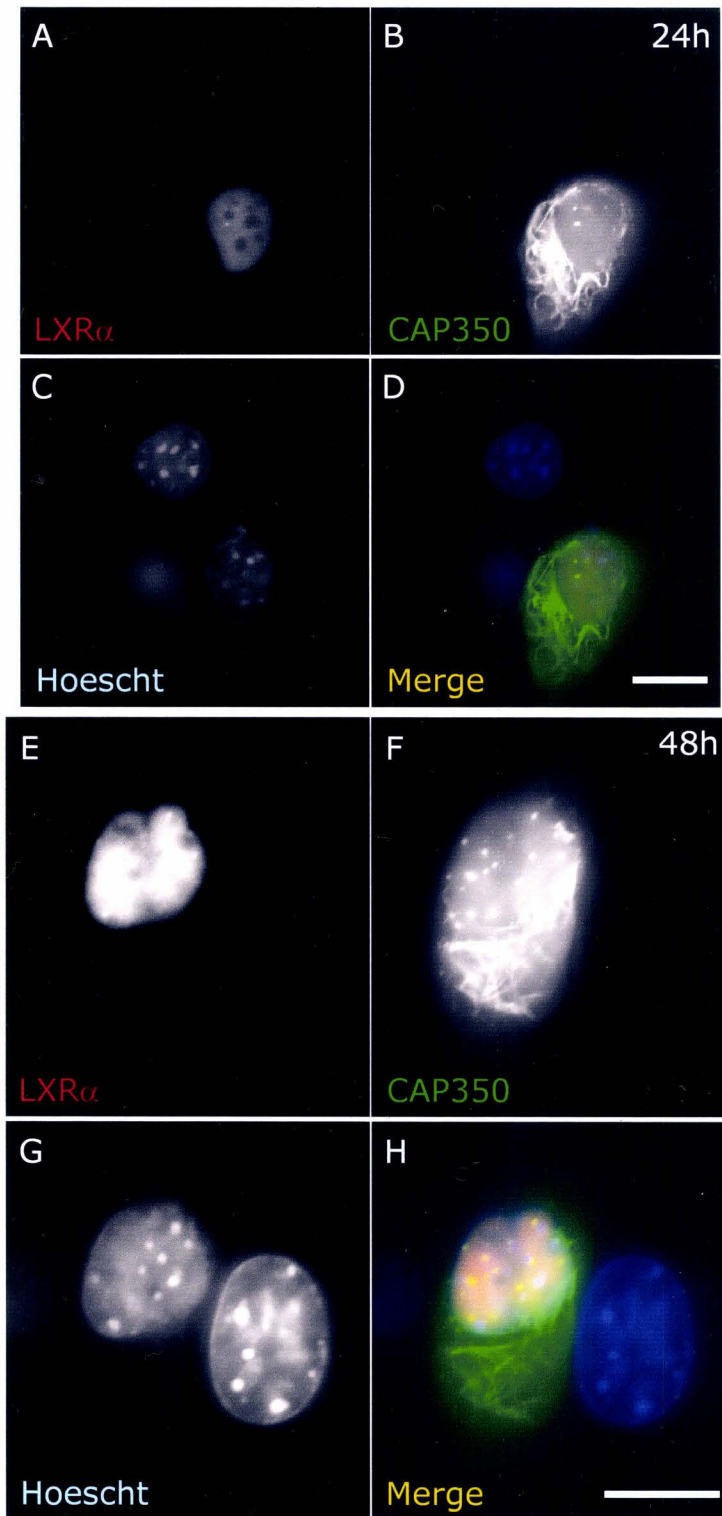
Figure 17. CAP350 colocalizes with LXRα at 24h and 48h.

Figure 17. CAP350 colocalizes with LXRα 24h and 48h.

YFP-CAP350 and mRFP-LXRα colocalize in the nucleus to CAP350-defined foci in NIH/3T3 cells. Representative live-cell fluorescence images YFP-CAP350 and mRFP-LXRα co-expressed in NIH/3T3 cells at 24h (Panels A-D) and 48h (Panels E-H) post-transfection. 2 µg of YFP-CAP350 and 1 µg of mRFP-LXRα were transiently co-transfected using ExGen500 in NIH/3T3 cells. CAP350 shows a nuclear localization in foci and cytoplasmic localization to intermediate filaments at both 24h and 48h post-transfection. LXRα colocalizes with the CAP350 only in the nucleus at the CAP350-defined nuclear foci at both 24h and 48h. The scale is approximately 10 µm.

Panel A-D, shows YFP-CAP350 and mRFP-LXRα expression at 24h in NIH/3T3 cells .

Panel A, represents LXRα as viewed in the red channel, where nuclear foci are evident that are colocalized with CAP350 foci. Panel B, represents CAP350 as viewed in the green channel, where CAP350 foci appear in the nuclei and CAP350 localizes to filaments. Panel C, represents hoescht staining of the DNA to indicate the location of the nucleus as viewed in the blue channel. Panel D, shows the merged image, that shows that the foci that appear for LXRα and CAP350 are colocalized.

Panel E-H, shows YFP-CAP350 and mRFP-LXRα expression at 48h in NIH/3T3 cells .

Panel E, represents LXRα as viewed in the red channel, where nuclear foci are evident that are colocalized with CAP350 foci. Panel F, represents CAP350 as viewed in the green channel, where CAP350 foci appear in the nuclei and CAP350 localizes to filaments. Panel G, represents hoescht staining of the DNA to indicate the location of the nucleus as viewed in the blue channel. Panel D, shows the merged image, that shows that the foci that appear for LXRα and CAP350 are colocalized.

Table 2.

	Time (h)	# of Cells	Nuclear (% of cells)		# of Foci		Cytoplasmic (% of cells)		Filaments (% of cells)	
			LXR	CAP350	LXR	CAP350	LXR	CAP350	LXR	CAP350
CAP350 + LXRα	24	44	100	100	3.43 +/- 2.38	4.79 +/- 2.34	4.55	97.7	0	56.82
	48	23	100	100	2.37 +/- 1.46	6.27 +/- 4.26	0	100	0	70
CAP350$_{1-890}$ + LXRα	24	98	100	90.82	11.2 +/- 6.62	14.42 +/- 7.0	17.35	20.41	10.2	20.41
	48	60	100	98.3	13.69 +/- 8.45	18.75 +/- 10.21	1.7	1.7	1.7	1.7
CAP350$_{1-890(LSHAA)}$ + LXRα	24	94	100	92.55	0.72 +/- 1.8	11.01 +/- 6.21	12.77	12.77	1.06	10.64
	48	79	100	93.7	0.64 +/- 1.97	15.51 +/- 9.7	6.3	6.3	2.53	6.3

3.3.3 *LXRα colocalizes with CAP350$_{1-890}$ at 24h and 48h.*

Using the YFP-CAP350$_{1-890}$ construct in transient cotransfection studies with mRFP-LXRα will allow observation under fluorescence microscope of the interaction between LXRα and CAP350$_{1-890}$ in live NIH/3T3 cells. At 24h post-transfection, CAP350$_{1-890}$ shows the expected nuclear expression in CAP350-defined foci and no expression in the cytoplasm; and LXRα is found to be diffusely expressed in the nucleus and colocalized to the CAP350-defined foci (Figure 18 Panels A-D). LXRα is recruited to CAP350-defined foci with a mean of 11 and 14 respectively at 24h (Table 2). This indicates that CAP350$_{1-890}$ is capable of recruiting LXRα to nuclear foci. At 48h post-transfection, colocalization between LXRα and CAP350 is evident in the nucleus in CAP350-defined foci (Figure 18 Panels E-H). LXRα exhibits diffuse expression and colocalization to the nuclear foci in the presence of CAP350$_{1-890}$, with mean of 14 for LXRα and 19 for CAP350$_{1-890}$ foci (Table 2). These results show that LXRα intranuclear distribution can be altered by the N-terminal fragment of CAP350 in a similar manner to that of PPARα, and that the N-terminal region of CAP350 is important in foci formation and colocalization with LXRα.
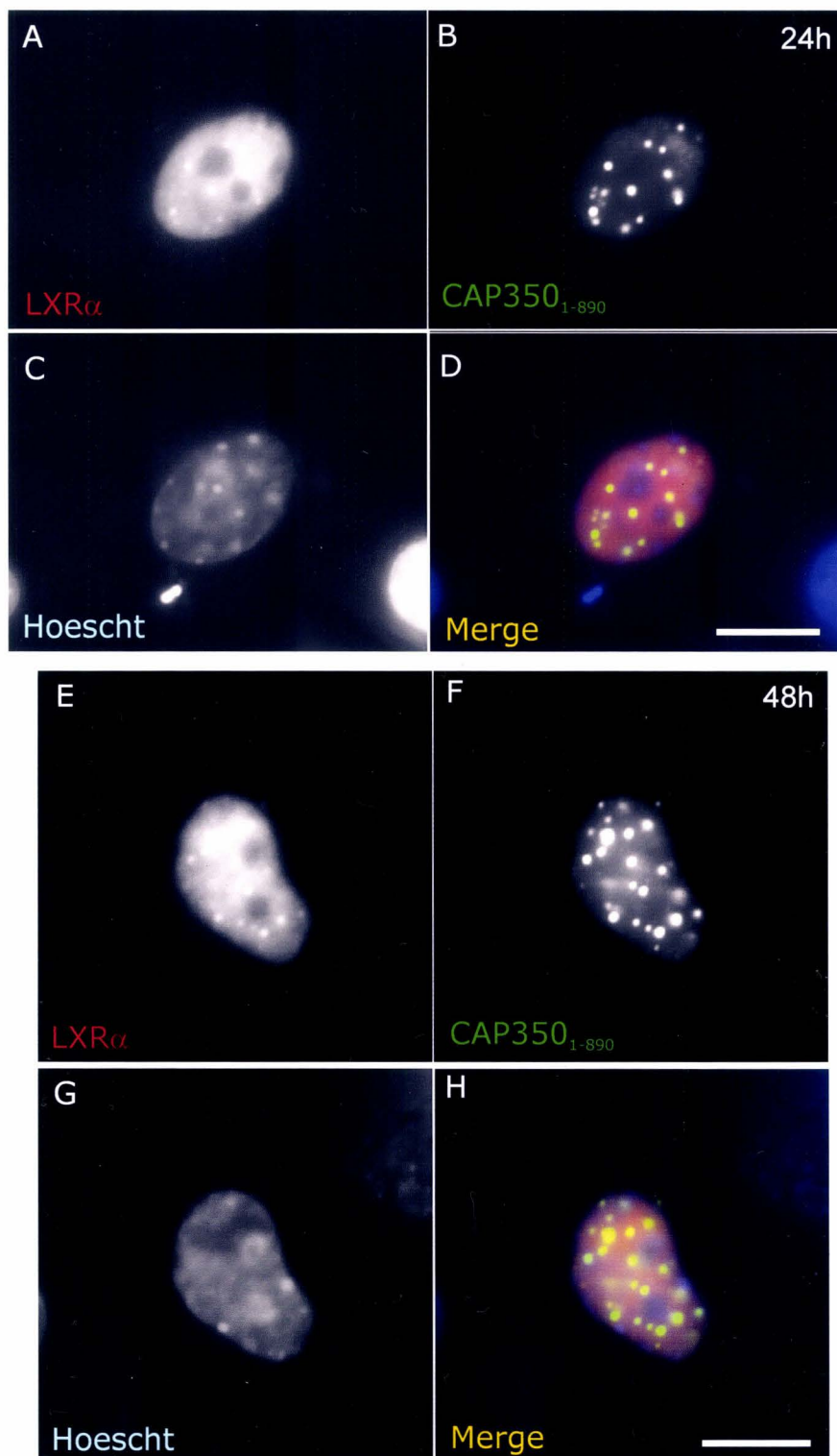
Figure 18. LXRα and CAP350$_{1\text{-}890}$ colocalize at 24h and 48h.

Figure 18. CAP350$_{1-890}$ colocalizes with LXRα 24h and 48h.

YFP-CAP350$_{1-890}$ and mRFP-LXRα colocalize in the nucleus to CAP350-defined foci in NIH/3T3 cells. Representative live-cell fluorescence images YFP-CAP350$_{1-890}$ and mRFP-LXRα co-expressed in NIH/3T3 cells at 24h (Panels A-D) and 48h (Panels E-H) post-transfection. 1 µg of YFP-CAP350$_{1-890}$ and 1 µg of mRFP-LXRα were transiently co-transfected using ExGen500 in NIH/3T3 cells. CAP350 shows a nuclear localization in foci and no cytoplasmic localization 24h and 48h post-transfection. LXR colocalizes with the CAP350$_{1-890}$ in the nucleus at the CAP350-defined nuclear foci at both 24h and 48h. The scale is approximately 10 µm.

Panel A-D, shows YFP-CAP350$_{1-890}$ and mRFP-LXRα expression at 24h in NIH/3T3 cells. Panel A, represents LXRα as viewed in the red channel, where nuclear foci are evident that are colocalized with CAP350 foci. Panel B, represents CAP350 as viewed in the green channel, where CAP350 foci appear in the nuclei. Panel C, represents hoescht staining of the DNA to indicate the location of the nucleus as viewed in the blue channel. Panel D, shows the merged image, that shows that the foci that appear for LXR and CAP350$_{1-890}$ are colocalized in the nucleus.

Panel E-H, shows YFP-CAP350$_{1-890}$ and mRFP-LXR expression at 24h in NIH/3T3 cells. Panel E, represents LXRα as viewed in the red channel, where nuclear foci are evident that are colocalized with CAP350$_{1-890}$ foci. Panel F, represents CAP350$_{1-890}$ as viewed in the green channel, where CAP350$_{1-890}$ foci appear in the nuclei. Panel G, represents hoescht staining of the DNA to indicate the location of the nucleus as viewed in the blue channel. Panel H, shows the merged image, that shows that the foci that appear for LXRα and CAP350$_{1-890}$ are colocalized in the nucleus.

3.3.4 *LXRα does not colocalize with CAP350$_{1-890(LSHAA)}$ at 24h and 48h.*

Using the YFP-CAP350$_{1-890(LSHAA)}$ construct in transient cotransfection studies with mRFP-LXRα allowed observation of the importance of the LXXLL motif in the interaction between CAP350 and LXRα in live NIH/3T3 cells. At 24h and 48h post-transfection, CAP350$_{1-890(LSHAA)}$ shows the expected nuclear expression in CAP350-defined foci and no expression in the cytoplasm; and LXRα is found to be expressed only in the nucleus in a diffuse nuclear pattern (Figure 19). LXRα does not colocalize to the foci formed by CAP350$_{1-890(LSHAA)}$. The mean of the CAP350$_{1-890(LSHAA)}$ foci at 24h and 48h are 11 and 15 respectively, while the number foci formed by LXRα at 24h and 48h are 0.7 and 0.6 respectively (Table 2). This indicates that the LXXLL motif is important in the ability of CAP350 to influence the intranuclear localization of LXRα.
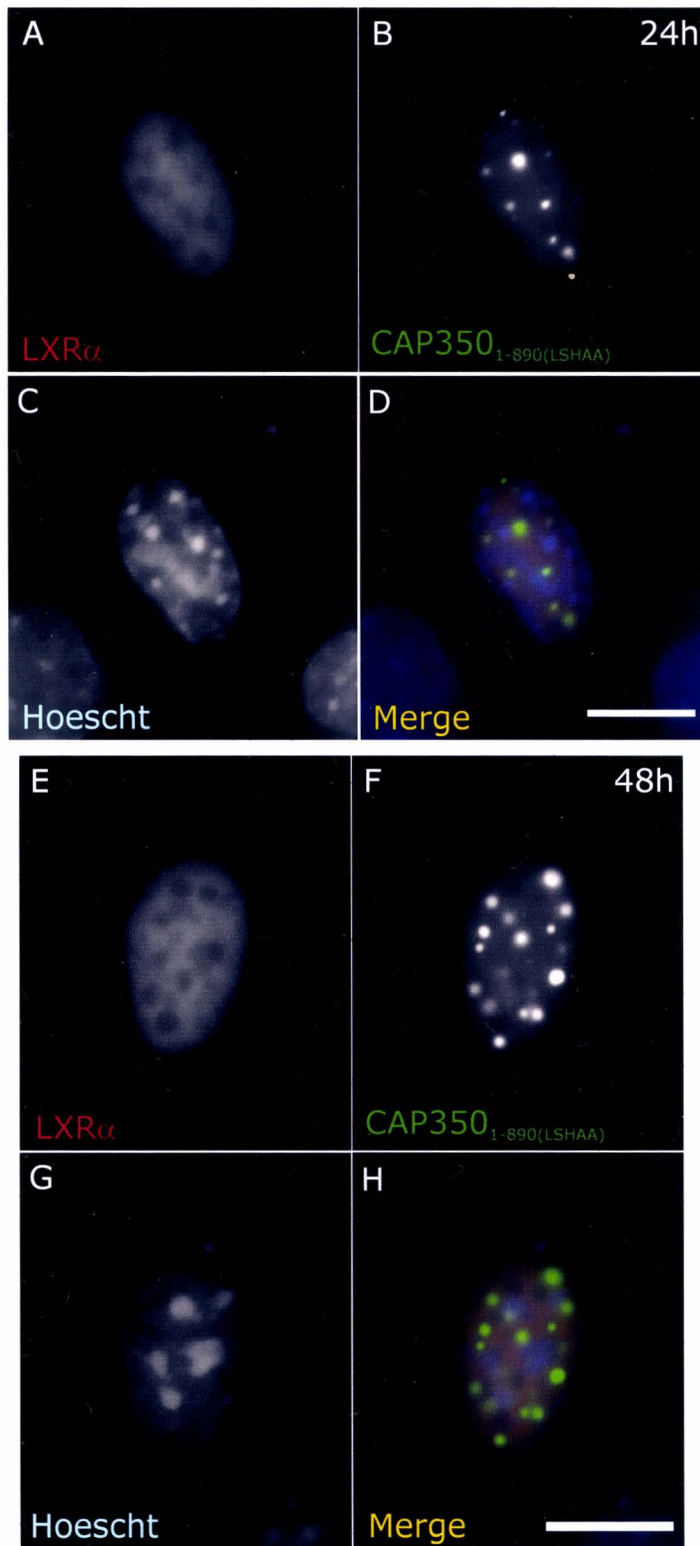
Figure 19. CAP350$_{1-890(LSHAA)}$ does not colocalize with LXRα

Figure 19. CAP350$_{1-890(LSHAA)}$ does not colocalize with LXRα 24h and 48h.

YFP-CAP350$_{1-890(LSHAA)}$ and mRFP-LXRα do not colocalize in NIH/3T3 cells. Representative live-cell fluorescence images YFP-CAP350$_{1-890(LSHAA)}$ and mRFP-LXRα co-expressed in NIH/3T3 cells at 24h (Panels A-D) and 48h (Panels E-H) post-transfection. 1 µg of YFP-CAP350$_{1-890(LSHAA)}$ and 1 µg of mRFP-LXRα were transiently co-transfected using ExGen500 in NIH/3T3 cells. CAP350$_{1-890(LSHAA)}$ shows a nuclear localization in foci and no cytoplasmic localization 24h and 48h post-transfection. LXRα does not colocalizes with the CAP350$_{1-890(LSHAA)}$ and shows a diffuse nuclear distribution in the nucleus at both 24h and 48h. The scale is approximately 10 µm.

Panel A-D, shows YFP-CAP350$_{1-890(LSHAA)}$ and mRFP-LXRα expression at 24h in NIH/3T3 cells . Panel A, represents LXRα as viewed in the red channel, where LXRα exhibits a diffuse nuclear distribution. Panel B, represents CAP350$_{1-890(LSHAA)}$ as viewed in the green channel, where CAP350$_{1-890(LSHAA)}$ foci appear in the nuclei. Panel C, represents hoescht staining of the DNA to indicate the location of the nucleus as viewed in the blue channel. Panel D, is the merged image.

Panel E-H, shows YFP-CAP350$_{1-890(LSHAA)}$ and mRFP-LXRα expression at 24h in NIH/3T3 cells . Panel E, represents LXRα as viewed in the red channel, where LXRα exhibits a diffuse nuclear distribution. Panel F, represents CAP350$_{1-890(LSHAA)}$ as viewed in the green channel, where CAP350$_{1-890(LSHAA)}$ foci appear in the nuclei. Panel G, represents hoescht staining of the DNA to indicate the location of the nucleus as viewed in the blue channel. Panel H, is the merged image.

DISCUSSION

The regulation of type II NRs includes multiple levels of control. One such level that has received attention is the possible effect of compartmentalization on the activity of the NR. Using improved cytological imaging technology has allowed the monitoring of protein localization and protein interactions in live cells. This is leading to the development of a more dynamic model of type II NR behavior in the cell that encompasses compartmentalization, protein interactions and the involvement of the nuclear matrix.

4.1   *Characterization of fluorescent protein constructs*

In order to monitor and study the behavior or type II NRs, four fluorescent protein constructs were created. They are all N-terminal fusions with either mRFP or eGFP. N-terminal fusions were constructed based on prediction from NR structure. The AF-2 domain in the C-terminal end of the protein is responsible for ligand-dependant function, thus in order to create functional NR fusions that can be used as models, N-terminal fusion were constructed to avoid non-functional constructs. An mRFP-fusion was constructed with PPARα, LXRα, and RXRα. Also an eGFP-fusion was created with RXRα. All constructs created were of the expected size and can be monitored under the fluorescence microscope following transient transfection in NIH/3T3 cells. The mRFP-LXRα and eGFP-RXRα were functionally characterized to be similar to the wildtype NR, despite an overall decrease in transactivation levels. Other groups have shown that the addition of the fluorescent protein moiety is useful, allowing labeled NRs to retain their normal transcriptional activity and ligand dependence (Carey *et al.* 1996; Chang and Puga 1998; Fejes-Toth *et al.* 1998; Georget *et al.* 1997; Htun

et al. 1996; Htun *et al.* 1998; Lim *et al.* 1999; Roderick *et al.* 1997; Zhu *et al.* 1998). This indicates their usefulness as a model for NR localization in the cell. The function of mRFP-PPARα and mRFP-RXRα has not been determined, however this mRFP-PPARα has been utilized in a PPARα localization study (Patel *et al.* 2005), and the mRFP-RXRα is expected to behave similarly to the eGFP-RXRα construct due to the similar size and nature of the eGFP and mRFP proteins.

4.2   CAP350$_{1-890}$ interacts with LXRα

Compartmentalization is influenced by a variety of factors that allow for intracellular trafficking, and changes in intranuclear distribution allowing the regulation of the activity of type II NRs (Baumann *et al.* 1999; Baumann *et al.* 2001b; Hager *et al.* 2002). Contrary to the classical model of type II NR behavior, various type II NRs have been shown to be dynamic, capable of collecting in intranuclear compartments, and shuttling in and out of the nucleus (Barsony and Prufer 2002, Baumann *et al.* 2001a). The mechanisms that mediate continuous exchanges of type II NRs between subnuclear macromolecular complexes are not described and the significances are largely unknown. CAP350, a predicted cytoskeletal interacting protein, was recently described to influence the intracellular distribution of PPAR in the cell and regulates PPAR activity (Patel *et al.* 2005). The protein contains an LXXLL motif that is known to interact with NRs, which possibly could be the motif forming the interacting surface with PPARα. An interesting feature of CAP350 is the presence of Cap-Gly domain in the C-terminal end of the protein. This domain is known to be responsible for association with cytoskeletal elements and the centrosome. Indeed a recent study indicated CAP350s role in microtubule anchoring (Yan *et al.* 2006). The added

feature of cytoskeletal association indicates a possible role for CAP350 in organization of PPARα and possibly other NRs.

The interaction between CAP350 and PPARα was confirmed in an interaction assay using an N-terminal fragment of CAP350 with PPARα (Patel *et al.* 2005). Using GST-CAP350$_{1-890(LSHAA)}$, which has the LXXLL mutated, demonstrated that the integrity of the LXXLL motif was not necessary for PPARα interaction *in vitro*. The integrity of this motif however is needed *in vivo* to maintain the colocalization observed between CAP350 and PPARα. This indicates that the motif is not needed for direct interaction with PPARα but must play some other role in the recruitment of PPARα to intranuclear foci.

The LXXLL motif is common among many coactivators that are shared across many of the NR-pathways. The above GST interaction assay was tested with LXRα. An interaction between LXRα and CAP350$_{1-890}$ is also evident, and similar to that observed for PPARα. The mutation of the LXXLL motif does not affect this interaction with LXRα. This shows that the integrity of the LXXLL motif is also not necessary for interaction with LXRα *in vitro*. This finding leads to the idea that LXRα may also be regulated by compartmentalization and the demonstration that CAP350 can interact with another type II NR shows that CAP350 may play a general role in regulation of type II NRs. Also since PPAR and LXR are involved in regulating metabolic pathways that are known to influence each others activity, CAP350 may be important in this cross-talk.

4.3 Mutation of the LXXLL motif abolishes colocalization of CAP350$_{1-890}$ with LXRα

Nuclear compartmentalization plays an important role in gene regulation, and many transcription factors and NRs, such as GR, ER, TR, and RAR along with coregulators GRIP-1, SMRT, SRC-1 and RIP140 have been shown to accumulate in discrete foci distributed throughout the nucleoplasm (Carmo-fonseca *et al.* 2001; Doucas *et al.* 2002; Hendzel *et al.* 2001; Zilliacus *et al.* 2001; Tazawa *et al.* 2003; van Steensel *et al.* 1995). The identity, composition and function of these foci remain to be elucidated. CAP350 redirects PPARα from a diffuse nuclear distribution to discrete CAP350-defined foci. These foci are distinct from PML/ND10 bodies, nuclear speckles and Nup98 bodies (Patel *et al.* 2005), which are NR-containing subnuclear foci that are suggested to represent sites of transcriptional activity (Htun *et al.* 1996). Foci are thought to represent sites of transcriptional inactivity and may serve to regulate the local concentration of regulatory molecules in the nucleus and/or represent domains for the assembly/disassembly of multicomponent transcription complexes (Hendzel *et al.* 2001). The findings that CAP350-dependant localization of PPARα in subnuclear foci correlates with an inhibition of PPARα-mediated transcriptional transactivation are consistent with such a scenario (Patel *et al.* 2005).

CAP350 influences the intranuclear distribution of LXRα from a diffuse nuclear distribution to discrete to nuclear foci. This was determined when viewing the interaction using fluorescent protein constructs of each protein. Colocalization was observed when CAP350 and LXRα are expressed in NIH/3T3 cells in the CAP350-defined nuclear foci. CAP350 does not influence the shuttling of LXRα as observed with PPARα, despite cytoplasmic expression of CAP350 to intermediate filaments. The N-terminal 890 amino acid of CAP350 is sufficient to maintain this recruitment of

LXRα to nuclear foci. When the N-terminal LXXLL motif is mutated in $CAP350_{1\text{-}890(LSHAA)}$ from LSHLL to LSHAA, the nuclear foci are not disrupted and a colocalization is not observed, despite the LXRα interaction with the $CAP350_{1\text{-}890(LSHAA)}$ *in vitro*. This indicates that the LXXLL motif is required for mediating the colocalization of LXRα and CAP350 in nuclear bodies *in vivo*, however the integrity of this motif is not necessary for their direct physical interaction, suggesting that the amino-terminal subfragment of CAP350 must harbor other determinants that mediate its interaction with LXRα. This behavior is observed with PPARα (Patel *et al.* 2005), and suggest that the LXXLL motif serves some other role in the colocalization of CAP350 and LXRα to subnuclear bodies perhaps through recruitment of auxiliary proteins that mediate these events.

CAP350 colocalization with PPARα is correlated to the inhibition of PPARα-mediated transactivation in rat hepatoma cells (Patel *et al.* 2005). This provides evidence that distribution or exchange of NRs among subcellular or nuclear sites through protein-protein interactions can modulate biological activity by compartmentalization. The significance of the colocalization between CAP350 and LXRα remains to be determined. This could be solved by utilizing an LXRα transcriptional assay in an LXRα-responsive cell. CAP350 has potential to be a regulator of LXRα action.

In summary, CAP350 has been observed to interact with another type II NR, LXRα, and is capable of altering the nuclear distribution of LXRα from a diffuse nuclear patter to discrete intranuclear foci. As observed with PPARα the CAP350 foci are likely transcriptionally inactive regions of the nucleus that serve to sequester LXRα to control its availability. These foci are also likely to act as an organization center linked to the cytoskeleton and protein mobility. The possibility remains that

CAP350 regulation can represent a general mechanism for limiting type II NR activity.
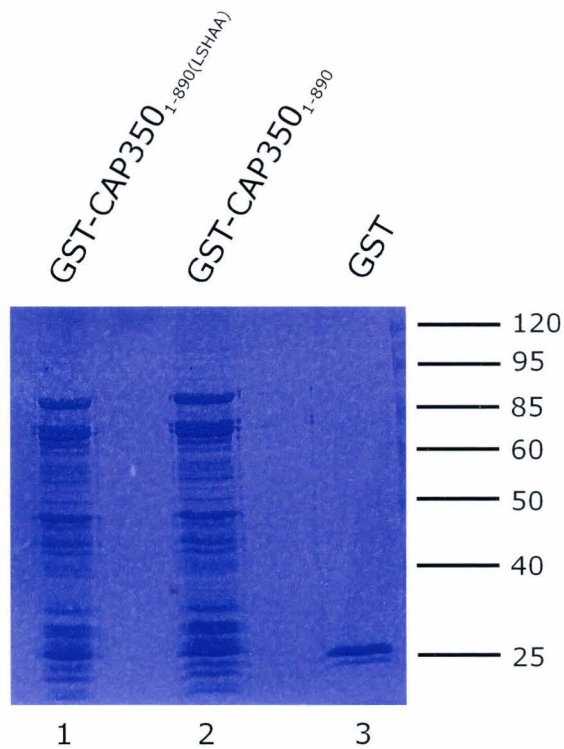
Appendix 1. Purification of CAP350$_{1-890}$ and CAP350$_{1-890(LSHAA)}$.

GST-CAP350$_{1-890}$ and GST-CAP350$_{1-890(LSHAA)}$ were bacterially synthesized in BL-21 cells and extracted using a sonication method. They were immobilized on glutathione sepharose 4B beads (Amersham). To determine the proteins that were purified using the immobilization the beads were denatured and the soluble fraction run on 10% SDS-PAGE. Lane 1, GST-CAP350$_{1-890(LSHAA)}$. Lane 2, GST-CAP350$_{1-890}$. Lane 3, GST control. These extracts were used in all the interaction experiments shown above. The gel was stained with coomassie blue and dried. The products of the extraction show that there is minimal breakdown with the major bands representing the approximate size of the CAP350$_{1-890}$ fragment.

REFERENCES

Akiyama, T.E., Baumann, C.T., Sakai, S., Hager, G.L., and Gonzalez, F.J. (2002). Selective intranuclear redistribution of PPARα isoforms by RXRα. *Mol. Endocrinol.* 16, 707-721.

Almlof, T., Wallberg, A.E., Gustaffson, J.-A., and Wright, A.P. (1998). Role of important hydrophobic amino acids in the interaction between the glucocorticoid receptor τ1-core activation domain and target forces. *Biochemistry* 37, 9586–9594.

Almlof, T., Gustaffson, J.-A., and Wright, A.P.H. (1997). Role of hydrophobic amino acid clusters in the transactivation of the human glucocorticoid receptor. *Mol. Cell. Biol.* 17, 934–945.

Anzick, S.L., Kononen, J., Walker, R.L., Azorsa, D.O., Tanner, M.M., Guan, X.Y., Sauter, G., Kallioniemi, O.P., Trent, J.M., and Meltzer, P.S. (1997). AIBI, a steroid receptor coactivator amplified in breast and ovarian cancer. *Science*, 277, 965–958.

Aronica, S.M., and Katzenellenbogen, B.S. (1993). Stimulation of estrogen receptor-mediated transcription and alteration in the phosphorylation state of the rat uterine estrogen receptor by estrogen, cyclic adenosine monophosphate, and insulin-like growth factor-1. *Mol. Endocrinol.* 7, 743–752.

Ausubel, F. M., Brent, R., Kingston, R. E., Moore, D. D., Seidman, J.G., Smith, J.A., and Struhl, K. (1994) *Current Protocols in Molecular Biology.* John Wiley & Sons, New York

Barettino, D., Ruiz, M.d.M.V., and Stunnenberg, H.G. (1994). Characterization of the ligand-dependent transactivation domain of thyroid hormone receptor. *EMBO J.* 13, 3039-3049

Barsony, J., Renyi, I., and McKoy, W. (1997). Subcellular distribution of normal and mutant vitamin D receptors in living cells. Studies with a novel fluorescent ligand. *J. Biol. Chem.* 272, 5774–5782.

Barsony, J., and Prufer, K. (2002). Vitamin D receptor and retinoid X receptor interactions in motion. *Vitam. Horm.* 65, 345–376.

Baumann, C.T., *et al* (1999). Intracellular localization and trafficking of steroid receptors. *Cell. Biochem. Biophys.* 31, 119-127.

Baumann, C.T., Maruvada, P, Hager, G.L., and Yen, P.M. (2001a). Nuclear cytoplasmic shuttling by thyroid hormone receptors. Multiple protein interactions are required for nuclear retention. *J. Biol Chem.* 276, 11237-11245.

Baumann, C.T., Ma, H., Wolford, R., Reyes, J., Marudava, P, Lim, C., Yen, P.M., Stallcup, M.R., and Hager, G.L. (2001b). The glucocorticoid receptor

interacting protein 1 (GRIP1) localizes in discrete nuclear foci that associate with ND10 bodies and are enriched in components of the 26S proteasome. *Mol. Endocrinology* 15, 485–500.

Beato, M., and Sanchez-Pacheco, A. (1996). Interaction of steroid hormone receptors with the transcription initiation complex. *Endocr. Rev.* 17, 587–609.

Berezney, R., and Jeon, K.W. (1995). *Nuclear matrix. Structural and functional organization.* Academic Press, New York.

Berger, J., Patel, H.V., Woods, J., Hayes, N.S., Parent, S.A., Clemas, J., Leibowitz, M.D., Elbrecht, A., Rachubinski, R.A., Capone, J.P., and Moller, D.E. (2000) A PPARγ `mutant serves as a dominant negative inhibitor of PPAR signaling and is localized in the nucleus. *Mol. Cell. Endocrinol.* 162, 57-67.

Black, B.E., Holaska, J.M., Rastinejad, F., and Paschal, B.M. (2001). DNA binding domains in diverse nuclear receptors function as nuclear export signals. *Curr. Biol.* 11, 1749–1758.

Bocher, V., Pineda-Torra, I., Fruchart, J.-C., and Staels, B. (2002). PPARs: transcription factors controlling lipid and lipoprotein metabolism. *Ann. N.Y. Acad. Sci.* 967, 7-18.

Bordji, K., Grillasca, J.P., Gouze, J. N., Magdalou, J., Schohn, H., Keller, J.M., Bianchi, A., Dauca, M., Netter, P., Terlain, B. (2000). Evidence for the presence of peroxisome proliferator-activated receptor (PPAR) α and γ and retinoid X receptor in cartilage *J. Biol. Chem.* **275**, 12243–12250.

Brinkmann, A.O., Blok, L.J., de Ruiter, P.E., Doesburg, P., Steketee, K., Berrevoets, C.A., and Trapman, J. (1999). Mechanisms of androgen receptor activation and function. *J. Steroid Biochem. Mol. Biol.* 69, 307-313.

Brown, C.E., Lechner, T., Howe, L., and Workman, J.L. (2000) The many HATs of transcription coactivators. *Trends Biochem. Sci.* 25, 15-19.

Bunn, C.F., Neldig, J.A., Freidinger, K.E., Stankiewicz, T.A., Weaver, B.S., McGrew, and Allson, L.A. (2001). *Mol. Endocrinol.* 15, 512–533.

Campbell, R. E., Tour, O., Palmer, A. E., Steinbach, P. A., Baird, G. S., Zacharias, D. A., and Tsien, R. A. (2002). A monomeric red fluorescent protein. *Proc. Natl. Acad. Sci. U.S.A.* 99, 7877–7882.

Carey, K.L, Richards, S.A., Lounsbury, K.M., and Macara, I.G., (1996). Evidence using green fluorescent protein-glucocorticoid receptor chimera that the Ran/TC4 GTPase mediate an essential function independent of nuclear protein import. *J. Cell Biol.* 133, 985–996.

Carno-Fonseca, M. (2002). The contribution of nuclear compartmentalization to gene regulation. *Cell* 108, 513–521.

Chang, C.Y., and Puga, A. (1998). Constitutive activaiotn fo the aromatic hydrocarbon receptor. *Mol. Cell. Biol.* 18, 525–535.

Chawla, A., Repa J., Evans, R.M., and Magelsdorf, D.J. (2001a). Nuclear receptors and lipid physiology: opening the X-files. *Science* 294, 1866-1870.

Chawla, A., Boisvert, W.A., Lee, C.-H., Laffitte, B.A., Barak, Y., Joseph, S.B., Liao, D., Nagy, L., Edwards, P.A., Curtiss, L.K., Evans, R.M., and Tontonoz, P. (2001b). A PPARγ-LXR-ABCA1 pathway in macrophages is involved in cholesterol efflux and atherogenesis. *Mol. Cell* 7, 161–171.

Chen, J.D., and Evans, R.M. (1995). A transcriptional co-repressor that interacts with nuclear hormone receptors. *Nature* 377, 454–457.

Chen, J.D., Umensono, K., and Evans, R.M. (1996). SMRT isoforms mediate repression and anti-repression of nuclear receptor heterodimers. *Proc. Natl. Acad. Sci. U.S.A.* 93, 7567–7571.

Chen, H., Lin, R.J., Schiltz, R.L., Chakravarti, D., Nash, A., Nagy, L., Privalsky, M.L., Nakatani, Y., and Evans, R.M. (1997). Nuclear receptor coactivator ACTR is a novel histone acetyltransferase and forms a multimeric activation complex with p/CAF and CBP/p300. *Cell* 90, 569–580.

Cheung, P., Allis, C.D. and Sassone-Corsi, P. (2000). Signaling to chromatin through histone modifications. *Cell* 103, 263-271.

Chinetti, G., Griglio, S., Antonucci, M., Torra, P.I., Delerive, P., Majd, Z., Fruchart, J.-C., Chapman, J., Najib, J., and Staels, B. (1998). Activation of proliferator-activated receptors α and γ induces apoptosis of human monocyte-derived macrophages. *J. Biol. Chem.* 273, 25573-25580.

Chinetti, G., Lestavel, S., Bocher, V., Remaley, A.T., Neve, B., Torra, I.P., Tessier, E., Minnich, A., Jaye, M., Duverger, N., Brewer, H.B., Fruchart, J.-C., Clavey, V., and Staels, B. (2001). PPAR-α and PPAR-γ activators induce cholesterol removal from human macrophage foam cells through stimulation of the ABCA1 pathway. *Nature Med.* 7, 53–58.

Claeseens, F, and Gewirth, D.T. (2004). DNA recognition by nuclear receptors. *Essays Biochem.* 40, 59–72.

ClonTECHniques (1997) April.

Cohen, R.N., Putney, A., Wondlisford, F.E., and Hollenberg, A.N. (2000). The nuclear corepressors recognize distinct nuclear receptor complexes. *Mol. Endorcrinol.* 14, 900–914.

Cohen, R.N., Brzostek, S., Kim, B., Chorev, M., Wondisford, F.E., and Hollenberg, A.N. (2001). The specificity of interaction between nuclear hormone receptors and corepressors is mediated by distinct amino acid sequences within in interacting domains. *Mol. Endorcrinol.* 15, 1049–1061.

Colingwood, T.N., Umov, F.D. and Wolffe, A.P. (1999). Nuclear receptors: coactivators, corepressors and chromatin remodeling in the control of transcription. *J. Mol. Endocrinol.* 23, 255-275.

Costet, P., Luo, Y., Wang, N., and Tall, A.R. (2000). Sterol-dependant transactivation of the *ABC1* promoter by the Liver X Receptor/Retinoid X Receptor. *J. Biol. Chem.* 275, 28240–28245.

Danielian, P. S., White, R., Lees, J.A., and Parker, M.G. (1992). Identification of a conserved region required for hormone dependent transcriptional activation by steroid hormone receptors. *EMBO J.* 11, 1025-1033.

de Jong, L., Grande, M.A., Mattern, K.A., Schul, W., and can Driel, R. (1996). Nuclear domains involved in RNA synthesis, RNA processing and replication. *Crit. Rev. Eukaryot. Gene Expr.* 6, 215–246.

Deroo, B.J. and Archer, T.K. (2001). Glucocoricoid receptor-mediated chromatin remodeling *in vivo. Oncogene* 20, 3039-3046.

Dilworth, F.J. and Chambon, P. (2001). Nuclear receptors coordinate the activities of chromatin remodeling complexes and coactivators to facilitate initiation of transcription. *Oncogene* 20, 3047–3054.

Doucas, V. (2000). The promyelocytic (PML) nuclear compartment and transcription control. *Biochem Pharmacol.* 60, 1197–1201.

Dundr, M., and Misteli, T. (2001). Functional architecture in the cell nucleus. *Biochem. J.* 356, 297–310.

Durand, B., Saunders, M., Gaudon, C., Roy, B., Losson, R., and Chambon, P. (1994) Activation function 2 (AF-2) of retinoic acid receptor and 9-cis retinoic acid receptor: presence of a conserved autonomous constitutive activating domain and influence of the nature of the response element on AF-2 activity. *EMBO J.* 13, 5370-5382

Eisen, J.A., Sweder, K.S., and Hanawalt, P.C. (1995). Evolution of the SNF2 family of proteins: subfamilies with distinct sequences and functions. *Nucleic Acids Res.* 23, 2715–2723.

Elefanty, A.G., Antoniou, M., Custodio, N., Carmo-Fonseca, M., and Grosveld, F.G. (1996). GATA transcription factors associate with a novel class of nuclear bodies in erythroblasts and megakaryocytes. *EMBO J.* 15, 319–333.

Fejes-Toth, G., Pearce, D., and Naray-Fejes-Toth, A. (1998). Subcellular localization of mineralocoricoid receptors in living cells: effects of receptor agonists and antagonists. *Proc. Natl. Acad. Sci. U.S.A.* 95, 2973–2978.

Fiedler, U. and Marc Timmers, H.T. (2000). Peeling by binding or twisting by cranking: models for promoter opening and transcription initiation by RNA polymerase II. Bioessay 22, 316-26.

Ford, J., McEwan, I.J., Wright, A.P., and Gustafsson, J.-A., (1997). Involvement of the transcription factor IID protein complex in gene activation by the N-terminal transactivation domain of the glucocorticoid receptor *in vitro*. *Mol. Endocrinol.* 11, 1467–1475.

Forman, B.M., and Samuels, H.H. (1990). Dimerization among nuclear hormone receptors. *New Biol.* 2, 587–594.

Forman, B.M., Ruan, B., Chen, J., Schroepfer, G.J. Jr., and Evans, R.M. (1997) *Proc. Natl. Acad. Sci. U.S.A.* The orphan nuclear receptor LXRα is positively and negatively regulated by distinct products of mevalonate metabolism. **94**, 10588–10593.

Gan, X., Kaplan, R., Menke, J.G., MacNaul, K., Chen, Y., Sparrow, C.P. Xhou, G., Wright, S.D., and Cai, T.-Q. (2001). Dual mechanisms of ABCA1 regulation by geranylgeranyl pyrophosphate. *J. Biol. Chem.* 276, 48702–48708.

Georget, V., Lobaccaro, J.M., Terouanne, B., Mangeat, P., Nicolas, J.-C., and Sultan C. (1997). Trafficking of the androgen receptor in living cells fused with green fluorescent protein-androgen receptor. *Mol. Cell. Endocrinol.* 129, 17–26.

Georget, V., Terouanne, B., Nicolas, J.-C., and Sultan, C. (2002). Mechanism of antiandrogen action: key role of Hsp90 in conformational change and transcriptional activity of the androgen receptor. *Biochemistry* 41, 11824–11831.

Glass, C.K., Lipkin, S.M., Devary, O.V., and Rosenfeld, M.G. (1989). Positive and negative regulation of gene transcription by a retinoic acid-thyroid hormone receptor heterodimer. *Cell* 59, 697–708.

Glass, C.K. (1994) Differential regulation of target genes by nuclear receptor monomers, dimers, and heterodimers. *Endocr. Rev.* 15, 391-407.

Glass, C.K., and Rosenfeld, M.G. (2000). The coregulator exchange in transcriptional function of nuclear receptors. *Genes Dev.* 14, 121–141.

Glass, C.K., and Witztum, J.L. (2001). Artherosclerosis: The road ahead. *Cell* 104, 503–516.

Gobinet, J., *et al* (2002) Molecular action of androgens. *Mol. Cell. Endocrinol.* 198, 15-24.

Grande, M.A., van der Kraan, I., de Jong, L., and van Driel, R. (1997). Nuclear distribution of transcription factors in relation to sites of transcription and RNA polymerase II. *J. Cell Sci.* 110, 1781 – 1791.

Grunstien, M. (1997). Histone acetlyation in chromatin structure and transcription. *Nature* 389, 349–352.

Guichon-Mantel, A., Lescop, P., Christin-Maitre, S., Loosfelt, H., Perrot-Applanat, M., and Milgrom E (1991). Nucleocytoplasmic shuttling of the progesterone receptor. *EMBO* 10, 3851–3859.

Hager, G.L., Lin, C.S., Elibi, C., and Baumann, C.T. (2000). Trafficking of nuclear receptors in living cells. *J. Steroid Biochem. Mol. Biol.* 74, 249-254.

Heery, D.M., Kalkhoven, E., Hoare, S., and Parker, M.G. (1997). A signature motif in transcriptional co-activators mediates binding to nuclear receptors. *Nature* 387, 733–736.

Hendzel, M.J., Kruhlak, M.J., MacLean, N.A., Boisvert, F., Lever, M.A., and Bazett-Jones, D.P. (2001). Compartmentalization of regulatory protein in cell nucleus. *J. Steroid Biochem. Mol. Biol.* 76, 9–21.

Henriksson, A., Almlof, T., Ford, J., McEwan, I.J., Gustafsson, J.-A., and Wright, A.P. (1997). Role of the Ada adaptor complex in gene activation by the glucocorticoid receptor. *Mol. Cell. Biol.* 17, 3065–3073.

Hernandez, N. (1993). TBP, a universal eukaryotic transcription factor? Genes and Development, 7(7B):1291-308.

Hihi, A.K., *et al* (2002) PPARs : transcriptional effectors of fatty acids and their derivatives. *Cell. Mol. Life Sci.* 59, 790-798.

Hittelman, A.B., Burakov, D., Iniguez-Luhi, J.A., Freedman, L.P., and Garabedian, M.J. (1999). Differential regulation of glucocorticoid receptor transcriptional activation via AF-1 associated proteins. *EMBO J.* 18, 5380–5388.

Holstege, F.C.P., van der Vliet, P.C., and Timmers, H.T. (1996). Opening of an RNA polymerase II promoter occurs in two distinct steps and requires the basal transcription factors IIE and IIH. *EMBO* 15, 1666–1677.

Hong, L., Schroth, G.P., Mathews, H.R., Yau, P., and Bradbury, E.M. (1993). Studies of the DNA binding properties of histone H4 amino terminus: thermal denaturation studies reveal that acetylation markedly reduces the binding constant of the H4 "tail" to DNA. *J. Biol. Chem.* 268, 305–314.

Hong, H., Kohli, K., Triverdi, A., Johnson, D.L., and Stallcup, M.R. (1996). GRIP1, a novel mouse protein that serves as a transcriptional co-activator in yeast for the hormone binding domains of steroid receptors. *Proc. Natl. Acad. Sci. U.S.A.* 93, 4948–4952.

Hong, H., Kohli, K., Garabedian, M.J., and Stallcup, M.R. (1997). GRIP1, a transcriptional coactivator for the AF-2 transactivation domain of steroid, thyroid, retinoid, and vitamin D receptors. *Mol. Cell Biol.* 17, 2735-2744.

Horlein, A.J., Naar, A.M., Heinzel, T., Torchia, J., Gloss, B., Kurokawa, R., Ryan, A., Kamei, Y., Soderstrom, M., Glass, C.K., and Rosenfeld, M.G. (1995). Ligand-independent repression by the thyroid hormone receptor mediated by a nuclear co-repressor. *Nature* 377, 397–403.

Hsiao, P.W., Deroo, B.J., and Archer, T.K. (2002). Chromatin remodeling and tissue-selective responses of nuclear hormone recepors. *Biochem. Cell. Biol.* 80, 343–351 .

Htun, H., Barsony, J., Renyi, I., Gould, D.L., and Hager, G.L. (1996). Visualization of glucocorticoid receptor translocation and intranuclear organization in living cells with a green fluorescent protein chimera. *Pro. Natl. Acad. Sci. U.S.A.* 14, 4845–4850.

Htun, H., Holth, L.T., Hoth, Walker, D., Davie, J.R., and Hager, G.L. (1999). Direct visualization of the human estrogen receptor α revels a role for ligand in the nuclear distribution of the receptor. *Mol. Biol. Cell* 10, 471–486.

Hu, X., and Lazar, M.A. (1999). The CoRNR motif controls recruitment of corepressors by nuclear hormone receptors. *Nature* 402, 93–96.

Hudson, L.G., Santon, J.B., Glass, C.K., and Gill, G.N. (1990). Ligand-activated thyroid hormone and retinoic acid receptors inhibit growth factor receptor promoter expression. *Cell* 62, 1165–1175.

Ide, T., Shimano, H., Yokishawa, T., Yahagi, N., Amemiya-Kudo, M., Matsuzaka, T., Nakakuki, M., Yatoh, S., Iizuka, Y., Tomita, S., Ohashi, K., Takahashi, A., Sone, H., Gotoda, T., Osuga, J.-I., Ishibashi, S., and Yamada, N. (2003). Cross-talk between peroxisome proliferator-activated receptor (PPAR) α and Liver X receptor (LXR) in nutritional regulation of fatty acid metabolism. II. LXRs suppress lipid degeneration gene promoters through inhibition of PPAR signaling. *Mol. Endocrinol.* 17, 1255–1267.

Issemann I, and Green S. (1990). Activation of a member of the steroid hormone receptor family by peroxisome proliferators. *Nature* 347, 645–650 .

Jackson, D.A., McCready, S.J., and Cook, P.R. (1984). Replication and transcription depend on attachment of DNA to the nuclear cage. *J. Cell Sci. Suppl.* 1, 59–79.

Jackson, D.A., Hassan, B.A., Errington, R.J., and Cook, P.R. (1993). Visualization of focal sites of transcription within human nuclei. *EMBO J.* 12, 1059–1065.

Janowski, B.A., Willy, P.J., Devi, T.R., Falck, J.R., and Magelsdorf, D.J. (1996). An oxysterols signaling pahthway mediated by the nuclear receptor LXR alpha. *Nature* 383, 728–731.

Kamei, Y., Xu, L., Heinzel, T., Torchia, J., Kurokawa, R., Gloss, B., Lin, S.C., Heyman, R., Rose, D., Glass, C., and Rosenfeld, M. (1996). A CBP integrator

complex mediates transcriptional activation and AP-1 inhibition by nuclear receptors. *Cell* 85, 403–414.

Kumar, R., and Thompson, B.E. (2003). Transactivation functions of the N-terminal domains of nuclear hormone receptors: protein folding and coactivator interactions. *Mol. Endorcrinol.* 17, 1–10.

Laffitte, B.A., Repa, J.J., Joseph, S.B., Wilpitz, D.C., Kast, H.R., Mangelsdorf, D.J., and Tontonoz, P. (2001). LXRs control lipid-inducible expression of the apolipoprotein E gene in macrophages and adipocytes. *Proc. Natl. Acad. Sci. U.S.A.* 98, 507–512.

Lamond, A.I., and Earnshaw, W.C. (1998). Structure and Function in the Nucleus. *Science* 280, 547–553.

Lee, C.H., *et al* (2003) Lipid metabolism, metabolic diseases, and peroxisome proliferator-activated receptors. *Endocrinology* 144, 2201-2207.

Lee, I.T., and Young, R.A. (2000). Transcription of eukaryotic protein-coding genes *Annu. Rev. Genet.* 34, 77–137.

Lehmann, J.M., Kliewer, S.A., Moore, L.B., Smith-Oliver, T.A., Oliver, B.B., Su, J.-L., Sundseth, S.S., Winegar, D.A., Blanchard, D.E., Spencer, T.A., and Wilson, T.M. (1997). Activation of the nuclear receptor LXR by oxysterols defines a new hormone response pathway. *J. Biol. Chem.* 272, 3137–3140.

Lemon, B., and Tjian, R. (2000). Orchestrated response: a symphony of transcription factors for gene control. *Genes Dev.* 14, 2551–2569.

Leidig, F., Shepard, A.R., Zhang, W.G., Stelter, A., Cattini, P.A., Baxter, J.D., and Eberhardt, N.L. (1992). Thyroid hormone responsiveness in human growth hormone-related genes. Possible correlation with receptor-induced DNA conformational changes. *J. Biol. Chem.* 267, 913–21.

Lemberger, T., Desvergne, B., and Wahli, W. (1996). Peroxisome proliferator-activated receptors: a nuclear receptor signaling pathway in lipid physiology. Annu. Rev. Cell Dev. Biol. 12, 335-63.

Li, A.C., and Glass, C.K. (2004). PPAR- and LXR-dependant pathways controlling lipid metabolism and the development of artherosclerosis. *J. Lipid Res.* 45, 2161 – 2173.

Lim, C.S., Baumann, C.T., Htun, H., Xian, W., Irie, M., Smith, C.L., and Hager, G.L. (1999). Differential localization and activity of the A and B forms of the human progesterone receptor using green fluorescent protein chimeras. *Mol. Endocrinol.* 13, 366–375.

Linton, M.F., Atkinson, J.B., and Fazio, S. (1995). Prevention of artherosclerosis in apolipoprotein E-deficient mice by bone marrow transplantation. *Science* 267, 1034–1037.

Li, H., Gomes, P.J., and Chen, J.D. (1997). RAC3, a steroid/nuclear receptor-associated coactivator that is related to SRC-1 and TIF-2. *Proc. Natl. Acad. Sci. U.S.A.* 94, 8479–8484.

Li, H., Leo, C., Schroen, D.J., and Chen, J.D. (1997). Characterization of receptor interaction and transcriptional repression by the corepressor SMRT. *Mol. Endorcrinol.* 11; 2025–2037.

Luger, K., Mader, A.W., Richmond, R.K., Sargent, D.F., and Richmond T.J. (1997). Crystal structure of the nucleosome core particle at 2.8 angstron resolution. *Nature* 389, 251–260.

Mackem, S., *et al* (2001). A glucocorticoid/retinoic acid receptor chimera that displays cytoplasmic/nuclear translocation in response to retinoic acid. A real time sensing assay for nuclear receptor ligands. *J. Biol. Chem.* 276, 45501-45504.

Madan, A.P., and DeFranco, D.B. (1993). Bideirectional transport of glucocorticoid receptors across the nuclear envelope. *Proc. Natl. Acad. Sci. U.S.A.* 90, 3588–3592.

Mangelsdorf, D.J., Ong, E.S, Dyck, J.A., and Evans, R.M. (1990). Nuclear receptor that identifies a novel retinoic acid response pathway. *Nature* 345, 224–229.

Mangelsdorf, D.J., and Evans R.M. (1995). The RXR heterodimers and orphan receptors. *Cell* 83, 841–850.

Marcus, S. L., Miyata, K. S., Zhang, B., Subramani, S., Rachubinski, R. A., and Capone, J. P. (1993). Diverse peroxisome proliferator-activated receptors bind to the peroxisome proliferator-responsive elements of the rat hydratase/dehydrogenase and fatty acyl-CoA oxidase genes but differentially induce expression. *Proc. Natl. Acad. Sci. U.S.A.* 90, 5723–5727.

Martin, S., and Pombo, A. (2003). Transcription factories : quantitative studies of nanostructures in the mammalian nucleus. *Chromosome Res.* 11, 461–470.

Maruvada, P., *et al* (2003). Dynamic shuttling and intranuclear mobility of nuclear receptors. *J. Biol. Chem.* 278, 12425-12432.

McInerney, E.M., Rose, D.W., Flynn, S.E., Westin, S., Mullen, T.-M., Krones, A., Inostroza, J., Torchia, J., Nolte, R.T., Assa-Munt, N., Milburn, M.V., Glass, C.K., and Rosenfeld, M.G. (1998). Determinants of coactivator LXXLL motif specificity in nuclear receptor transcriptional actiation. *Genes Dev.* 12, 3357–3368.

McKenna, N.J., Lanz, R.B., and O'Malley, B.W. (1999). Nuclear receptor coregulators: cellular and molecular biology. *Endocr. Rev.* 20, 321–344.

McNabb, F.M. (1995). Thyroid hormone, their activation, degradation and effects on metabolism. *J. Nutr.* 125(6 suppl.), 1773S–1776S.

McNally, J.G., Muller, W.G., Walker, D., Wolford, R., and Hager, G.L. (2000) The glucocorticoid receptor: rapid exchange with regulatory sites in living cells. *Science* 287, 1262-1265.

McNeish, J., Aiello, R.J., Guyot, D., Turi, T., Gabel, C., Aldinger, C., Hoppe, K.L., Roach, M.L., Royer, L.J., de Wet, J., Broccardo, C., Chimini, G., Francone, O.L. (2000). *Proc. Natl. Acad. Sci. U.S.A.* 97, 4245.

Meyer, M.E., Gronemeyer, H., Turcotte, B., Bocquel, M.T., Tasset, D., and Chambon, P. (1989). Steroid hormone receptors compete for factors that mediate their enhancer function. *Cell* 57, 433–442.

Michalik, L., and Wahli, W. (1999) Peroxisome proliferator-activated receptors: three isotypes for a multitude of functions. *Curr. Opin. Biotechnol.* 10, 564-70.

Miyata, K. S., McCaw, S. E., Patel, H. V., Rachubinski, R. A., and Capone, J. P. (1996). The orphan nuclear hormone receptor LXRα interacts with the peroxisome proliferator-activated receptor and inhibits peroxisome proliferator signaling. *J. Biol Chem.* 271, 9189–9192.

Moras, D., and Gronemeyer, H. (1998) The nuclear receptor ligand-binding domain: structure and function. *Curr. Opin Cell Biol.* 10, 384-391.

Mukherjee, R., Strasser, J., Jow, L., Hoener, P., Paterniti, J.R.Jr., and Heyman, R.A. (1998). RXR agonists activate PPARα-inducible genes, lower triglycerides, and raise HDL levels *in vivo*. *Arterioscler. Thromb. Vasc. Biol.* 18, 272–276.

Murata, Y., Yamaguchi, S., Nomura. Y., Ohmori, S, Fujieda, M., Katunuma, N., Yen, P. M., Chin, W. W., Seo, H. (1998) *J. Biol. Chem.* **273**, 33166-73

Nagy, L., Kao, H.-Y., Love, J.D., Li, C., Banayo, E., Gooch, J.T., Krishna, V., Chatterjee, K., Evans, R.M., and Schwabe, J.W.R. (1999). Mechanism or corepressor binding and release from nuclear hormone receptors. *Genes Dev.* 13, 3209–3216.

Nelson, W.G., Pienta, K.J., Barrack, E.R., and Coffet, D.S. (1986). The role of the nuclear matrix in the organization an function of DNA. *Annu. Rev. Biophys. Biophys. Chem.* 15, 457–475.

Nickerson, J. (2001) Experimental observations of a nuclear matrix. *J. Cell. Sci.* 114, 463–474.

Noy, N. (2000). Retinoid-binding proteins: mediators of retinoid action. *Biochem. J.* 348, 481–495.

Onate, S.A., Tsai, S.Y., Tsai, M.J., and O'Malley, D.P. (1995). Sequence and characterization of a coactivator for the steroid hormone receptor family. *Science* 270, 1354–1357.

Olkkonen, V.M., and Lehto, M. (2004). Oxysterols and oxysterols binding proteins: role in lipid metabolism and artherosclerosis. *Ann. Med.* 36, 562–572.

Ordentlich, P., Downes, M., Xie, W., Genin, A., Spinner, N.B., and Evans, R.M. (1999). Unique forms of human and mouse nuclear receptor corepressor SMRT. *Proc. Natl. Acad. Sci. U.S.A.* 96, 2639–2644.

Orphanides, G., Lagrange, T., and Reinberg, D. (1996). The general transcription factors of RNA polymerase II. Genes and Development 10, 2657-83.

Orphanides, G. and Reinberg, D. (2000). RNA polymerase II elongation through chromatin. *Nature* 407, 471-475.

Ou, J., Bei-Shan, H.T., Luk, A., DeBose-Boyd, R.A., Bashmakov, Y., Goldstein, J.L., and Brown, M.S. (2001). Unsaturated fatty acids inhibit transcription of the sterol regulatory element-binding protein-1c (SREBP-1c) gene by antagonizing ligand-dependant activation of the LXR. *Proc. Nat. Acad. Sci. U.S.A.* 98, 6027–6032.

Parfenov, V.N., Pochukalina, G.N., Davis, D.S., Reinbold, R., Scholer, H.R., and Kuruganti, M.G. (2003). Nuclear distribution of Oct-4 transcription factor in transcriptionally active and inactive mouse oocytes and its relation to RNA polymerase II and splicing factors. *J. Cell. Biochem.* 89, 720–732.

Patel, H., Truant, R., Rachubinski, R. A., and Capone, J. P. (2005). Activity and subcellular compartmentalization of peroxisome proliferator-activated receptor α are altered by the centrosome-associated protein 350. *J. Cell Sci.* 118, 175-186.

Pearce, D., Naray-Fejes-Toth, A., and Fejes-Toth, G. (2002). Determinants of subnuclear organization of mineralocorticoid receptor characterized through analysis of wild type and mutant receptors. *J. Biol. Chem.* 277, 1451–1456.

Pederson, T. (1998). Thinking about a nuclear matrix. *J. Mol. Biol.* 277, 147–159.

Pederson, T. (2000). Half a century of "the nuclear matrix". *Mol. Biol. Cell* 11, 799–805.

Peet, D.J., Turley, S.D., Ma, W.Z., Janowski, B.A., Lobaccaro, J.M. Hammer, R.E., and Mangelsdorf, D.J. (1998). Cholesterol and bile acid metabolism are impaired in mice lacking the nuclear oxysterols receptor LXR alpha. *Cell* 93, 693–704.

Perlmann, T., and Evans, R.M. (1997). Nuclear receptors in Sicily: All in the Famiglia. *Cell* 90, 391–397.

Perissi, V., Staszewski, L.M., McInerney, E.M., Kurokawa, R., Krones, A., Rose, D.W., Lambert, M.H., Milburn, M.V., Glass, C.K., and Rosenfeld, M.G. (1999). Molecular determinants of nuclear receptor-corepressor interaction. *Gene Dev.* 13, 3198–3208.

Petkovich, P.M. (2001). Retinoic acid metabolism. *J. Am. Acad. Dermatol.* 45, S136–S142.

Pollard, K.J., and Peterson, C.L. (1998). Chromatin remodeling: a marriage between two families? *Bioessays* 20, 771–780.

Pombo, A., Cuello, P., Schul, W., Yoon, J.-B., Roeder, R.G., Cook, P.R., and Murphy, S. (1998). Regional and temporal specialization in the nucleus: a transcripitionally-active nuclear domain rich in PTF, Oct1 and PIKA antigens associates with specific chromosomes early in the cell cycle. *EMBO J.* 17, 1768–1778.

Pombo, A., Jones, E., Iborra, F.J., Kimura, H., Sugaya, K., Cook, P.R., and Jackson, D.A. (2000). Specialized transcription factories within mammalian nuclei. *Crit. Rev. Eukaryot. Gene Expr.* 10, 21–29.

Pratt, W.B. (1992). Control of steroid receptor function and cytoplasmic-nuclear transport by heat shock proteins. *Bioessays* 14, 841–848.

Prufer, K., Racz, A., Lin, G.C., and Basrony, J. (2000) Dimerization with retinoid X receptors promotes nuclear localization and subnuclear targeting of vitamin D receptors. *J. Biol. Chem.* 275, 41114-41123.

Qi, C., *et al* (2002) Peroxisome proliferator-activated receptors, coactivators and downstream targets. *Cell Biochem. Biophys.* 32, 187-204.

Racz, A., and Barsony, J. (1999). Hormone-dependant translocation of vitamin D receptor is linked to transactivation. *J. Biol. Chem.* 274, 19352–19360.

Reddy, J. K., Warren, J. R., Reddy, M. K., and Lalwani, N.D. (1982). Hepatic and renal effects of peroxisome proliferators: biological implications. *Ann. N. Y. Acad. Sci.* 386, 81-110.

Renaud, J. P., *et al* (1995) Crystal structure of the RAR-gamma ligand-binding domain bound to all-trans retinoic acid. *Nature* 378, 681-9.

Repa, J.J., and Mangelsdorf, D.J. (2000). The role of orphan nuclear receptors in the regulation of cholesterol homeostasis. *Annu. Rev. Cell Dev. Biol.*16, 459-81.

Repa, J.J., Liang, G., Ou, J., Bashmakov, Y., Lobaccaro, J.M., Shimomura, I., Shan, B., Brown, M.S., Goldstein, J.L., and Mangelsdorf, D.J. (2000a). Regulation of mouse sterol regulatory element-binding protein-1c gene (SREBP-1c) by oxysterols receptors LXRα and LXRβ. *Genes Dev.* 14, 2819–2830.

Repa, J.J., Turley, S.D., Lobaccaro, J.-M.A., Medina, J., Li, L., Lustig, K., Shan, B., Heyman, R.A., Dietschy, J.M., and Mangelsdorf, D.J. (2000b). Regulation of absorption and ABC1-mediated effluz of cholesterol by RXR heterodimers. *Science* 289, 1524–1529.

Roderick, H.L., Campbell, A.K., and Llewellyn, D.H. (1997). Nuclear localization of calreticulin in vivo is enhanced by its interaction with glucocorticoid receptors. *FEBS Lett.* 405, 181–185.

Rosen, E.D. and Spiegelman, B.M. (2001). PPARγ: a nuclear regulator of metabolism, differentiation, and cell growth. *J. Biol. Chem.* 276, 37731–37734.

Russell, D.W., and Setchell, D.R. (1992). Bile acid biosynthesis. *Biochemistry* 31, 4737–4749.

Saito, K., *et al* (2004). The CAP-Gly domain of CYLD associates with the proline-rich sequence in NEMO/IKKgamma. *Structure (Camb).* 12, 1719-1728.

Sarge, K.D., Murphy, S.P., and Morimoto, R.I. (1993). Activation of heat schock gene transcription by heat shcok factor 1 involves oligomerization, acquisition of DNA-binding activity, and nuclear localization and can occur in the absence of stress. *Mol. Cell. Biol.* 13, 1392–1407.

Saporita, A.J., Zhang, Q., Navali, N., Dincer, Z., Hahn, J., Cai, X., and Wang, Z. (2003). Identification and characterization of a ligand-regulated nuclear export signal in androgen receptor. *J. Biol. Chem.* 278, 41998–42005.

Schoonjans, K., Staels, B., Auwerx, J. (1996). Role of the peroxisome proliferator-activated receptor in mediating the effects of fibrates and fatty acids on gene expression. *J. Lipid. Res.* 37, 907-925.

Schultz, J.R., Tu, H., Luk, A., Repa, J.J., Medinca, J.C., Li, L., Scwendner, S., Wang, S., Thoolen, M., Mangelsdorf, D.J., Lustig, K.D., and Shan, B. (2000). Role of LXRs in control of lipogenesis. *Genes Dev.* 14, 2831–2838.

Seol, W., Mahon, M.J., Lee, Y.-K., and Moore, D.D. (1996). Two receptor interacting domains in the nuclear hormone receptor corepressor RIP13/N-CoR. 10, 1646–1655.

Shoenmakers, E., Verrijdt, G., Peeters, B., Verhoeven, G., Rombauts, W., and Claessens, F. (2000) Differences in DNA binding characteristics of the androgen and glucocorticoid receptors can determine hormone-specific responses. *J. Biol. Chem.* 275, 12290–12297.

Spector, D.L. (2003). The dynamics of chromosome organization and gene regulation. *Annu. Rev. Biochem.* 72, 573–608.

Spencer, T.A., LI, D., Russel, J.S., Collins, J.L., Bledsoe, R.K., Consler, T.G., Moore, L.B., Galardi, C.M., McKee, D.D., Moore, J.T., Watson, M.A., Parks, D.J.,

Lambert, M.H., and Willson, T.M. (2001). Pharmacophore analysis of the nuclear oxysterols receptor LXRα. *J. Med. Chem.* 44, 886–897.

Strahl, B.D. and Allis, C.D. (2000). The language of covalent histone modifications. *Nature* 403, 41-45.

Sumanasekera, W.K., *et al* (2003) Evidence that peroxisome proliferator-activated receptor α is complexed with the 90-kDa heat shock protein and the hepatitis virus B X-associated protein 2. *J. Biol. Chem.* 278, 4467-4473.

Takeshita, A., Cardona, G.R., Koibuchi, N., Suen, C.S., and Chin, W.W. (1997). TRAM-1, a novel 160-kDa thyroid hormone receptor activator molecule, exhibits distinct properties from steroid coactivator-1. *J. Biol. Chem.* 272, 27629–27634.

Tazawa, H., Osman, W., Shoji, Y., Treuter, E., Gustafsson, J.-A., and Zilliacus, J. (2003). Regulation of subnuclear localization is associated with a mechanism for nuclear receptor corepression by RIP140. *Mol. Cell. Biol.* 23, 4187–4198.

Teboul, M., Enmark, E., Li, Q., Wikstrom, A.C., Pelto-Huikko, M., and Gustafsson, J.A. (1995). OR-1, a member of the nuclear receptor superfamily that interacts with the 9-cis-retinoic acid receptor. *Proc. Natl. Acad. Sci. U.S.A.* 92, 2096-100.

Torchia, J., Rose, D.W., Inostroza, J., Kamei, Y., Westin, S., Glass, C.K., and Rosenfeld, M.G. (1997). The transcriptional coactivator p/CIP binds CBP and mediates nuclear receptor function. *Nature* 387, 677–684.

Torchia, J., Glass, C.K., and Rosenfeld, M.G. (1998). Co-activators and co-repressors in the integration of transcriptional response. *Curr. Opin. Cell. Biol.* 10, 373–383.

Tormura, A., Kiminobu, G., Morinaga, H., Nomura, M., Okabe, T., Yanase, T., Takayanagi, R., and Nawata, H. (2001). The subnuclear three-dimensionl image analysis of androgen receptor fused to green fluorescence protein. *J. Biol. Chem.* 276, 28395–28401.

Tsien, R. (1998). The green fluorescent protein. *Annu. Rev. Biochem.* 67, 509–544 .

Tyagi, R.K., Amazit, L., Lescop, P., Milgrom, E., and Guiochon-Mantel, A. (1998) Mechanisms of progesterone export form nuclei: role of nuclear localization signal, nuclear export signal, and ran guanosine triphosphate. *Mol. Endocrinol.* 12, 1684–1698.

Tzukerman, M.T., Esty, A., Santiso-Mere, D., Danielian, P., Parker, M.G., Stein, R.B., Pike, J.,W., and McDonnel, D.P. (1994). Human estrogen receptor transactivational capacity is determined by both cellular and promoter context and mediated by two functionally distinct intramolecular regions. *Mol. Endocrinol.* 8, 21–30.

van Steensel, B., Marike, B., van der Meulen, K., van Binnendijk, E.P., Wansink, D.G., de Jong, L., de Kloet, R.E., and van Driel, R. (1995). Localization of the glucocorticoid receptor in discrete clusters in the cell nucleus. *J. Cell Sci.* 108, 3003–3011.

van Steensel, B., van Binnendijk, E.P., Hornsby, D.C., van der Voort, H.T.M. Krozowski, Z.S., de Kloet, E.R., and van Driel, R. (1996). Partial colocalization of glucocorticoid and mineralocorticoid recepors in discrete compartments in nuclei of rat hippocampus neuron. *J. Cell Sci.* 109, 787–792.

Venkateswaran, A., Repa, J.J., Lobaccaro, J.-M.A., Bronson, A., Mangelsdorf, D.J., and Edwards, P.A. (2000a). Human white/Murine ABC8 mRNA levels are highly induced in lipid-loaded macrophages. *J. Biol. Chem.* 275, 14700–4707.

Venkateswaren, A., Lafitte, B.A., Joseph, S.B., Mak, P.A., Wilpitz, D.C., Edwards, P.A., and Tontonoz, P. (2000). Control of cellular cholesterol efflux by the nuclear oxysterols receptor LXRα. *Proc. Natl. Acad. Sci. U.S.A.* 97, 12097–12102.

Vignali, M., Hassan, A.H., Neely, K.E. and Workman, J.L. (2000). ATP-dependant chromatin-remodeling complexes. *Mol. Cell. Biol.* 20, 1899-1910.

Voegel, J.J., Heine, M.J.S., Zechel, C., Chambon, P., and Gronemeyer, H. (1996). TIF2, a 160 kDa transcriptional mediator for the ligand-dependant activation function AF-2 of nuclear receptors. *EMBO J.* 15, 3667–3675.

Voegel, J.J., Heine, M.J., Tini, M., Vivat, V., Chambon, P., and Gronemeyer, H. (1998). The coactivator TIF2 contains three nuclear receptor-binding motifs and mediates transactivation through CBP binding-dependant and – independent pathways. *EMBO J.* 17, 507–519.

Wansink, D.G., Schul, W., van der Kraan, I., van Steensel, B., van Driel, R., and de Jong, L. (1993). Fluorescent labeling of nascent RNA reveals transcription by RNA polymerase II in domains scattered throughout the nucleus. *J. Cell Biol.* 122, 283–293.

Watanabe, Y., Tanaka, T., Uchiyama, Y., Takeno, T., Izumi, A., Yamashita, H., Kumakura, J., Iwanari, H., Shu-Ying, J., Naito, M., Mangelsdorf, D. J., Hamakubo, T., and Kodama, T. (2003). Establishment of a monoclonal antibody for human LXRα: detection of LXRα protein expression in human macrophages. *Nucl. Recept.* 1, 1.

Wiebel, F.F., and Gustafsson, J.A. (1997). Heterodimeric interaction between retionoid X receptors α and orphan nuclear receptor OR1 reveals dimerization-induced activation as a novel mechanism of nuclear receptor activation. *Mol. Cell. Biol.* 17, 3977–3986.

Willy, P. J., Umesono, K., Ong, E. S., Evans, R.M., Heyman R.A., and Mangelsdorf, D. J. (1995). LXR, a nuclear receptor that defines a distinct retinoid response pathway. *Genes. Dev.* 9, 1033-1045.

Willy, P. J., and Mangelsdorf, D.J. (1997). Unique requirements for retinoid-dependent transcriptional activation by the orphan receptor LXR. *Genes Dev.* 11, 289–298.

Wilson, T.M., Brown, P.J., Sternbach, D.D., and Henke, B.R. (2000). The PPARs: From orphan receptors to drug discovery. *J. Med. Chem.* 43, 527 – 550.

Wurtz, J. M., *et al* (1996). A canonical structure for the ligand-binding domain of nuclear receptors. *Nature Struct. Biol.* 3, 87-94.

Xu, L., *et al* (1999). Coactivator and corepressor complexes in nuclear receptor function. *Curr. Opin. Genet. Dev.* 9, 140-147.

Xu, J., and Li, Q. (2003). Review of the *in vivo* functions of the p160 steroid receptor coactivator family. *Mol. Endocrinol.* 17, 1681–1692.

Yan, X., Habedanck, R., and Nigg, E.A. (2006). A complex of two centrosomal proteins, CAP350 and FOP, cooperates with EB1 in microtubule anchoring. *Mol. Biol. Cell* 17, 634–644.

Yokishawa, T., Ide, T., Shimano, H., Yahagi, N., Amemiya-Kudo, M., Matsuzaka, T., Yatoh, S., Kitamine, T., Okazaki, H., Tamura, Y., Sekiya, M., Takahashi, A., Hasty, A.H., Sato, R., Sone, H., Osuga, J.-I., Ishibashi, S., and Yamada, N. (2003). Cross-talk between peroxisome proliferator-activated receptor (PPAR) α and Liver X receptor (LXR) in nutritional regulation of fatty acid metabolism. I. PPARs suppress sterol regulatory element binding protein 1c through inhibition of LXR signalling. *Mol. Endocrinol.* 17, 1240–1254.

Zamir, I., Harding, H.P., Atkins, G.B., Horlein, A., Glass, C.K., Rosenfeld, M.G., and Lazar, M.A. (1996). A nuclear hormone receptor corepressor mediates transcriptional silencing by receptors with distinct repression domains. *Mol. Cell. Biol.* 16, 5458–5465.

Zhang, B., *et al* (1992). Identification of a peroxisome proliferator-responsive element upstream of the gene encoding rat peroxisoml enoyl-CoA hydratase/3-hydroxyacyl-CoA dehydrogenase. *Proc. Natl. Acad. Sci. U.S.A.,* 89, 7541-7545.

Zhang, B., *et al* (1993). Characterization of protein-DNA interactions within peroxisome proliferator-responsive element of the rat hydratase dehydrogenase gene. *J. Biol. Chem.* 268, 12939-12945.

Zhang, Z., Li, D., Blanchard, D.E., Lear, S.R., Erickson, S.K., Spencer, T.A. (2001). Key regulatory oxysterols in liver: analysis as delta4-3-ketone derivatives by HPLC and response to physiological perturbations. *Lipid Res.* 42, 649 – 658.

Zhou, Z.-X., Madhabananda, S., Simental, J.A., Lane, M.V., and Wilson, E.M. (1994). A ligand-dependant bipartite nuclear targeting signal in the human androgen receptor. *J. Biol. Chem.* 269, 13115–13123.

Zhu, X.G., Hanover, J.A., Hager, G.L, and Cheng, S.Y. (1998). Hormone-induced translocation of thyroid hormone receptors in living cells visualized using a receptor green fluorescent protein chimera. *J. Biol. Chem.* 273, 27058-27063.

Zilliacus, J., Wright, A.P.H, Carlstedt-Duke, J., and Gustafsson, J.-A. (1995). Structural determinants of DNA-binding specificity by steroid receptors. *Mol. Endocrinol.* 9, 389–400.

Zilliacus, J., Holter, E., Wakui, H., Treuter, E., and Gustafsson, J.-A. (2001). Regulation of glucocorticoid receptor activity by 14-3-3-dependant intracellular relocalization of the corepressor RIP140. *Mol. Endocrinol.* 15, 501–511.